ERDC TR-13-7

US Army Corps
of Engineers®
Engineer Research and
Development Center

ERDC
INNOVATIVE SOLUTIONS
for a safer, better world

Analysis Techniques, Materials, and Methods for Treatment of Thermal Bridges in Building Envelopes

Benjamin P. Barnes, Axy Pagán-Vázquez, Andrew P. Heffron, Brenda B. Mehnert, Michael P. Case, Ashok Kumar, Jeffrey L. Lattimore, Richard J. Liesen, Larry D. Stephenson, Jonathan C. Trovillion, and Jeffrey B. Allen

August 2013

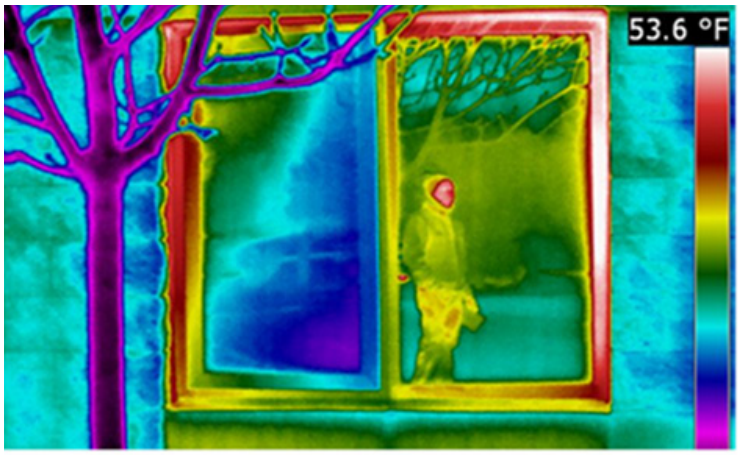

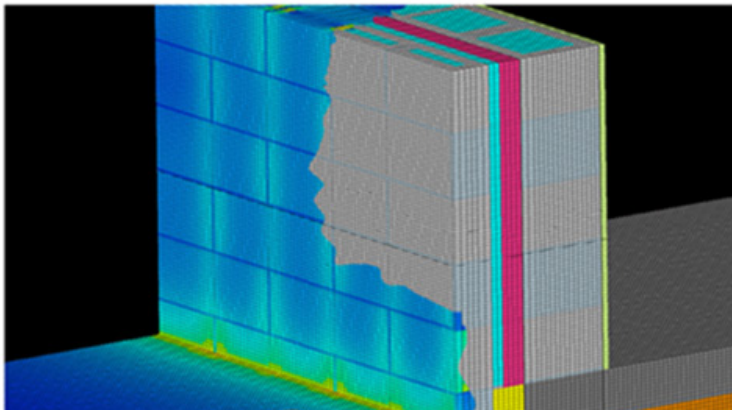

Construction Engineering
Research Laboratory

ERDC TR-13-7
August 2013

Analysis Techniques, Materials, and Methods for Treatment of Thermal Bridges in Building Envelopes

Benjamin P. Barnes, Axy Pagán-Vázquez, Andrew P. Heffron, Brenda B. Mehnert, Michael P. Case, Ashok Kumar, Jeffrey L. Lattimore, Richard J. Liesen, Larry D. Stephenson, and Jonathan C. Trovillion

US Army Engineer Research and Development Center
Construction Engineering Research Laboratory (CERL)
PO Box 9005
Champaign, IL 61826-9005

Jeffrey B. Allen

US Army Engineer Research and Development Center
Information Technology Laboratory (ITL)
Waterways Experiment Station, 3909 Halls Ferry Road
Vicksburg, MS 39180-6199

Final Report

Prepared for Headquarters, US Army Corps of Engineers
Washington, DC 20314-1000

Abstract

To meet mandated energy reduction goals, this work developed capabilities to characterize energy losses through building envelopes (especially thermal bridge losses), and to devise potential mitigation strategies using advanced techniques and materials. This report reviews existing thermal bridge quantification and mitigation strategies, as well as Army and building code requirements. It is proposed that, first, additional guidance must be authored to encourage treatment of thermal bridges and, second, that an easy to use thermal bridge catalogue must be composed. To this end, important thermal bridges in Army buildings are identified by infrared imaging and drawings review. Next, several 3-D heat transfer simulations are performed on these details as the first step to predicting their performance for inclusion in a details catalogue. Finally, advanced materials are characterized to better serve as mitigation options for thermal bridge retrofits.

Contents

Illustrations

Figure **Page**

Figure **Page**

Figure **Page**

Figure **Page**

Table **Page**

Preface

This study was conducted for Headquarters, US Army Corps of Engineers (HQUSACE) and the Office of the Assistant Secretary of the Army for Acquisition, Logistics, and Technology, ASA (ALT) under program element 622784T45, "Energy Technology Applied to Military Facilities." The HQUSACE technical monitor was Harry Goradia, CEMP-CI-I.

The work was managed and executed by Dr. Ashok Kumar, Dr. M. Case and Dr. L.D. Stephenson of the Materials and Structures Branch (CEERD-CF-M), and the Energy Branch (CEERD-CF-E) of the US Army Engineer Research and Development Center – Construction Engineering Research Laboratory (ERDC-CERL), Champaign, IL. At the time of publication, the Chief of the ERDC-CERL Materials and Structures Branch was Vicki L. Van Blaricum (CEERD-CF-M), and the Chief of the Energy Branch was Franklin H. Holcomb (CEERD-CF-E), the Chief of the Facilities Division was L. Michael Golish, (CEERD-CF), and the Technical Director for Installation was Martin J. Savoie (CEERD-CV-ZT). The Deputy Director of ERDC-CERL was Dr. Kirankumar Topudurti and the Director was Dr. Ilker Adiguzel. CERL's principal investigators were Dr. Michael Case and Dr. L.D. Stephenson.

The Commander and Executive Director of ERDC is COL Jeffrey R. Eckstein, and the Director of ERDC is Dr. Jeffery P. Holland.

Unit Conversion Factors

Multiply	By	To Obtain
British thermal units (International Table)	1,055.056	joules
degrees Fahrenheit	(F-32)/1.8	Degree Celsius
Feet	0.3048	meters
Inches	0.0254	meters
Square feet	0.09290304	Square meters
Btu/(ft-°F-h) (conductivity or linear thermal transmittance)	1.7307	W/(m-K)
Btu/(sq ft-°F-h) (U-factor)	5.6783	W/(m^2-K)
sq ft-°F-h/Btu (R-value)	0.17611	m^2-K/W
kWh (kilowatt-hour)	3,600	kilojoules
Pounds	0.45455	kilograms

1 Introduction

1.1 Background

Approximately 25% of the Department of Defense's total energy use is consumed by buildings—over 577,000 buildings on more than 5300 sites. The US Department of Defense (DoD) spent over $3.5 billion for energy for fixed installations in 2006. The Energy Independence and Security Act (EISA 2007), and Energy Policy Act (EPAct 2005) require the Army to dramatically reduce overall facility primary energy usage over the coming decades. The Army Energy Security Implementation Strategy (DA 2009) laid out the Department of the Army's strategy for large energy reductions. More recently, the Army published the "Army Vision for Net Zero," which states the ambitious goal of reaching Net Zero Energy at all fixed installations (ASAIEE 2012).

This goal implicitly includes an enormous stock of existing buildings, and achieving this goal will require the implementation of building envelope performance requirements not yet seen in the Federal government. The building envelope represents an area of much needed improvement in these facilities. Guidance has already been published to encourage much more efficient building envelopes. However, that guidance does not address thermal bridging despite the fact that failure to mitigate it has been shown to represent losses of 8.45 kWh/m²-year (2.68 kBtu/sq ft-year) to 12.6 kWh/m²-a (3.99 kBtu/sq ft-a) in otherwise zone H1A (Paris) high performing buildings (Citterio, Cocco, and Erhorn-Kluttig 2008).

A "thermal bridge" (TB) is a part of an envelope in which heat transfer is greater than would be expected in a wall made up of planar layers such as gypsum wallboard, insulation, sheathing, and cladding. TBs often result from the inclusion of materials of higher conductivity that "bridge" from inside to outside. Structural steel studs are a typical example; steel has a conductivity value three orders of magnitude higher than typical insulation materials (ASHRAE 2009a). Geometrical differences can also cause TBs, e.g., where increased surface area on either side causes a "fin effect," transferring more heat than a planar surface would. Figure 1 shows a simulation of a detail comprising both types of TB, done during heating conditions in which a balcony acts as a heat transfer fin that would increase conduction even if it was made from a material similar to the wall. The concrete slab, being more conductive than the wall around it, further increases heat transfer.

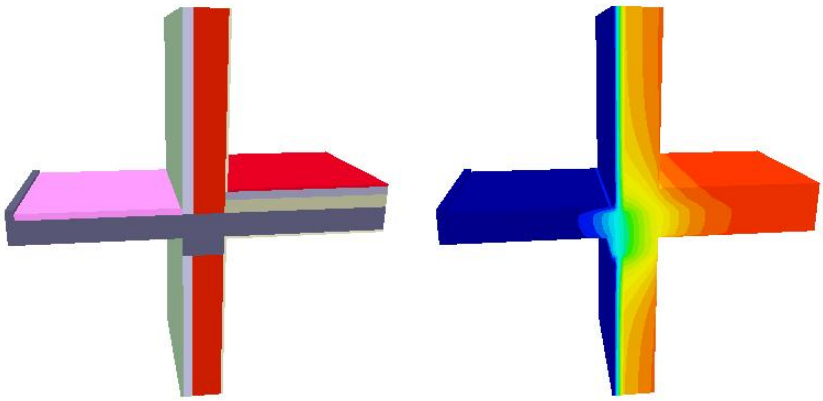

Figure 1. A finite difference heat transfer model, done using KOBRA (CSTC 2011), of a concrete slab extending through the building envelope to create a balcony.

Achieving high-performance building envelopes requires high performing materials throughout the wall, especially where TBs are involved and even more so in the case of retrofits; the development of novel materials may offer improved strategies for mitigating energy losses. However, the potential for novel materials to contribute to more efficient building envelopes is also not well exploited in existing practice, in part because the properties of such materials are not well understood.

Erhorn-Kluttig and Erhorn (2009) compiled the results of several studies that estimated the impacts of TBs, and concluded that:

- The total impact of TBs on heating energy required is significant. A study done in France found that it is possible to save 8.45 kWh/m²-a (2.68 kBtu/sq ft-a) in heating energy by retrofitting a residential concrete building with TB mitigation. A German study found that, when compared to standard construction, a "double house" treatment of TBs can save 9.9-12.6 kWh/m²-a (3.14-3.99 kBtu/sq ft-a) (Erhorn, Gierga and Erhorn-Kluttig 2002, Lahmidi and Leguillon Undated). In some cases, avoiding and mitigating TBs in the design can save more primary energy than installing solar hot water systems.
- The impact on cooling energy, the relative conductive contribution of which is much smaller, is less significant. However, the impact on cooling peak load is significant. A simulation study done in Greece found that, for typical Greek masonry construction, the calculated peak cooling load is 10% higher when TBs are considered (Theodosiou and Papadopoulous 2008).

- Where a Member State's building code requires a default U-factor increase in buildings for which calculations do not explicitly address TBs (discussed further in Section 2.1.1.6), this value is usually found to be worse than if the thermal bridges had been explicitly calculated. That is, detailed calculation tends to predict a a lower overall U-factor for a building than does the addition of a default increment. For instance, a study done in Poland, using an aerated concrete building, found that standard prediction methods lead to an additional 0.036 W/m²K (0.0063 Btu/sq ft-°F-h), compared to the default of 0.05 W/m²K (0.0088 Btu/sq ft-°F-h) for premium construction and 0.1 W/m²K (0.018 Btu/sq ft-°F-h) for standard construction. Similarly, a study done in the Netherlands found a 3.75-11.25% improvement in their "Energy reduction value" when they use detailed calculation measures rather than the default TB penalty (Wojnar, Firlag and Panek 2009, Spiekman 2009).

The absolute impact of TBs has often been thought of as small relative to an envelope's overall losses, but this relative contribution has been increasing as buildings become more energy efficient. In fact, thermal bridging effects can be as high as a 30% of the total energy loss through the envelope (CITE) Singular TB will not necessarily create a considerable impact but their superposition along the entire building certainly will. In the past, much attention was paid to improving the "clear-wall" portion of the envelope – those planar areas that have regularly spaced structural components and that are free of windows, doors, etc. As additional insulation improvements in the clear wall show diminishing returns (Figure 2), mitigating TBs becomes the wiser investment. For example, a fenestration load for a blast resistant window that is dominated by the thermal bridging of the frame and steel reinforced rough opening becomes increasingly worthwhile to consider.

TBs present four primary challenges to the building designer:

1. Determining what is necessary to achieve compliance with codes and Army regulations
2. Determining how one minimizes the energy cost implications by mitigating and avoiding TBs
3. Determining whether necessary TBs present a condensation risk
4. Predicting the energy penalty of a TB, or the cost effectiveness of mitigation the TB.

This work draws on work done for the European Union's ASIEPI project, and applies the results in the US and (more specifically) in the Army context. Table 1 summarizes relevant ASIEPI publications.

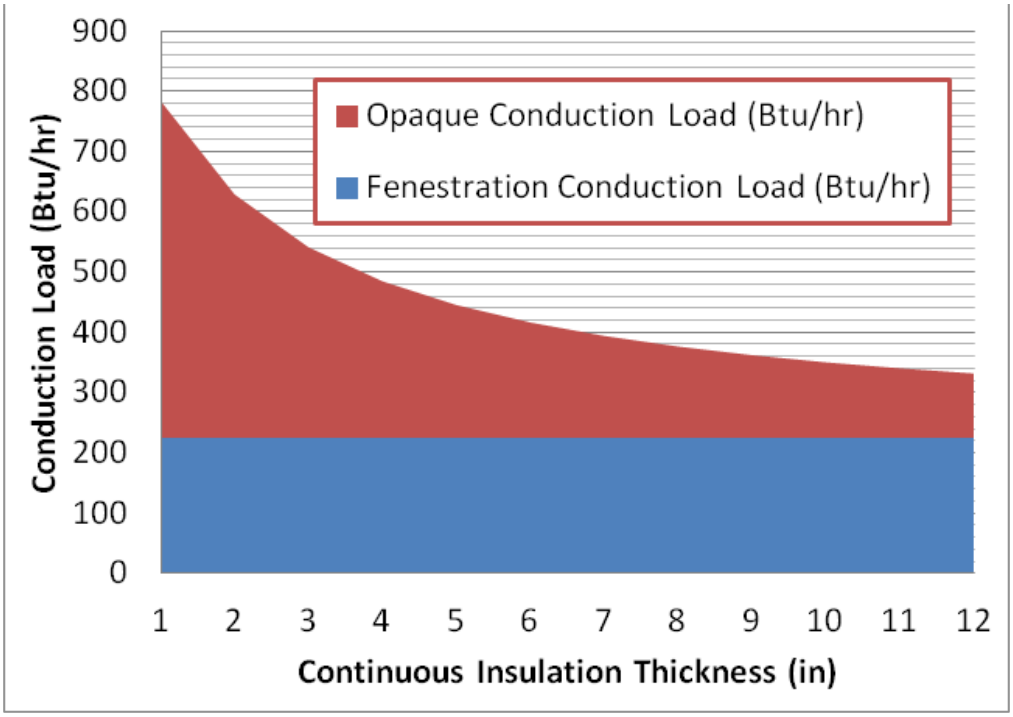

Figure 2. A calculation, using the simplified methods discussed in Section 2.1.1, for a typical 12x12-ft concrete masonry unit (CMU) wall with a 3x4-ft window retrofitted for blast resistance, with varying levels of continuous insulation applied on the exterior surface.

Table 1. List of publications from ASIEPI's "Thermal Bridges" task.

No.	Title	Citation
N/A	Final Report of the Institution of Electrical Engineers (IEE) ASIEPI Work on Thermal Bridges	(Erhorn et al. 2010)
P188	Good practice guidance on thermal bridges & construction details, Part I: Principles	(Schild and Blom. 2010)
P189	Good practice guidance on thermal bridges & construction details, Part II: Good examples	(Schild 2010)
P190	Advanced Thermal Bridge Driven Technical Developments	(Erhorn and Erhorn-Kluttig 2010)
P159	Analysis of Execution Quality Related to Thermal Bridges	(Thomsen and Rose 2009)
P148	Impact of Thermal Bridges on the Energy Performance of Buildings	(Erhorn-Kluttig and Erhorn 2009)
P198	Software and Atlases for Evaluating Thermal Bridges	(Tilmans and Orshoven 2010)
P064	Thermal Bridges in the "Energy Performance of Buildings Directive" Context: Overview on Member State Approaches in Regulations	(Citterio, Cocco and Erhorn-Kluttig 2008)

1.2 Objectives

The objectives of this work were to:

1. Determine the building details that require attention to identify, predict, and mitigate TB impact in Army buildings. The criteria for selection were: (a) that a detail either represents a particularly severe TB, or (b) that it is used in very common Army construction types. It follows that the first objective is to develop an understanding of important construction types, and, within them, important specific details.
2. Review similar efforts in the field of building envelope research, to avoid duplication of effort, and to determine what is lacking in the field, specifically in areas of special relevance to the Army, where such work is not likely to be accomplished by other entities.
3. Identify possible causes of TBs and to propose alternative treatments for them, i.e., to develop practical, accurate, usable methods to help designers in quantify TB impacts. An "atlas" of details relevant to Army buildings would augment this task. Preliminary simulation results from analyzing these details are included in Chapter 4.

1.3 Approach

The objectives of this project were accomplished in the following steps:

1. Important construction types were identified by:
   a. Interviewing Directorate of Public Works (DPW) personnel and other staff during visits to installations.
   b. Reviewing the Army Real Property Inventory to determine total building areas belonging to different building categories.
   c. Reviewing reports on the Army's existing building stock, such as "Unaccompanied Personnel Housing (UPH) During The Cold War (1946-1989)" (Kuranda et al. 2003) and "Antiterrorism Measures for Historic Properties" (Webster, Reicher, and Cohen 2006) to distinguish specific construction types that may represent an important stock of buildings that require retrofit.
2. High impact details (prominent TBs observed in important buildings) were listed. This will be determined by Centers of Standardization (COS) drawing review for new buildings, and by as-built drawing review for existing buildings, where available. Another primary technique for determining high impact details has been the use of thermographic imaging of build-

ings on actual installations. This technique reveals details that allow high heat transfer in several types of existing Army buildings.

3. Current methods were reviewed and solutions proposed. The review of current work examined available simplified methods, detail catalogues, and numerical tools, with a specific focus on why such methods and tools are not widely used. Existing regulations concerning TBs were examined to determine why TBs are not more successfully treated. In addition, a brief review of whole-building simulation tools was included to illustrate how the predictive fidelity of such tools is biased by their treatment (or lack of treatment) of TBs.

1.4 Mode of technology transfer

It is anticipated that the results of this work will be integrated into a detailed TB guide that may be referenced by Unified Facilities Criteria 1-200-01 "General Building Requirements," and that may also supplement the USACE "Energy and Water Conservation Design Requirements for SRM Projects" web publications (DoD 2011).

2 Review of Thermal Bridge Guidance and Standards

2.1 Calculation methods and tools

The many methods for quantifying and/or mitigating the impact of TBs may be grouped into three categories:

1. Simplified methods, which can be done by hand calculation
2. Catalogues, which give examples of approved details for compliance and, in some cases, provide quantitative information for predicting heat transfer
3. Numerical methods, which discretize and solve the heat diffusion equation, coupled with radiation and convection models where necessary.

It is important to understand the two general paradigms for incorporating TBs into a whole-building calculation. The first, "area weighting," is more common in the United States. For example, the National Fenestration Rating Council (NFRC) Standard 100 uses area weighting to combine the effects of window frame, edge-of-glass, and center-of-glass areas, as does Christian and Kosny's (1995) method for opaque walls. Some of the simplified methods discussed below also use area weighting. The second, "linear and point transmittances" method (or "Ψ and χ method") is more commonly used in Europe, as described in International Standards Organization (ISO) 13789 for non-repeating and geometrical TBs (ISO 2007c). Most TB catalogues also use Ψ- and χ-values.

The typical TB example in which a structural member interrupts an insulated wall illustrates the two approaches. In Figure 3, the heat flux varies along the length of the wall. For much of the wall, the flux at the outside surface can be taken as constant over the area and equal to the flux at the inside surface at steady state, since the conduction is effectively 1-D over those areas. In the neighborhood of a TB, however, the conduction path is more complex. These separate areas are referred to as zones (see Section 2.1.1, Simplified methods).

At a large enough distance from the bridge, one can effectively draw "cut-off planes," which are planes through the wall that can be considered adiabatic. They separate areas of the wall in which conduction can be assumed

to be 1-D, from areas where more complex heat transfer occurs. In this example, the heat flux is q''_{base} through the areas not impacted by the TB. To capture the impact of the TB, designers would first determine the zone that is impacted – that is, identify x_1 and x_2. They would then find the average heat flux over this "zone," q''_{ave} (Figure 4).

This is the point at which the area-weighted method and the Ψ and χ method diverge. In the area-weighted method, the two heat fluxes, q''_{ave} and q''_{base}, are divided by the temperature difference used to calculate (or test) them. This produces U-factors for the two zones. These U-factors, called $U_{A,C,}$ and U_B, are area weighted to generate a whole-wall U-factor:

$$U = \frac{U_{A,C}A_{A,C} + U_B A_B}{A_{A,C} + A_B}$$

where:

the subscript "A,C" denotes the area in which q''_{base} applies
the subscript "B" denotes the area in which q''_{ave} applies.

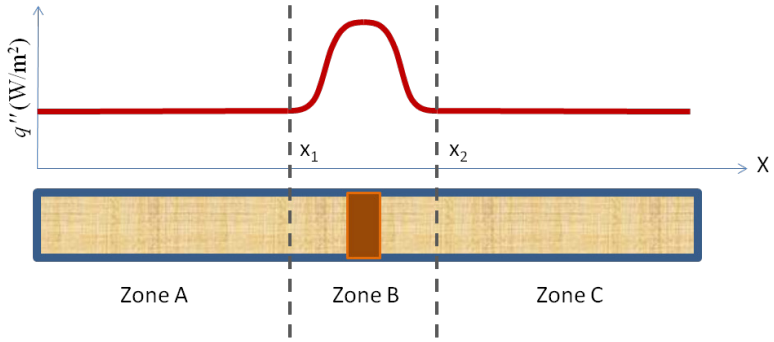

Figure 3. A long, structural TB viewed from the top of a wall.

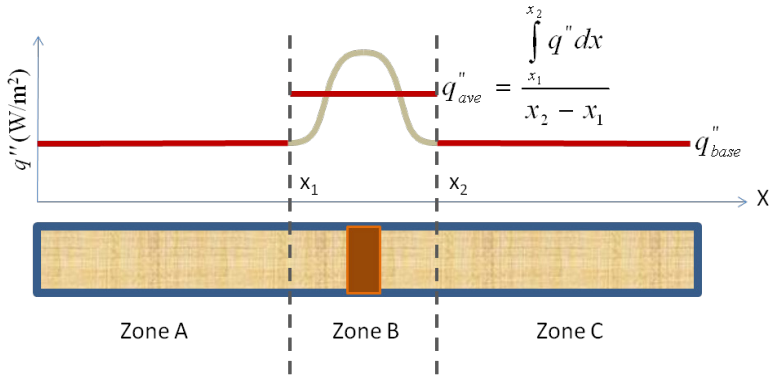

Figure 4. In the area affected by the TB, a new average heat flux is determined.

To implement this method, the user requires both U_B and the affected width, $x_2 - x_1$, both of which are typically taken from look-up tables, as well as the length of the feature causing the TB (in this case, the height of the stud).

In the "Ψ and χ method," only the *difference* between the overall flux and q''_{base} is integrated from x_1 to x_2, and this produces Q_Ψ/h (Figure 5). In fact, one can think of the difference as being integrated over the entire wall, though it is close to zero in most locations. This value, expressed per degree of temperature difference, is called a linear thermal transmittance or Ψ-value and has units of power per length per temperature difference (i.e., W/m-K or Btu/ft-°F-h). This only an incremental change in the overall conduction, and is not to be confused with the U-factor, which typically has units of power per *area* per temperature difference (i.e., W/m²-K or Btu/sq ft-°F-h) and is intended to express the wall's conductance. To use this method, the user only needs the Ψ-value and the length of the TB.

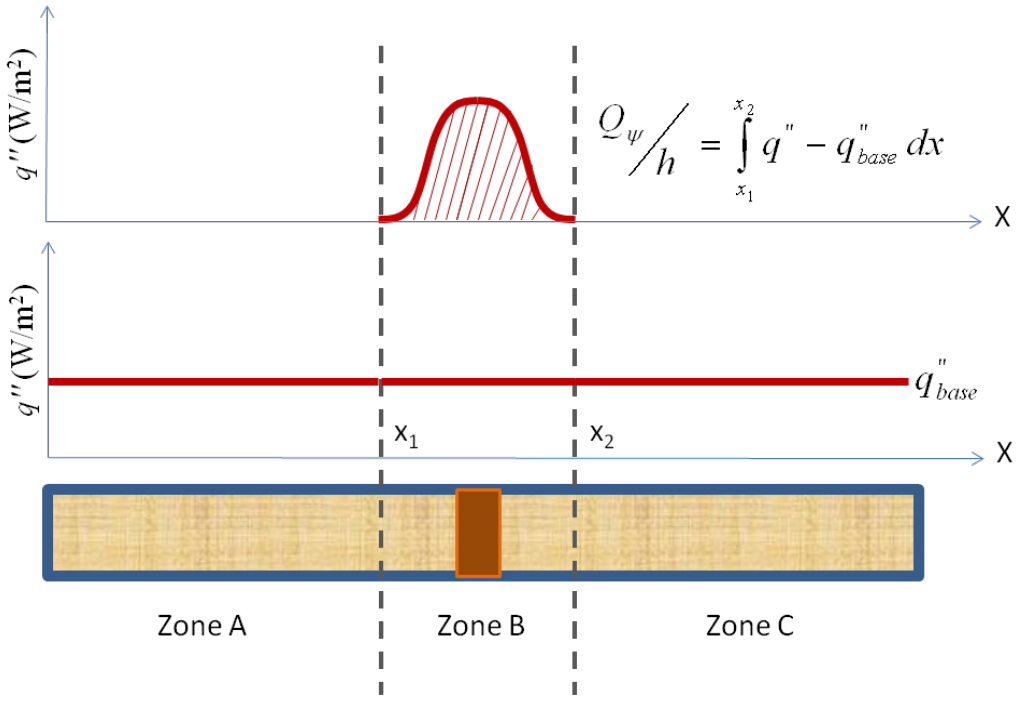

Figure 5. The striped portion reflects the difference between the total heat flux and that expected in a wall with no thermal anomaly.

The χ-values are similar, except that the units are power per temperature difference (i.e., W/K or Btu/hr-°F). Referred to as point thermal transmittance, χ-values apply to point bridges such as a steel beam perpendicular to the wall, or a fastener or brick tie. In this case, the user needs only the χ-values and the number of occurrences of the bridge.

The primary issue with the weighted area approach is that the effective lengths (i.e., $x_2 - x_1$) must be determined. American Society of Heating, Refrigerating, and Air-Conditioning Engineers (ASHRAE) RP-1365 "Thermal Performance of Building Envelope Details for Mid- and High-Rise Buildings" (referred to below as ASHRAE RP-1365) justifies the authors' decision to use "Ψ and χ":

> … defining the effective area … is either a very challenging or arbitrary process and using this information with the area-weighted average method for whole building load calculations is tedious.
>
> This work highlights a few major drawbacks for using the area-weighted average method to account for thermal anomalies contained within opaque building envelope assemblies:
>
> 1. Assigning effective areas to three-dimensional heat flow paths can be a complex procedure; judgment must be exercised and consistency is difficult to achieve.
> 2. A catalogue of effective lengths specific to simulated details and U-factors is undesirable.
> 3. Using the area-weighted average method to account for all the significant thermal anomalies of typical buildings is a tedious process at best.
>
> These drawbacks can be partially overcome by setting standard effective lengths for groups of anomalies. However, this simplification leads to the assigned value being at least partly arbitrary without any true significance. This leads to the concept of linear and point transmittances to overcome these drawbacks.
>
> First, one has to accept that there cannot be effective lengths specific to each simulated detail and simplifications are necessary for a generic thermal performance catalogue to be useful for practitioners. The effective length might as well be zero.
>
> Second, one has to be open to the idea of letting go of the area-weighted average method, at least for thermal anomalies contained within opaque building envelope assemblies, if another method provides the same end result, but with a lot less effort, in this case, by the use of predefined/standardized values found in catalogs based on heat conduction simulations.

> The concept of linear and point thermal transmittances (Ψ or χ respectively) is quite simple. The heat flow through an assembly with a thermal anomaly is compared to the same assembly without the thermal anomaly for the same gross area. The difference in magnitude of the heat flow is attributed to the effect the thermal anomaly has on the clear field assembly. For whole-building load calculations, the linear and point transmittances is simply added to the clear value U-factor for a given total assembly area (wall/roof) to calculate the overall thermal transmittance. Splitting the total assembly area into areas affected by individual thermal anomalies and clear field areas is not necessary *(ASHRAE 2011b)*.

Although this work reviews methods of both types, proposed deliverables will use linear and point thermal transmittances.

2.1.1 Simplified methods

Simplified methods can be applied by hand calculation, though they are often developed using numerical methods or experiments. Their application has limited accuracy and cannot address all bridge types. However, the following sections demonstrate that they could be used much more often than they are, if there were motivation in codes and standards to do so.

2.1.1.1 Parallel path and isothermal planes (ASHRAE 2009a)

Two very simple methods for handling TBs are the parallel paths method and the isothermal planes method, both of which are presented in ASHRAE Fundamentals (2009a).

The parallel paths method is essentially area averaging in its simplest form. The cutoff planes, discussed above, are simply placed at the edge of the anomaly, as shown in Figure 6. The method assumes that heat flows one-dimensionally through the "normal" wall area and the anomaly, and that the boundary between these areas is an adiabatic plane. In theory, parallel paths could be used for point TBs such as fasteners, but it seldom is. To calculate the overall heat flux, the resistances shown in Figure 6 can be added in series, then parallel, as the electrical analogy would suggest:

$$R_{anomaly} = R_A + R_B + R_C + R_E + R_F$$

$$R_{normal} = R_A + R_B + R_D + R_E + R_F$$

$$U_{total}A_{total} = \frac{A_{anomaly}}{R_{anomaly}} + \frac{A_{normal}}{R_{normal}}$$

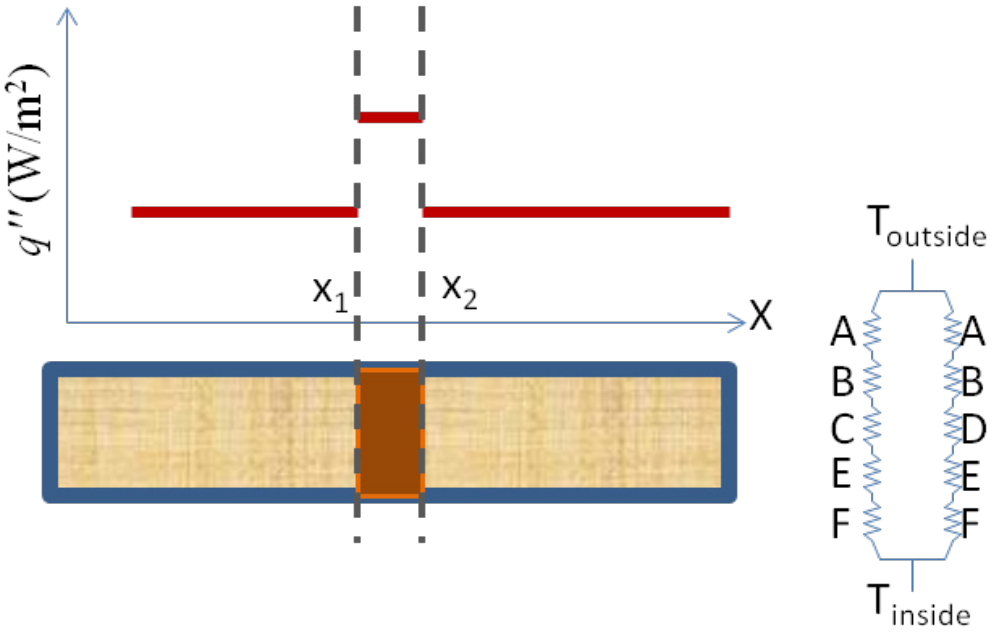

Figure 6. The "parallel paths" method assumes 1-D heat flows through both the anomalous area and the normal area; the boundary between the two is assumed to be an adiabatic plan. A = outside air film, B = outside sheathing and siding, C = insulation, D = structural member, E = inside wallboard, F = inside air film.

The method typically gives an upper bound to the R-value of a wall, which is appropriate where the structural material's conductivity is close to that of the insulation (within an order of magnitude) and where there is no layer in the plane of the wall likely to allow for high lateral conduction. If the structural material has a higher conductivity by multiple orders of magnitude than the insulation (e.g., in steel framing), the isothermal planes method (Figure 7) provides an R-value likely to be closer to the measured value.

In the isothermal planes method, each layer of the wall is resolved with the parallel paths method, where necessary; only those layers with anomalies require this. The remaining layers are added in series. This effectively assumes that each plane separating the layers is an isotherm, or, using the electrical analogy, composes a "node" with one "voltage." Note that, in Figure 7, $R_{anomaly}$ and R_{normal} refer here to the resistance of only the layer that contains the anomaly, not the series-combined resistances used in the parallel paths method above; an example would be the resistance of the stud only and the insulation batt only.

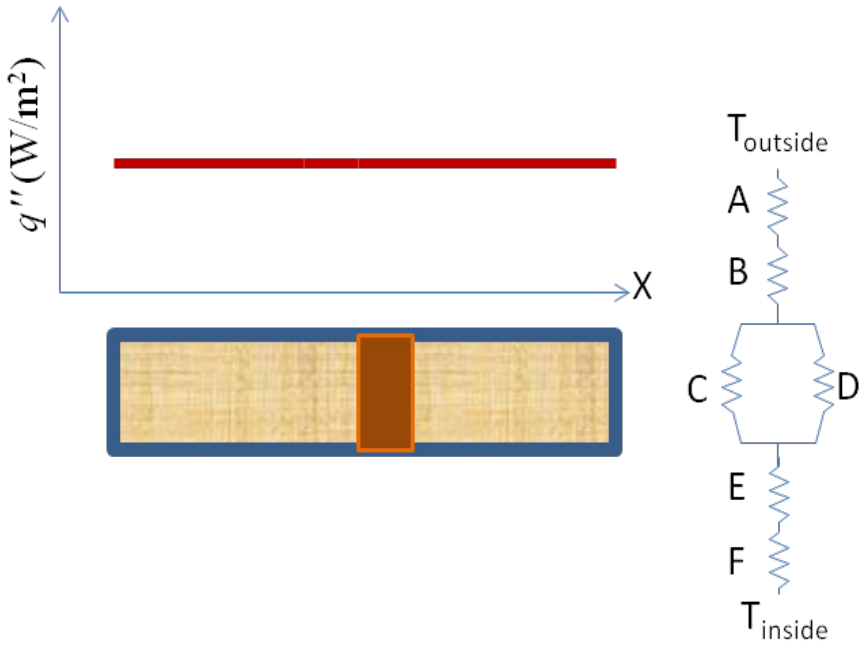

Figure 7. The isothermal planes method,

The overall U-factor can be calculated as suggested by the electrical analogy:

$$R_{anomalous\ layer} = \frac{A_{anomaly}}{R_{anomaly}A_{total}} + \frac{A_{normal}}{R_{normal}A_{total}}$$

$$R_{total} = R_A + R_B + R_{anomalous\ layer} + R_E + R_F$$

ASHRAE Fundamentals (2009a) provides an example calculation for a masonry wall. The isothermal planes method produces an R-value of 0.604 m²-K/W (3.43 sq ft-°F-h/Btu) while a parallel paths method produces 1.04 m²-K/W (5.89 sq ft-°F-h/Btu). Hot-box testing gives 0.551 m²-K/W (3.13 sq ft°F/Btu), which is close to the value produced by the isothermal planes method (though one would typically expect this isothermal planes to provide a lower bound). In a masonry wall, the concrete faces provide a good layer for lateral heat conduction, so higher accuracy is expected of the isothermal planes method.

Wood framing, in comparison, has no such layer and the structural members are only about three times as conductive as the insulation material. In this case, the parallel paths method will be more accurate. In fact, errors have been known to be less than 2% using this method when the correct amount of framing is accounted for (Kosny and Christian 2001).

These two methods form the backbone of many other simplified correlations. Indeed, they are used to construct many of the tables in two widely used buildings energy standards:

- ASHRAE/ANSI/IES Standard 90.1 "Energy Standard for Buildings Except Low-Rise Residential Buildings" (referred to as "ASHRAE 90.1")
- ASHRAE/USGBC/IESNA Standard 189.1 "Standard for the Design of High-Performance, Green Buildings Except Low-Rise Residential Buildings" (referred to as "ASHRAE 189.1").

The simplified methods are also approved by these standards for use in determining the performance of many custom wall types (ASHRAE 2007, ASHRAE 2009b). The methods are fundamentally limited, however, and have difficulty addressing situations such as:

- Steel studs, which have a very high thermal conductivity, but a very narrow cross-section and flanges on both sides.
- Geometrically interesting details, like balconies, corners and interior wall intersections. Since the inside surface area and the outside surface area of the analyzed wall are different, these simplified methods cannot be used here.
- Areas with very high amounts of structural framing, where studs cannot simply be considered as regularly repeating bridges that can be analyzed separately.
- Slab-ground interactions, which contain multiple time scales and boundary conditions.

To address the above list accurately, other methods are usually required. Bombino et al. (2010) produces results that motivate caution when using simplified methods for more complex details. A parallel paths approach to calculating a mid-floor slab-edge U-factor gives results within 3% of a 2-D numerical simulation, even though it ignored the fin effect of the slab continuing into the interior (see Section 2.2.2 for more discussion of surface area effects). However, a small amount of insulation on the slab edge increases the discrepancy to 12% (Bombino and Finch 2010). The higher discrepancy occurs when the slab-wall interaction becomes more significant, invalidating the implicit 1-D assumption of the parallel paths method.

2.1.1.2 ASHRAE Zone and modified zone methods (ASHRAE 2009a)

A steel member in a clear wall has a conductivity that exceeds that of the surrounding insulation by roughly three orders of magnitude. The radically different temperature distribution in the steel stud and the insulation causes 3-D heat transfer paths to become important. The dramatically different temperature profile becomes evident by using a sophisticated 2-D conduction simulation as in Figure 8) . Resulting heat conduction in this simulated wall is 70% higher than would be predicted by the simple, clear-wall R-value.

A common method for treating this issue without resorting to numerical simulation is called the "zone method," detailed in ASHRAE Fundamentals (2009a). It is an area-weighted method with specific rules for choosing the width of each zone.

The basic zone method is useful for highly conductive, large metal members that are widely spaced. It suggests the width of the anomalous zone based on an empirical function:

$$W = w+2d$$

where:

w = the width of the metal member
d = its depth into the wall.

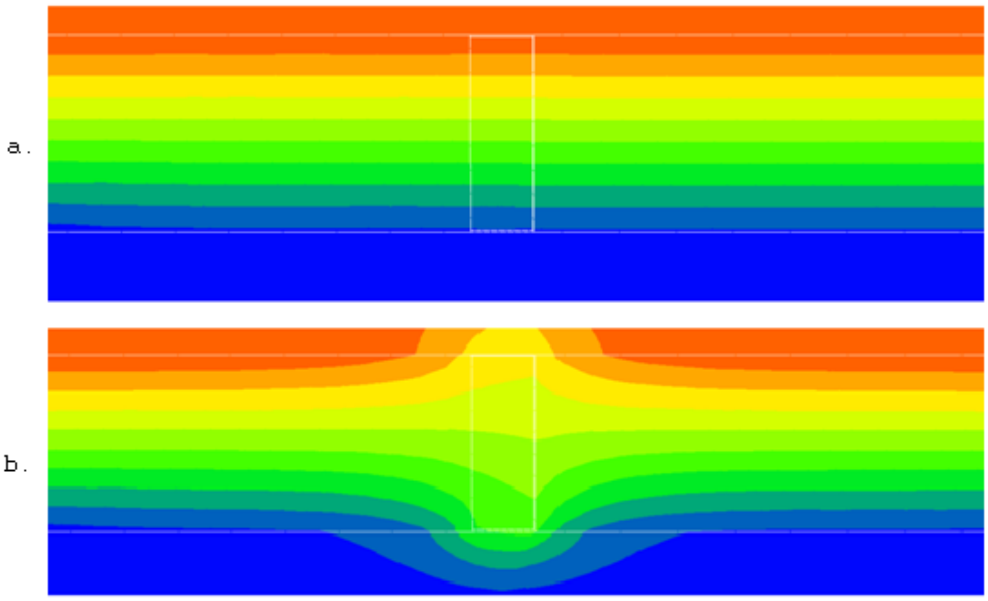

Figure 8. Temperature profiles in a steel stud wall (shown by colors).

Within this zone, the U-factor of the wall is computed using the isothermal planes method. In the remaining wall, the R-value is found simply by series addition and inverted to find the U-factor. The two zones are then combined by area weighting the U-factors. An example calculation is given for a roof composed of a steel bulb tee bridging through fiber glass insulation and covered by gypsum concrete and roofing. The zone method gives 0.812 m^2-K/W (4.61 h-sq ft°F/Btu), while two actual hot-box measurements produce 0.805 and 0.854 m^2-K/W (4.57 and 4.85 h-sq ft°F/Btu) (ASHRAE 2009a).

For metal stud walls in insulated cavities, the modified zone method provides a more accurate result. The primary difference is in the way that the anomalous zone width is calculated, with such inputs as the stud flange size, and the thickness and resistivity of materials on the inside or outside of the studs. This method has been very well validated by over 200 simulations and 15 walls measured in a hot box (Kosney et al. 1994).

2.1.1.3 Whole-wall R-values (Kosny and Christian 2001)

Kosney and Christian (2001) developed a method for capturing the difference between clear-wall R-values and whole-wall R-values. This method:

1. Tests an 8 x 8-ft section of the wall in a guarded hot box (see Section 2.1.3)
2. Uses the test results to calibrate a numerical simulation
3. Uses the numerical simulation on corner, wall-roof, window and door openings, and other details, and then
4. Finds the "whole-wall" U-factor by applying the results of the detail simulations to a realistic "reference building" with four corners and realistically spaced windows and doors.

It was found that, when the "clear-wall" R-value is used, the thermal resistance of the wall is overstated by as much as 26.5%. Results were gathered for 18 wall types. This type of information can be used in a table of values, as in ASHRAE 90.1, but it is difficult to modify or generate new entries.

2.1.1.4 Gorgolewski's method (Gorgolewski 2007)

Gorgolewski (2007) developed a method for estimating U-factors in light steel framing that can be compared to the ASHRAE zone method. It has

been sanctioned for determining compliance with UK's building regulations. The first step is to identify R_{max} and R_{min} by the parallel paths and isothermal planes methods, respectively, using the appropriate framing factor. The two values are then weighted with:

$$R = pR_{max}(1-p)R_{min}$$

where:

$$p = 0.8\frac{R_{min}}{R_{max}} + 0.1$$

This results in a 3% average absolute error, and over-estimates R-value by no more than 10%. By refining the value of p further, using table-lookups for different framing geometries, the average absolute error is brought down to 2.7%, with a maximum overestimate of 3%.

2.1.1.5 Statistical regression of common bridge types (Larbi 2005)

Larbi (2005) demonstrates a method of generalizing a particular detail type using a simplified equation based on a regression of dozens of variations of thicknesses and conductivity. There is one example each for slab-earth, mid-level slab-wall, and wall-roof connections. For these details, the fitted model achieved relative errors between the regression and the numerical model R-value of less than 3%. However, each regression applies only to one detail geometry. For instance, the wall to mid-level-slab bridge is modeled with the insulation on the inside, which is not often the case for new construction. Simplified methods such as this one can accompany detail catalogues to make each entry's information applicable to more variations.

2.1.1.6 Default values

One of the simplest ways to account for TBs in regulations is to supply either default Ψ-values to be multiplied by the lengths of important TB types, or to supply a default U-factor increment that is added to the calculated U-factor of the entire building area. ASIEPI Report P64 (see Figure 2) describes Member States' approaches to regulations, many of which include default values. Table 2 lists some examples.

Table 2. Examples of "default value" TB regulation from various European Union Member States.

Country	Approach
Denmark	Sets default values for specific TBs in certain types of construction: 0.06 W/m-K (0.034 Btu/ft-°F-h) for window edges and 0.40 W/m-K (0.23 Btu/ft-°F-h) for foundations. Detailed methods are allowed to prove that a constructed detail performs better than the default.
Belgium	A default value is allowed if all details are executed according to regulations. If not, a very severe default is used instead. The "K-level" is penalized.
Netherlands	A default U-factor increment of 0.10 W/m2-K (0.018 Btu/ft-°F-h) is added to the entire surface of the building unless detailed calculations prove otherwise.
Germany	Three levels of default U-factor increments exist: 0.05 W/m2-K (0.0088 Btu/ft-°F-h) for details at least as good as "approved details," 0.10 W/m2-K (0.018 Btu/ft-°F-h) for details in new construction and 0.15 W/m2-K (0.026 Btu/ft-°F-h) for existing buildings with internal insulation. The defaults can be overridden if detailed calculations are performed.
Poland	Two different default U-factor increments of 0.05 W/m2-K (0.0088 Btu/ft-°F-h) and 0.15 W/m2K (0.026 Btu/ft-°F-h) are available, the greater for walls with a cantilevered balcony. The defaults can be overridden if detailed calculations are performed.
United Kingdom	A default U-factor increment of 0.15 W/m2-K (0.026 Btu/ft-°F-h) is added to the entire surface of the building unless the only details used were drawn from "accredited construction details" catalogues, in which case 0.08 W/m^2-K (0.014 Btu/ft-°F-h) may be used. Another option is to use an "Enhanced Construction Details" document, which actually provides psi values for the details.

The U-factor increment is by far more common than default Ψ-values, likely because of its simplicity. In almost all cases, the default value can be overridden by performing detailed calculations on all TBs and, sometimes, various levels of default values are available for different prescriptive paths. As explained in Section 1.1, the default value is generally worse than the value computed by detailed calculation (Citterio, Cocco, and Erhorn-Kluttig 2008).

2.1.2 Catalogues

Detail catalogues (or "atlases") are growing in popularity as a method to treat TBs, especially in Europe. Their approaches can be divided into "compliance," "prediction," and both. Prediction catalogues provide a detail's ψ-value or χ-value. Temperature index is often included as well. For instance, if a user was attempting a more accurate energy model of a building, such a catalogue would greatly simplify the task. Ideally, a designer would do this to prove that a building's TBs do not increase an envelope's U-factor beyond an allowed maximum, but most standards and guidance do not require this treatment (see Section 2.2.3).

Compliance catalogues are those that provide approved details only. A designer would chose from these details either because it is prescribed by a standard or because choosing them grants some reward, such as the lower default values listed in Table 2. According to ASIEPI Report P198, "Software and Atlases for Evaluating Thermal Bridges":

> The latter approach is an important evolution in the way of dealing with thermal bridges. This change started about a decade ago. Focus has been shifting from ever more systematic and detailed analysis of thermal bridges to their avoidance as much as reasonably possible. A detailed quantification of thermal bridges is then usually considered as no longer necessary, and the designer is dispensed with this time-consuming task, a task that by itself does not solve the thermal bridge. This important new development will be presented in a future ASIEPI Information Paper (Tilmans and Orshoven 2010).

As such, even where a prediction catalogue is desired, it is beneficial to also gather approved details for certain standards, in case future guidance aims to take the prescriptive approach allowed by use of compliance catalogues. Some significant catalogues are briefly reviewed here.

2.1.2.1 Simple catalogues: ISO 14683 and ASHRAE Handbook of HVAC Applications

Some catalogues attempt to be general by providing little detail and only rough values. Chapter 44 of the ASHRAE Handbook of HVAC Applications (ASHRAE 2011a), for instance, gives a small catalogue of three sets of "preferred" and "not preferred" details, which address thermal and moisture issues. A more extensive, but still very simple example, is ISO 14683 "Thermal Bridges in Building Construction – Linear Thermal Transmittance – Simplified Methods and Default Values" (ISO 2007a). The details provided, however, are extremely simplistic and the ψ-values are intentionally on the high side. This makes them difficult to use in any framework other than a standard that requires default values for each TB type, rather than for the whole-building U-factor, as in the case of Denmark's building code (Tilmans and Orshoven 2010; Citterio, Cocco, and Erhorn-Kluttig 2008).

2.1.2.2 ASHRAE research project 1365: Thermal performance of building envelope details for mid- and high-rise buildings (ASHRAE 2011b)

RP-1365 provides ψ-values, χ-values, or U-factors for 40 details common in US commercial construction. The behavior of these values is also given

as a function of the conductivity of the insulation layer (though not the thickness, which is considered constant). It is the first major project in the United States to treat TBs using linear and point thermal transmittance. Results are based on sophisticated 3-D simulation; choice of contact resistances and film coefficients is based on extensive validation against a library of existing experimental results for 28 wall types, with references listed in Table 3.

The details presented are relevant to US commercial construction; they are also complex enough that many other quantification methods would fail. Particular attention is paid to steel framing in the clear wall, including the Z-girts used to support insulation or cladding often ignored in ASHRAE 90.1 calculations. Also included are mid-floor slab/wall intersections, flat-roof/parapet intersections, and window issues. Despite the fact that RP-1365 focuses on commercial construction not common in the Army, it would be wise to avoid redundancy with RP-1365 in any work produced by the current project.

Table 3. The studies containing the guarded hot box test results used to calibrate the numerical model used in ASHRAE RP-1365.

Desjarlais, A. O., and A. G. McGowan. 1997. Comparison of experimental and analytical methods to evaluate thermal bridges in wall systems. Proceedings of the 3rd ASTM Symposium on Insulation Materials: Testing and Applications, 3d vol. American Society for Testing and Materials (ASTM) STP 1320.
Brown, W. C., M. C. Swinton, and J. C. Haysom. 1998. A technique for calculating the effective thermal resistance of steel stud walls for code compliance. ASHRAE Transactions, Annual meeting in Toronto.
Kosny, J. and P. Childs. 2000. Dynamic Guarded Hot Box Measurements for RASTRA Wall Form System with Expanded Polystyrene-Beads. Oak Ridge National Laboratory Buildings Technology Center. (Part of ASHRAE Research Project 1145-RP final report prepared by Enermodal Engineering 2001).
Brown W. C., and D. G. Stephenson. 1993. Guarded hot box measurements of the dynamic heat transmission characteristics of seven wall specimens, Part II. ASHRAE Transactions. 99(2). Paper 3684. (ASHRAE 515-RP).
Kosny, J. P., J. E. Christian, E. Barbour, J. Goodrow. 1994. Thermal Performance of Steel-Framed Walls. CRADA Final Report, CRADA Number Oak Ridge National Laboratory (ORNL) 92-0235.

2.1.2.3 Details for passive houses: A catalogue of ecologically rated constructions

This work, printed in German and English, is perhaps the most complete catalogue for very high-performance details, all of which are designed to meet Passive House standards in Central European climate conditions. In addition to providing ψ-values, χ-values or U-factors for each detail, the long-term hygrothermal performance has been verified using a dynamic heat and moisture model. This catalogue also addresses fire protection and sound insulation, and the materials' ecological impacts and manufacturing emissions. The quantitative information for each detail is accompanied by thorough construction and maintenance notes. A complete introduction to Passive House design methods is also included (Pokorny et al. 2009).

2.1.2.4 UK catalogues of accredited construction details (ACDs) and enhanced construction details (ECDs) (UK Department for Communities and Local Government Undated)

The United Kingdom's ACDs give designers an efficient way to mitigate thermal bridges without excessive effort. If the details from the ACDs are used, the U-factor increment penalty, discussed in Section 2.1.1.6, is 0.08 W/m2-K (0.014 Btu/sq ft-°F-h) rather than the default 0.15 W/m2-K (0.026 Btu/sq ft-°F-h). The ECDs are higher performing that the ACDs and can be used for prediction in addition to compliance. (That is, they supply ψ-values and χ-values.) When using these details, building codes allow computing the actual TB impact rather than using either of the default values.

2.1.2.5 Other catalogues

ASIEPI Report P198, "Software and Atlases for Evaluating Thermal Bridges," provides a table of catalogues (Tilmans and Orshoven 2010), adapted Table 4, including the reference number from the original report.

2.1.3 Testing

Hot-box testing by American Society for Testing and Materials (ASTM) Standard C1363-11 can measure the heat flux through large, flat wall assemblies. As a way to quantify a unique TB, it is generally too expensive, but it provides excellent data for model validation. Table 3 lists the compilation of hot-box test results used by ASHRAE RP-1365 for calibrating their model (ASHRAE 2011b).

Table 4. Construction detail catalogues, adapted from Tilmans and Orshoven (2010); bracketed reference number refers to original report.

Title	Language	Number of details	Types of buildings	Flexibility	Integral part of EP regulation	In use in Member State
EN ISO 14683: Thermal bridges in building construction – Linear thermal transmittance – Simplified method and default values, [18]	English	76	residential	no	no	Europe
KOBRA v3.0w, [19]	French, Dutch	> 3000	all types	yes	no	Belgium
Construction details – Thermal Bridges, [20]	Czech	56	all types	yes	no	Czech Republic
U-values 2003, [21]	Danish	> 2000	all types	no	no	Denmark
Danish Standard 418. Calculation of heat loss from buildings, [22]	Danish	> 275	all types	no	yes	Denmark
2005 thermal regulation, TH-U 5/5 thermal bridges for new buildings, [23]	French	> 10000	new buildings	yes	yes	France
TH-U 5/5. Thermal bridges for existing buildings, [24]						
Thermal bridge atlas for wooden constructions, [25]	German	> 3000	wooden constructions (wall, ceiling, roof)	yes	no	Germany
Thermal bridge atlas for masonry constructions, [26]	German	> 8000	masonry constructions with/ without insulation (incl. ceiling, roof)	yes	no	Germany
Building Research Design Sheet 471.017, Thermal bridges – Tables with ψ-values, [27]	Norwegian	23	all types	yes	no	Norway
Electronic atlas of thermal bridges ("Kuldebroatlas"], [28]	Norwegian	> 23	all types	yes	no	Norway
Thermal bridges – Calculation, ψ-values and influence on energy consumption. Project report 25-2008, [29]	Norwegian	31	all types	yes	no	Norway
Thermal Bridges Catalogue Traditional Buildings, [30]	Polish	> 100		no	no	Poland
Thermal bridges. Basics, simple formula, heat loss, condensation, 100 calculated building details, [31]	German	100	all types	no	no	Austria
Thermal bridges in Constructive Elements Catalogue for Building Technical Code, [32]	Spanish	> 300	all types	yes	yes	Spain
Building regulation STR 2.05.01:2005 "Thermal technique of the building envelope", Annex 7, [33]	Lithuanian	200	all types	yes	yes	Lithuania
Thermal bridges catalogue, [34]	German	200	all types	yes	no	Switzerland
Code for thermal energy performance calculation of building elements C107/3-2005, [35]	Romanian	> 1500	all types	no	yes	Romania
Limiting Thermal Bridging and Air Infiltration. Acceptable Construction Details, [36]	English	150	all types	yes	yes	Ireland
Accredited construction details, [37]	English	150	dwellings	no	yes	United Kingdom
Accredited construction details (Scotland), [38]	English	130	dwellings	no	yes	United Kingdom
Enhanced Construction Details, [39]	English	47	dwellings	no	no	United Kingdom
Thermal bridge catalogue, [40]	German	323	all types	yes	no	Germany
BuildDesk [1], [41]	Polish	> 100	all types	no	no	Poland
CERTO [1], [42]	Polish	> 100	traditional and concrete panels	no	no	Poland
Thermal bridge catalogue for renovation and retrofit measures to prevent mould, [43]	German	92	all types, renovation	yes	no	Germany

2.1.1 Numerical methods

Numerical methods discretize a problem's geometry and solve, at a minimum, the heat diffusion equation within the boundary conditions specified. Where appropriate, convection and radiation equations can also be solved; often, they are just treated as conduction and a conductivity correlation is applied. Boundary conditions are typically chosen to represent interior and exterior temperatures and assumed convection heat transfer coefficients (i.e., interior and exterior convection is not directly modeled when simulating TBs). This section reviews available numerical heat transfer programs and summarizes ISO Standard 10211 "Thermal Bridges in Building Construction – Heat Flows and Surface Temperatures – Detailed Calculations" (207a), which governs numerical calculation of TB impacts.

2.1.1.1 Heat transfer simulation software

A number of heat transfer programs were evaluated to verify that their capabilities fulfill the modeling needs of this project. A minimum criterion was that the program include a conduction heat transfer solver. Other criteria included:

- Is it free?
- 3-D modeling, or 2-D only?
- Compatible with Windows OS?
- Able to model moisture transfer as well?
- Suitable for parallel computing?
- Able to model materials with non-linear properties?
- Capable of modeling processes other than heat conduction directly ("multiphysics")?
- Inputs and outputs directly to and from MATLAB?
- User can define free-form geometry, not just orthogonal blocks?
- Validated by ISO Standard 10211?
- Allows cross-section import?
- Allows batch runs?

The reviewed programs were:

1. **OpenFOAM**. Open Field Operation and Manipulation (OpenFOAM) is a free, open source computational fluid dynamics (CFD) software. It can solve complex fluids flows involving chemical reactions, turbulence and heat transfer, solid dynamics and electromagnetic. It contains library func-

tionality for turbulence models, transport/rheology models, thermophysical models, Lagrangian particle tracking and reaction kinetics. One of the most important features is that it is "open;" the users have complete freedom to customize and extend its existing functionality.
Disadvantages: OpenFOAM is not validated by ISO 10211, and its heat transfer solver is oriented more toward the heat transfer at a solid-liquid interface than conduction through solids. Furthermore, the software is not designed for a Windows operating system and has a steep learning curve, which is to be expected of a package so flexible.

2. **Elmer.** Elmer is an open source, multiphysics finite element analysis package. It processes partial differential equations in a discrete form, handles coupled systems, non-linearities and time-dependencies, and generates output data for post processing and visualization. Elmer's capabilities include heat transfer, fluid mechanics, electromagnetics, acoustics, quantum mechanics, and earth science. It has mesh capabilities and similarly, it can import mesh data files from ANSYS, Comsol, Gmsh, and other commercial FEA-meshing software. Simulation can be performed in parallel computing.
Disadvantages: Relatively little support is available compared to commercial software. Elmer is not validated by ISO 10211. Like OpenFOAM, Elmer has a steep learning curve.

3. **COMSOL.** COMSOL is a commercial multiphysics package that operates using module packages containing the algorithms and equations pertinent to the field of physics. These include: AC/DC, Heat Transfer, Structural Mechanics, Geomechanics, Acoustics, Fluid Dynamics, Chemical Reactions, Fuel Cells and more. Predefined multiphysics-application templates solve many common problem types. Users has the option of choosing different physics and defining the interdependencies, even going so far as to define their own partial differential equations. COMSOL has the capability to establish interfaces with recognized Computer-Assisted Design (CAD) and mesh software, which can simplify the process of the model construction. It is amenable to parallel computing and is validated by ISO 10211.
Disadvantages: COMSOL is extremely expensive; new capabilities often require purchasing new packages, and the license must be renewed annually.

4. **WUFI2-D.** WUFI, which stands for "Transient Heat and Moisture Transport" in German, calculates simultaneous heat and moisture transport in one- or two-dimensional building components. It takes into

account thermal conduction, enthalpy flows through moisture movement with phase-change, short-wave solar radiation, nighttime long-wave radiation cooling, vapor diffusion, solution diffusion and liquid transport mechanism such as capillary conduction.
Disadvantages: WUFI2-D works only with 2-D models and is not validated by ISO 10211.

5. **ANSYS Multiphysics.** ANSYS Multiphysics is capable of structural, thermal, fluid and electromagnetic analysis. These difference physics types can also be coupled together to solve complex multi-physical scenarios. It handles nonlinear materials properties (time dependent, temperature dependent, etc.), transient 3-D analysis. High-performance computing capability is available with the purchase of an additional module. Abundant support is available, including online assistance, examples and training sessions.
Disadvantages: An ANSYS license is expensive and must be renewed yearly. ANSYS also has a steep learning curve and is not validated by ISO 10211

6. **Trisco.** Trisco is a heat transfer modeling software made for building analyses. It can be coupled with several modules from the same developer, which, when combined, can solve complicated building heat transfer scenarios. It can also perform 3-D-transient analyses. Trisco automatically calculates ψ-value based on internal or external dimensions. It can import 2-D cross sections and build 3-D models quickly.
Disadvantages: Trisco does not handle nonlinear material properties. Depending on the module to be used, it may or may not handle transient, 3-D, and free-form drawing capabilities. As a consequence, several product licenses must be purchased to get more complete analysis capabilities.

7. **HEATING 7.2.** HEATING 7.2 is a finite difference conduction heat transfer code that can solve steady-state and transient heat conduction problems in 3-D and in multiple coordinate systems. Nonlinear, time and temperature dependent material properties are permitted. Some limited radiation problems can also be solved.
Disadvantages: HEATING 7.2 lacks a graphical user interface and is difficult to use.

8. **PLM with TMG Maya.** NX TMG Thermal Analysis (TMG) uses the finite element method. TMG can perform nonlinear and transient 3-D heat transfer analysis including conduction, radiation, convection, fluid flow,

and phase change.
Disadvantages: Full software capabilities are available only after purchasing several modules. For example, the Thermal/fluid coupled analysis (convective heat transfer) requires the combination of TMG Thermal Analysis module with the TMG-Flow module.

9. **FLUENT.** ANSYS FLUENT (ANSYS 2012) is CFD software that can be used for heat transfer problems as well. Sophisticated radiation and convection are also available. Nonlinear material properties and phase change is allowed.
Disadvantages: FLUENT has a steep learning curve and an expensive, annually renewed license.

10. **THERM.** THERM was developed by the Department of Energy (DOE) Lawrence Berkeley National Laboratory. It can simulate 2-D conductive heat transfer in building windows, walls, foundations, roofs, and doors. Convection in cavities, such as in window frames, is treated as conduction with conductivity derived from geometry correlations. The numerical approach is based on the finite element method, so the software can model a cross section with complex geometries.
Disadvantages: Scenarios such like 3-D corners (wall-wall-roof intersections) cannot be modeled in THERM because it only supports 2-D analysis. It has no CAD import feature, and no transient and nonlinear property capabilities. THERM has an automatic mesh refinement tool, which does not allow the user to specify the regions of desired mesh increase.

11. **HEAT 3.** HEAT3 is a PC-program for three-dimensional transient and steady-state heat conduction. The heat equation is solved with explicit forward finite differences. The successive over-relaxation technique is used in the steady-state case. One important restriction is that the problem has to be described in a rectangular mesh, i.e., all boundary surfaces are parallel to one of the Cartesian coordinate planes. Applications include: General heat conduction problems, TBs, U-factor calculation for building construction parts, surface temperature estimation, calculation of heat losses to the ground from a building, analysis of floor heating systems and analysis of window frames.
Disadvantages: HEAT 3 only accepts rectangular components and does not accept time dependant heat-flux boundary conditions or temperature dependant material input. Convection and radiation are not handled.

Table 5 summarizes how well each of the reviewed programs matched the first seven criteria. Ultimately, Heat3 was chosen as one of the simulation packages for use on this project, owing to its low cost, ease of use, and ability to achieve rapid turn-around on custom details.

2.1.1.2 Validation of software

Validation of a numerical heat transfer tool for use in TB analysis is carried out via ISO 10211 Standard Appendix A Cases 1, 2, 3, and 4. In general, these four cases are examples of components in building envelopes subjected to conductive heat transfer; the desired output is surface temperatures and heat flows. For all the cases, the difference between the temperatures in the standard and those calculated shall not exceed 0.1 °C. For cases 2, 3, and 4, the difference between the heat flows in the standard and those calculated should not exceed 1%. Modeling these cases can also be used to learn a software package and test the user's understanding. The four validation cases are described here, along with the results produced by Heat3 (ISO 2007a, BLOCON 2005).

Table 5. Summary of heat transfer modeling software.

	Free License?	3-D Modeling?	Windows Compatible?	Moisture Transfer?	Parallel Computing?	Nonlinear Materials?	Multiphysics?	Matlab direct I/O?
OpenFOAM	Y	Y	N	Y	Y	Y	Y	N
Elmer	Y	Y	Y	Y	Y	Y	Y	N
COMSOL	N	Y	Y	Y	Y	Y	Y	Y
WUFI 2-D	N	N	Y	Y	N	N	N	N
ANSYS	N	Y	Y	Y	Y	Y	Y	Y
Trisco	N	Y	Y	Y	N	N	N	N
HEATING 7.2	N	Y	Y	N	Y	Y	N	N
PLM/TMG	N	Y	Y	Y	Y	Y	Y	Y
FLUENT	N	Y	Y	Y	Y	Y	N	N
Therm	Y	N	Y	N	N	N	N	N
Heat3	N	Y	Y	N	N	N	N	N

Case 1: Heat transfer through a half square column/half of a square plate

This scenario (shown in Figure 9) has an analytical solution to which we can compare our results. The left image of Figure 9 represents the half square column, with 28 crosses indicating the nodes. The right image of Figure 9 shows the temperature from the analytical method. The temperature results from the method in question (Table 6) must be compared against those values for validation.

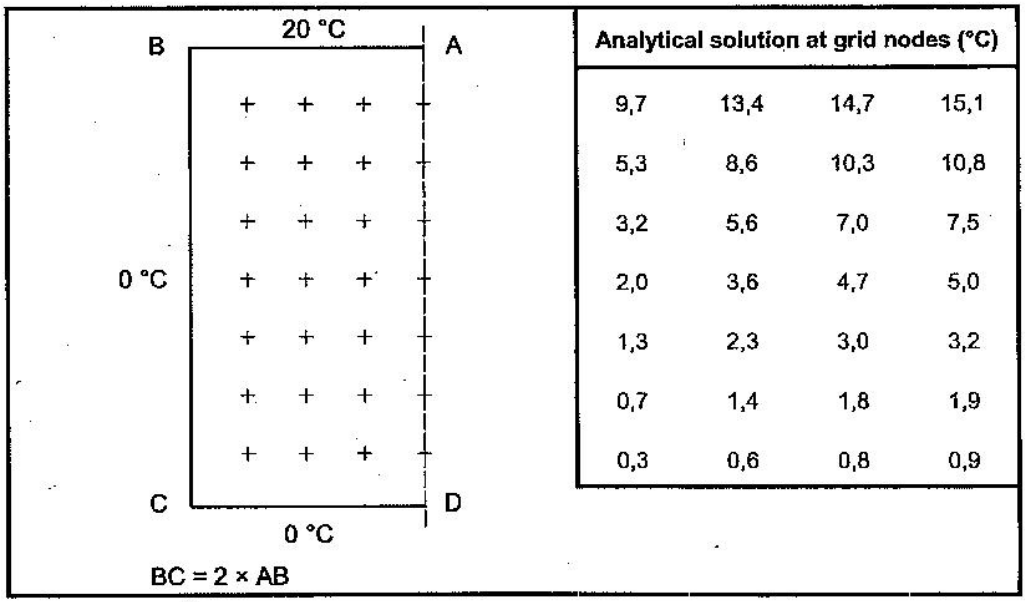

Figure 9. ISO 10211 Appendix A Case 1.

Table 6. HEAT2/3 ISO 10211 Appendix A Case 1 node temperature results.

9.66	13.38	14.73	15.09
5.25	8.64	10.32	10.81
3.19	5.61	7.01	7.47
2.01	3.64	4.66	5.00
1.26	2.31	2.99	3.22
0.74	1.36	1.77	1.91
0.34	0.63	0.82	0.89

2.1.1.3 Case 2: Two-dimensional model consisting of several materials

In Case 2, the two-dimensional model consists of a rectangle with sides AB, BI, IH, and HA (Figure 10). In Figure 10, the dashed lines AH and BI represent adiabatic surfaces (no heat transfer). Table 7 lists temperature and heat flow results at the indicated nodes. Table 8 lists the HEAT2/3 temperature and heat flow results. These results were computed using a total of 25000 nodes to define the geometry.

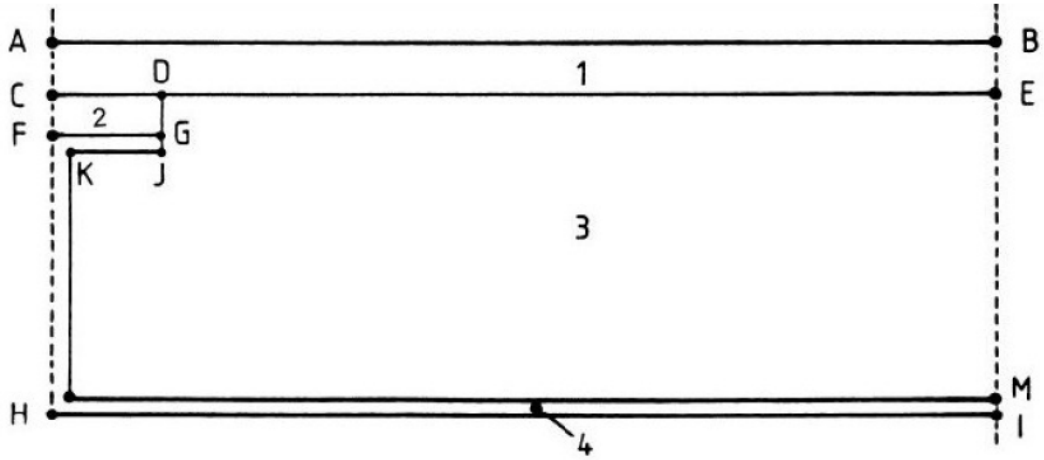

Figure 10. ISO 10211 Appendix A, Case 2.

Table 7. ISO 10211 Appendix A, Case 2, temperature and heat flow results at the indicated nodes.

Temperature °C		
A: 7.1		B: 0.8
C: 7.9	D: 6.3	E: 0.8
F: 16.4	G: 16.3	
H: 16.8		I: 18.3
Total Heat Flow Rate: 9.5 W/m		

Table 8. HEAT2/3 Temperature and heat flow results for ISO 10211 Appendix A Case 2.

Temperature °C		
A: 7.06		B: 0.7613
C: 7.8926	D: 6.2949	E: 0.8275
F: 16.4	G: 16.325	
H: 16.765		I: 18.333
Total Heat Flow Rate: 9.492 W/m		

2.1.1.4 Case 3: An example of a three-dimensional heat transfer section

The Case 3 model consists of a three-dimensional wall/wall intersection and a floor slab with an integrated representation of a balcony (Figure 11). This model has three temperature boundary conditions, indicated by the Greek letters α, β and γ.

Tables 9 and 10 list thermal coupling coefficients according to ISO 10211 and Heat 3, respectively. Tables 11 and 12 list surface temperature factors according to ISO 10211 and Heat 3, respectively.

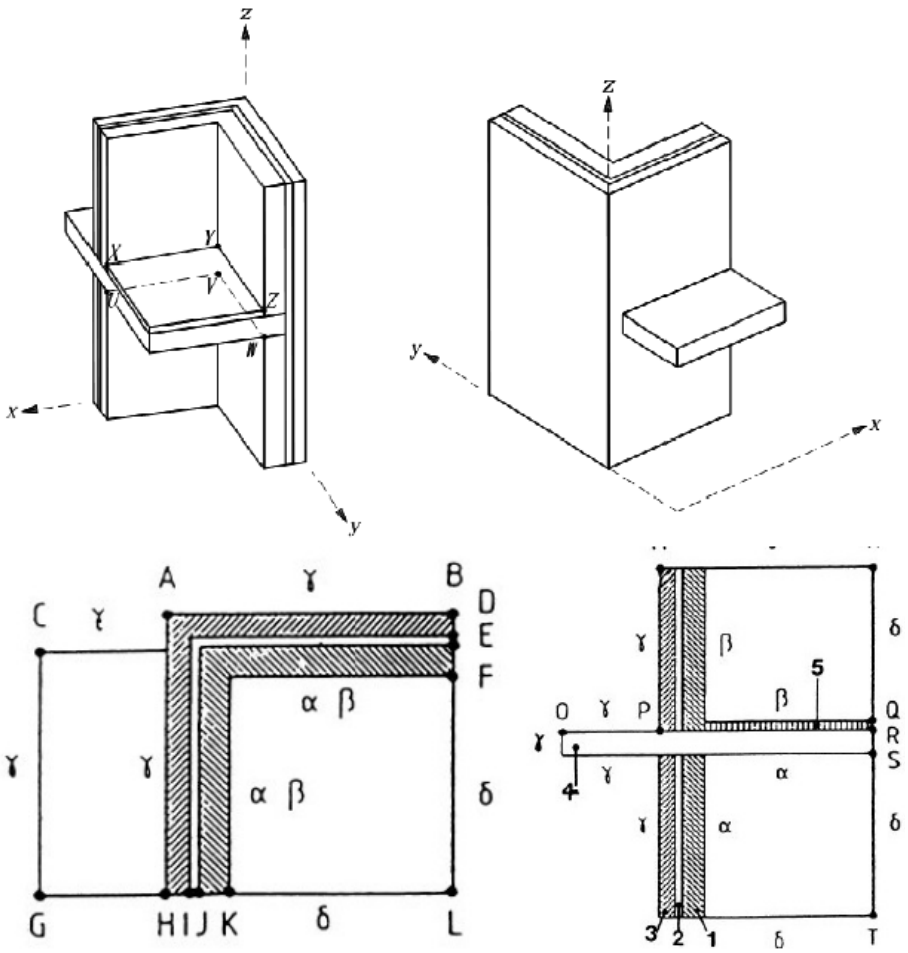

Figure 11. ISO 10211 Appendix A, Case 3 model schematic.

Table 9. Thermal coupling coefficients (W/K) results according to ISO 10211 Appendix A, Case 3.

ISO 10211	Γ	α	β
γ	-	1.781	1.624
α	1.781	-	2.094
β	1.624	2.094	-

Table 10. Thermal coupling coefficients (W/K) according to HEAT3 using 370000 nodes.

ISO 10211	Γ	α	β
γ	-	1.7804	1.6238
α	1.7804	-	2.0931
β	1.6238	2.0931	-

Table 11. Surface temperature factors according to ISO 10211 Appendix A, Case 3.

ISO 10211	gγ	A	β
gγ	1.000	0.000	0.000
gα	0.378	0.399	0.223
gβ	0.331	0.214	0.455

Table 12. HEAT3 computed surface temperature factors using 1100000 nodes.

ISO 10211	gγ	gα	gβ
γ	1.0000	0.0000	0.0000
α	0.3770	0.4003	0.2221
β	0.3311	0.2146	0.4545

The heat flow between pairs of environments is given here, with the ISO 10211 result given in brackets:

(β) and (γ) 24.357 W [ISO 10211: 24.36] difference: 0.0%

(β) and (α) 10.467 W [ISO 10211: 10.47] difference: 0.0%

(α) and (γ) 35.608 W [ISO 10211: 35.62] difference: <0.03%

The overall heat flow from the internal to the external environment is:

59.965 W [ISO 10211: 59.98] diff <0.03%

2.1.1.5 Case 4: Example of three-dimensional TB consisting of an iron bar penetrating an insulation layer.

For Case 4, the temperature difference between the lowest internal surface temperatures given in the standard and calculated by the method being validated should not exceed 0.005 °C.

The Case 4 three-dimensional model consists of an insulated wall with a penetrating bar (Figure 12).

Table 13 lists results using ISO 10211 Appendix A, and HEAT3 simulation using 840000 nodes. HEAT3 results shows that Case 4 complies with ISO 10211 Standard by having an exterior side maximum surface temperature difference of less than 0.005 °C (actually, 0.003 °C). Also, the heat flow difference is 0.1%, which is lower that the specified value of 1%.

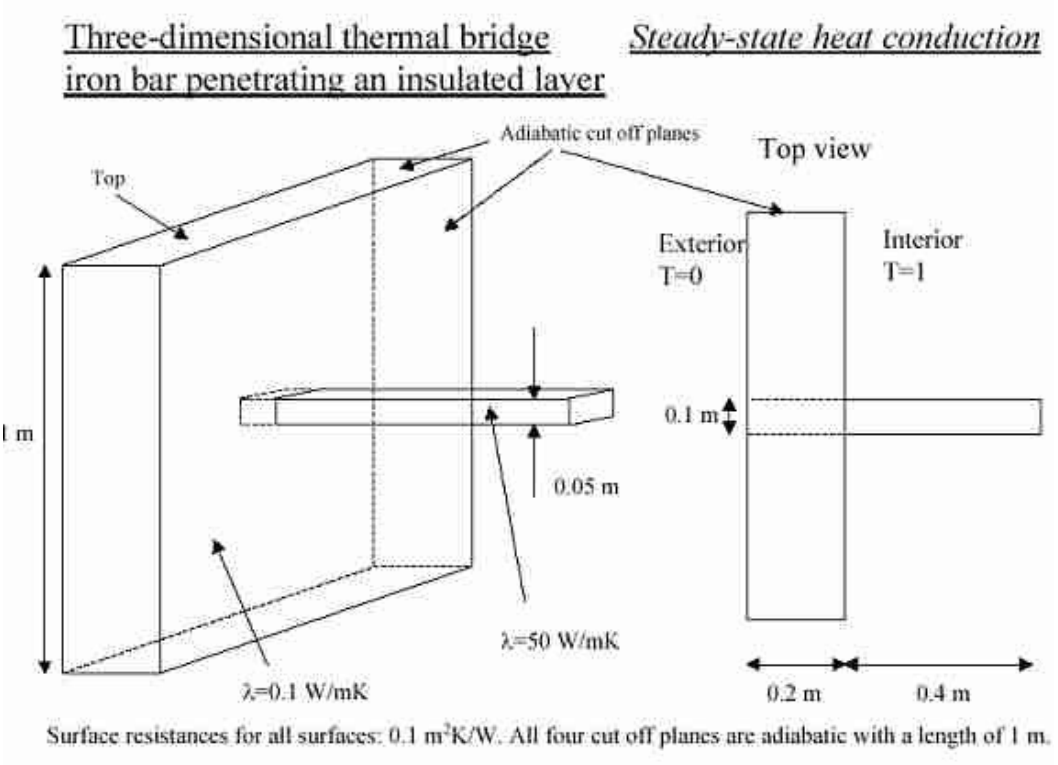

Figure 12. ISO 10211 Appendix A, Case 4 model schematic. Three-dimensional model consisting of an insulated wall with a penetrating bar.

Table 13. ISO 10211 Appendix A, Case 4 Results along with HEAT3 simulation results using 840000 nodes. HEAT3 results shows that it complies with ISO 10211 Standard by having an exterior side maximum surface temperature difference of less than 0.005 °C (actually, 0.003 °C). Also, the heat flow difference is 0.1%, which is lower that the specified value of 1%.

	ISO 10211 Specified Value	HEAT3 Result
Heat Flow	0.540 W	0.5394 W
Highest surface temperature on the external side	0.805	0.8047

2.1.2 Modeling calculation procedures

In addition to specifying the minimum requirements that an algorithm or software must meet, ISO Standard 10211 and 13770 also provide methodologies, guidance, and equations to be used to construct TB models for several scenarios, including ground heat conduction. Appendix A to this report briefly summarizes these methodologies, guidance, and equations.

2.2 Current treatment of TBs

The following sections discuss repeating and non-repeating TBs, their treatment by current methods, and coverage by codes and standards.

2.2.1 Repeating TBs

Repeating TBs occur in the “clear wall” —those planar areas that have regularly spaced structural components and that are free of windows, doors, and other irregularities. The classic example is the stud, 16 or 24 in. on center, bridging between the interior and exterior sheathing. Figure 8 (p 15) displays the results from a numerical heat transfer model for an example repeating TB. Other examples include fasteners, mortar joints, CMU webbing, and brick ties.

2.2.1.1 Structural members

In both the United States (ASHRAE 2007) and Europe (ISO 2007c), standards handle repeating structural TBs by averaging over the clear-wall area. ASIEPI Report P188, “Thermal Bridge Guidance Principles,” agrees with this approach (Schild and Blom 2010). This is not typically accomplished using numerical methods, as in Figure 8, but with some of the simplified methods discussed above, such as parallel paths, isothermal

planes, or one of the zone methods. In this way, ASHRAE 90.1 and ASHRAE 189.1 incorporate the effects of structural TBs, such as studs, rafters and CMU webbing (ASHRAE 2007, ASHRAE 2009b).

Where the percentage of the wall assumed to be framing, or "framing factor" is valid, using the results of simplified calculations and area averaging taken from published tables is a reasonable approach. For instance, the hot-box testing on concrete block clear walls has resulted in U-factors within 10% of results using the very simple isothermal planes method (ASHRAE 2009a). A recent four-part study commissioned by ASHRAE provides an excellent treatment of predictable, repeating TBs in metal roof construction where fiberglass insulation hangs over and is compressed by purlins (Choudhary and Kasprzak 2010a, 2010b; McBride and Gavin 2010; Christianson 2010). The project developed simple but accurate U-factor estimates validated by experiments and numerical simulations for a common type of metal building construction.

Unfortunately, many US codes do not require treatment of repeating TBs at all; the code requirement is often based on "nominal" insulation values, which are, in turn, based on the R-value of insulation in the stud cavities, not of the overall assembly (Lstiburek 2007, Kosny et al. 2007).

When repeating, clear-wall TBs are regulated by US building codes, and they are addressed by table-lookups that assume known, regular stud spacing (ASHRAE 2007). For instance, in the table entry for a wall with 1.5 in. wide studs 16 in. on center, the framing factor, might be taken as 1.5/16 = 9.4% (sometimes the sill and header plates are also included). One widely understood issue that has yet to be remedied is that virtually no wall is actually built this way. That is, it is very uncommon to see substantial stretches of wall without windows, doors, corners or intersections with interior walls, all of which involve significant additional framing that is no longer evenly spaced.

The Public Interest Energy Research Program found that residential buildings in California have an average framing factor of 27%, which is much higher than 9.4% or even the 12.2% that would be used if one included sills and headers (California Energy Commission 2001). Walls with this framing factor, built with 2X4 lumber, when tested in experimentally validated simulations, result in an average R-value of 1.6 m^2-K/W (9.3 sq ft-°F-

h/Btu), while the center-of-cavity R-value is 2.46 m²-K/W (13.95 sq ft-°F-h/Btu), and the R-value, assuming a 9.4% framing factor, would be 2.24 m²-K/W (12.7 13.95 sq ft-°F-h/Btu) (Kosny et al. 2007). Kosney and Christian (2001) refer to this disparity as the difference between the "clear-wall R-value" and the "whole-wall R-value" (Kosny and Christian 2001).

Even disparities this high are often exceeded, especially in steel construction, where the high thermal conductivity of the steel helps heat "bridge" around the cavity insulation much more effectively (as in Figure 8). Take, for instance, the realistic wall used by Bombino (2010): a wall with studs nominally spaced 24 in. on center with R_{SI}-3.7 m²-K/W (21 sq ft-°F-h/Btu) batt insulation, with 4x4-ft window every 8 ft. There is a double header plate to resist sagging from the above floor slab, a double stud at each window jamb, and double nested studs at window sills and heads. This adds up to 57.6% of opaque area. An area-weighted approach predicts a U-factor of 1.4 W/m²-K (0.26 Btu/sq ft-°F-h) for this wall, corresponding to R_{SI}-0.69 m²-K/W (3.9 sq ft-°F-h/Btu).

Photo used with author's permission from (Bombino and Finch 2010).

Figure 13. Photo of steel stud wall "where modified per the structural drawings" but where code compliance calculations were done without taking into account the additional framing.

Meanwhile, the U-factor in Table A3.3 of ASHRAE 90.1 of a nominal 2X6 wall with steel studs 24 in. on center, is 0.511 W/m²-K (0.090 Btu/sq ft-°F-h) or R_{SI}-1.95 m²-K/W (11.1 sq ft-°F-h/Btu). By failing to realistically consider the additional framing in this wall, a designer would underestimate the heat transfer by 60%.

Bombino (2010) provides another example in the case of a steel stud wall where "the architectural drawings depict the stud spacing at 16 in. on center … except where modified per the structure drawings" as in Figure 13. The vertical framing alone accounts for 71% of the wall area and, when simulated using THERM 5.2, results in a U-factor of 0.45 W/m²-K (0.08 Btu/sq ft-°F-h) or R_{SI}-2.20 m²-K/W (12.5 sq ft-°F-h/Btu). The majority of the insulation can be attributed to the R_{SI}-1.8 m²-K/W (10 sq ft-°F-h/Btu) exterior XPS insulation; simply summing the air film resistance, wallboard, and exterior XPS insulation leads to R_{SI}-2.11 m-K/W (12 sq ft-°F-h /Btu), indicating that the batt insulation achieves very little, despite being included in most code calculations. Indeed, Table A3.3 in ASHRAE Standard 90.1 would assign R_{SI}-3.43 m²-K/W (19.5 sq ft-°F-h /Btu) to such a wall if the user simply considers the stud spacing to be 16 in. on center. The designer, in this case, would underestimate heat transfer by 36%; the value would be much larger if not for the exterior insulation (ASHRAE 2007, Bombino and Finch 2010).

To the credit of ASHRAE 90.1 and ASHRAE 189.1, the standards are meant more for compliance than for accurate prediction. For instance, the tables require continuous exterior insulation for steel-framed walls in almost every climate, which mitigates TBs to some degree, whether or not the required R-value is actually achieved. This is certainly superior to the assumption that a wall with R-19 batts achieves R-19, no matter the framing factor or conductivity of the studs.

The examples above, however, indicate discrepancies severe enough that the walls in question should not comply, even though the standard has successfully encouraged basic use of exterior insulation. In the standard, there is in fact a distinction between walls that constitute real "clear wall," likely to be very rare in the actual building, and walls that contain too many repeating TBs. Section A1.2 of ASHRAE 90.1 describes the situation:

> If the building official determines that the proposed construction assembly is not adequately represented in Sections A2 through A8, the applicant shall determine appropriate values for the assembly using the assumptions in Section A9. An assembly is deemed to be adequately represented if:
>
> a. the interior structure, hereafter referred to as the base assembly, for the class of construction is the same as described in Sections A2 through A8 and
>
> b. changes in exterior or interior surface building materials added to the base assembly do not increase or decrease the R-value by more than 2* from that indicated in the descriptions in Sections A2 through A8.

As an example, Section A3.3 Steel-Framed Walls goes on to say:

> For the purpose of Section A1.2, the base assembly is a wall where the insulation is installed within the cavity of the steel stud framing but where there is not a metal exterior surface spanning member …

ASHRAE 90.1 Table A3.3, and A9.2B, which it is based on, contain only values for studs at 24 in. on center and at 16 in. on center. A designer encountering the example above would find that a 57.6% framing factor is not available in this table, but, as this wall is still "nominally" 24 in. on center, most applicants would use A3.3 for such a wall without complaint from the building official. The analysis required to determine whether or not the wall differs by R_{SI}-0.35 m²-K/W (2 sq ft-°F-h /Btu) or more is seldom carried out. In the rare case that an applicant uses Section A9 to determine a more accurate U-factor, that applicant may do so only "if approved by the building official." A9 does indeed contain methods that adequately treat the majority of repeating TBs, including:

- testing
- series addition of R-values
- parallel paths
- isothermal planes
- numerical methods
- zone methods
- modified zone methods.

One or more of these methods is permitted for each class of construction listed in ASHRAE 90.1 Section A9.

---

* This value is in standard units, i.e., 2 hr-ft²-°F /Btu, equivalent to an R_{SI}-value of 0.35 m²-K/W

2.2.1.2 Non-structural repeating thermal bridges

In addition to structural members, repeating TBs also include point TBs such as brick ties and fasteners. Conventional wisdom considers these insignificant, but they deserve a second look as envelope performance expectations rise. Christensen (2010) performed numerical simulations that examined fasteners in a 2X6 wall with 1.5 in. exterior insulation. Of primary concern is the siding nails that penetrate the continuous insulation. The wall's U-factor was estimated with the parallel paths method and with sophisticated finite element methods. The latter technique was used to give results both with and without siding nails and drywall screws. Including 3-D effects shows a similar change in expected U-factor as including fasteners does. In insulation levels approaching Passive House standards, a 3.3-12.0% reduction in R-value occurs when the impact of fasteners is included, with the vast majority of the impact from siding nails. For instance, a Parallel Path computed wall thermal resistance of R-29.24 with a 30% of framing factor can drop to R-25.73. The work developed a simple but robust correction factor for the parallel paths calculation method, but only guarantees its validity in walls of similar construction with similar quantities of fasteners (Christensen 2010).

In general, non-structural repeating TBs are covered by neither ASHRAE 90.1 nor ASHRAE 189.1. Some of the tables for clear-wall U-factors in 90.1 capture the impact of clips or girts penetrating insulation on concrete walls, but brick ties and fasteners are ignored. ASHRAE RP-1365, on the other hand, provides the results of detailed simulations for several clear walls, including the impact of continuous and broken Z-girts and brick ties; fasteners are, as usual, not explicitly considered (ASHRAE 2011b, ASHRAE 2007, ASHRAE 2009b).

ASIEPI Report P188, "Good Practice Guidance on Thermal Bridges and Construction Details," explicitly states that only non-repeating and geometrical thermal bridges should be considered with separate calculations (Schild and Blom 2010). The authors of this report agree and, as such, it is not recommended that repeating, non-structural TBs of the types discussed here be handled with separate χ-values, but, rather, that they be averaged into the clear-wall U-factors already used in most existing guidance.

2.2.2 Non-repeating TBs

Non-repeating TBs cover all those bridges that are not averaged into the clear-wall U-factor. Typical examples include:

- brick shelf angles
- non-repeating structural members, such as in exposed concrete frames
- window and door frames, frames for overhead doors
- balconies
- slab edges, both on the ground floor and exposed edges for upper floors
- wall-roof, corner, and wall-wall junctions.

2.2.2.1 Geometrical versus material-related impact

Non-repeating TBs can be geometrical or material-related or both. Figure 14 shows a corner TB calculated with KOBRA, where the concave side is to the exterior of the building (CSTC 2011).This is referred to here as a non-repeating TB, and it is not typically averaged into the construction-specific U-factor of the clear wall. The concrete column (dark grey) has a conductivity 2.8 times higher than that of the masonry wall (red) and it bridges through the exterior polystyrene insulation layer (light blue). A TB would be evident even if this was a flat wall, not a corner.

When the column and wall material are both replaced with polystyrene and the simulation is run again, however, the Ψ-value is still slightly positive (Figure 15) because of the differences in exposed surface area (Ψ-value = 0.039 W/m-K [0.023 Btu/ft-°F-h,] compared here to the UA calculations using the exterior building area).

The thermal insulation envelope is not bridged and there is no material behind the insulation of higher conductivity than the clear wall; the positive Ψ-value is due entirely to geometrical effects. Recall that Ψ-value is the sum per length of that part of the conduction that exceeds what is expected by simple multiplication of the clear-wall U-factor by the clear wall area. Here, there is more surface area in contact with the interior than the exterior, and the clear-wall UA calculation we are comparing to, in this case, used the exterior area of the building.

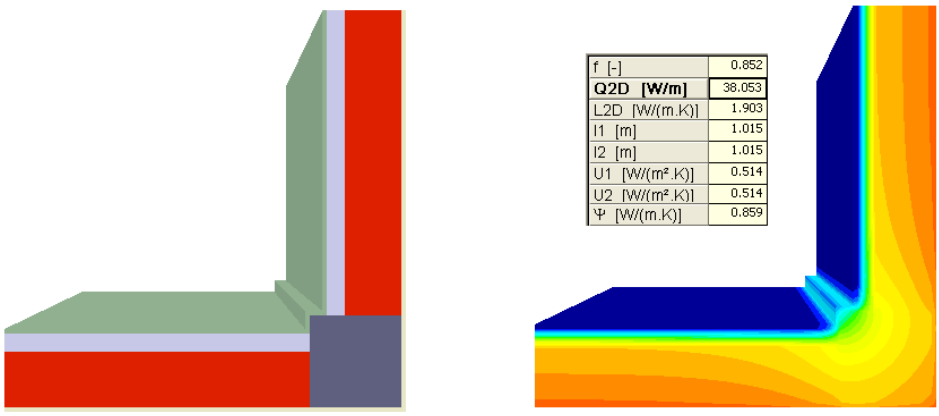

Figure 14. This corner features a concrete column in a masonry wall that, in the clear-wall portion, has exterior polystyrene insulation. The concave side of the corner is the exterior. Ψ-value = 0.859 W/m- K (0.496 Btu/ft-°F-h), comparing here to the U-factor if exterior building area is used.

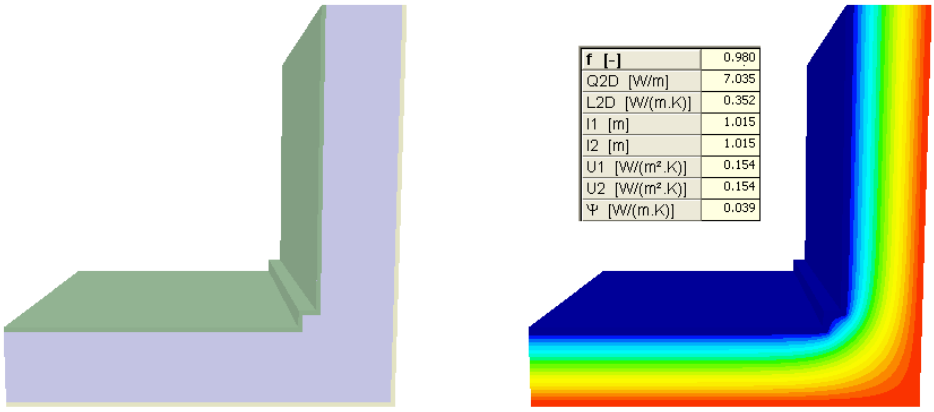

Figure 15. The same corner as in Fig. 14 except that the concrete column and masonry wall have both been replaced with polystyrene.

This is typical in whole-building energy simulation. The increased surface area available for heat transfer leads to a lower thermal performance, and that slight difference accounts for the positive Ψ-value. Note that, if the UA calculation used for comparison purposes had used the building's interior surface area, or if the concave side of the corner was on the building's interior, the geometrical impact on Ψ would be negative.

Another example is the balcony, derisively called "protruding fins that transfer every last available Btu across them" by building scientist Dr. Joseph Lstiburek (2007). Figures 16 and 17 show KOBRA simulations of the same balcony, except that in Figure 17, all elements that protrude inward or outward from the plane of the wall are removed, and the boundary conditions are applied directly to this cut-plane.

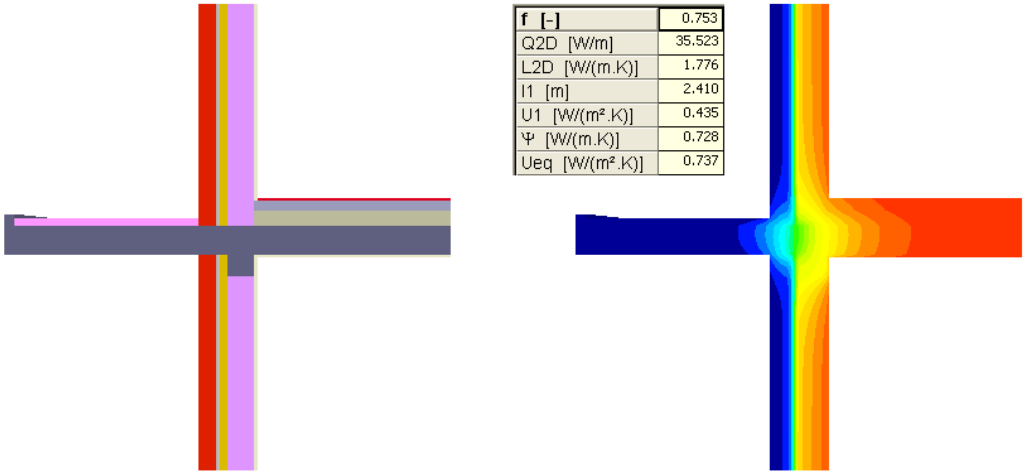

Figure 16. A simulation of a balcony as a slab continuing through the thermal insulation envelope. The balcony exterior is insulated on its top. Ψ-value = 0.728 W/m-K (0.421 Btu/ft-°F-h).

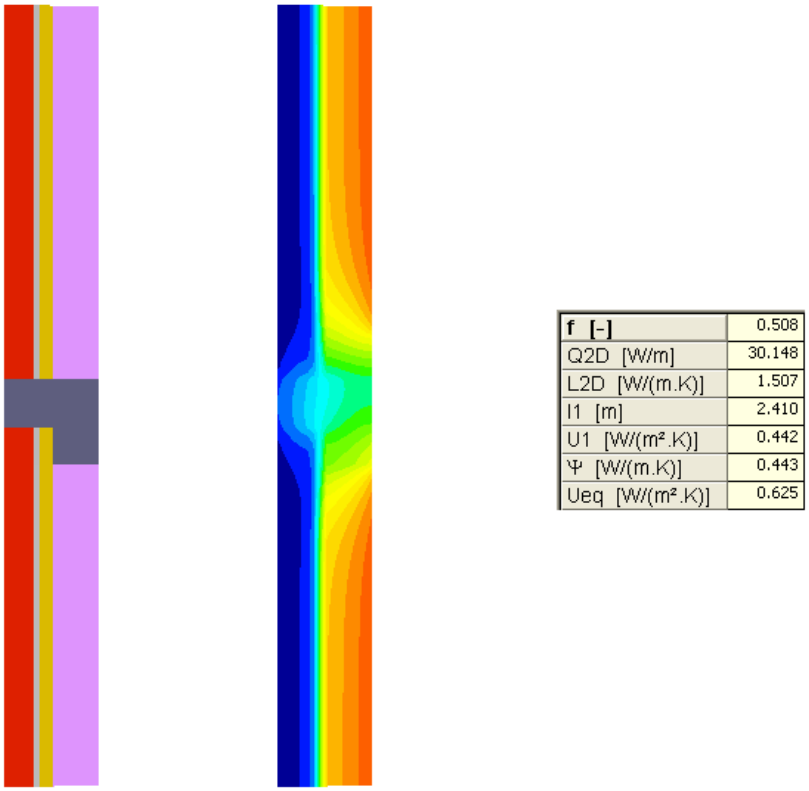

Figure 17. The same wall as in Fig. 16, except that all elements protruding past the interior or exterior surface of the wall are "cut-off," removing any potential fin effect and accounting only for the fact that a higher conductivity material bridges the insulation envelope. Ψ-value = 0.443 W/m-K (0.421 Btu/ft-°F-h), indicating that 39% of the thermal bridging is caused by the fin effect.

The Ψ-value calculated will be only that which can be attributed to a high-conductivity material bridging the thermal insulation, not the fin effect caused by protruding surfaces. By this analysis, 39% of the bridging effect is caused by the geometrical "fin effect" of this through-wall balcony.

2.2.2.1 Slab edges, shelf angles and balconies

Balconies and shelf angles typically occur at slab edges, where their impact is exacerbated by the availability of a conductive concrete fin bridging the insulation layer and protruding into the building interior. Figures 18 and 19 show examples of a balcony and slab-edge TB. In ASHRAE RP-1365, Details 05, 05a, and 06 give quantitative examples of a balcony bridge and a mitigation strategy that involves insulating the top and bottom of the balcony slab. Such a strategy would be relevant to existing buildings. For an 8-in. concrete slab bridging through a steel stud wall with R15 exterior insulation ψ = 0.770 W/m-K (0.445 Btu/ft-°F-h), if the slab is insulated on its top and bottom with 1-in. XPS to a distance of 800 mm from the wall, the ψ-value decreases to 0.496 W/m-K (0.287 Btu/ft-°F-h). Other examples in RP-1365 show instances where the slab simply terminates after it penetrates the insulation and cladding, serving as a brick shelf itself (and representing a much larger TB).

Details 35 and 36 in ASHRAE RP-1365 give examples of brick-block construction with exterior insulation. The brick is supported by a shelf angle, which is mounted to the structure at a slab edge. In the first detail, the insulation is penetrated by the shelf angle, which supports the brick. In the second detail, the shelf angle is supported by vertical knife edges attached to the slab edge, allowing the insulation to continue behind it. This mitigation reduces the ψ-value from 0.450 W/m-K (0.260 Btu/ft-°F-h) to 0.306 W/m-K (0.177 Btu/ft-°F-h) (ASHRAE 2011b).

Slab edges, shelf angles, and balconies receive much less attention than repeating bridges in ASHRAE 90.1 and ASHRAE 189.1. The language quoted in Section 2.2.1 might be considered to apply: "*If the building official determines that the proposed construction assembly is not adequately represented in Sections A2 through A8.*" It is unrealistic, however, to expect a building official to contest the values that appear to be sanctioned by the U-factor tables; to do so would fundamentally change the way the standard is applied. If the prescriptive path is used in either standard, essentially no requirement exists to treat slab edges, shelf angles, or balconies.

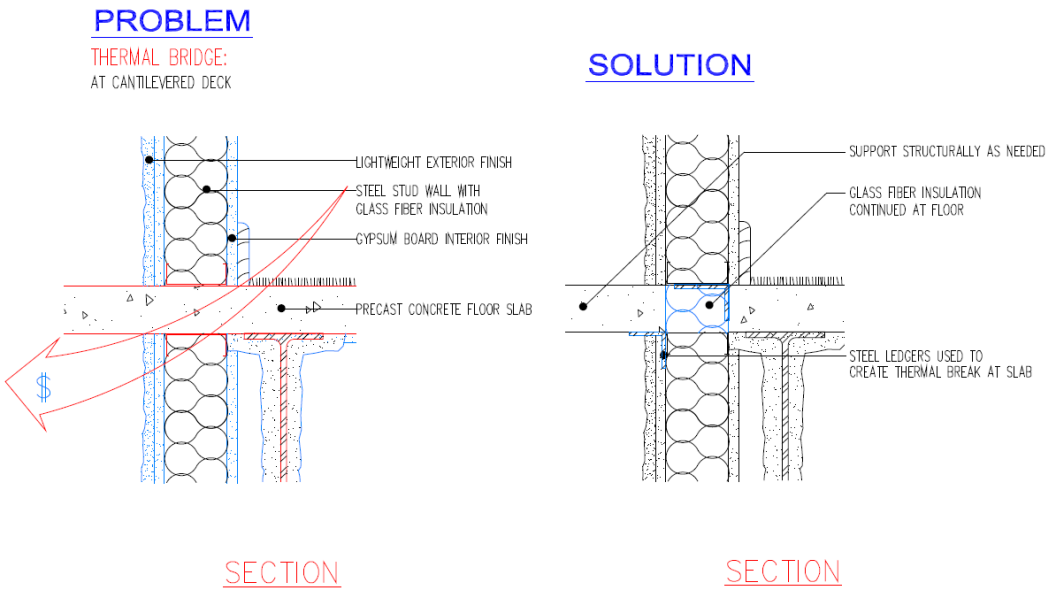

Source: Minnesota Department of Commerce (DOC) (2000).

Figure 18. Balcony TB with mitigation example.

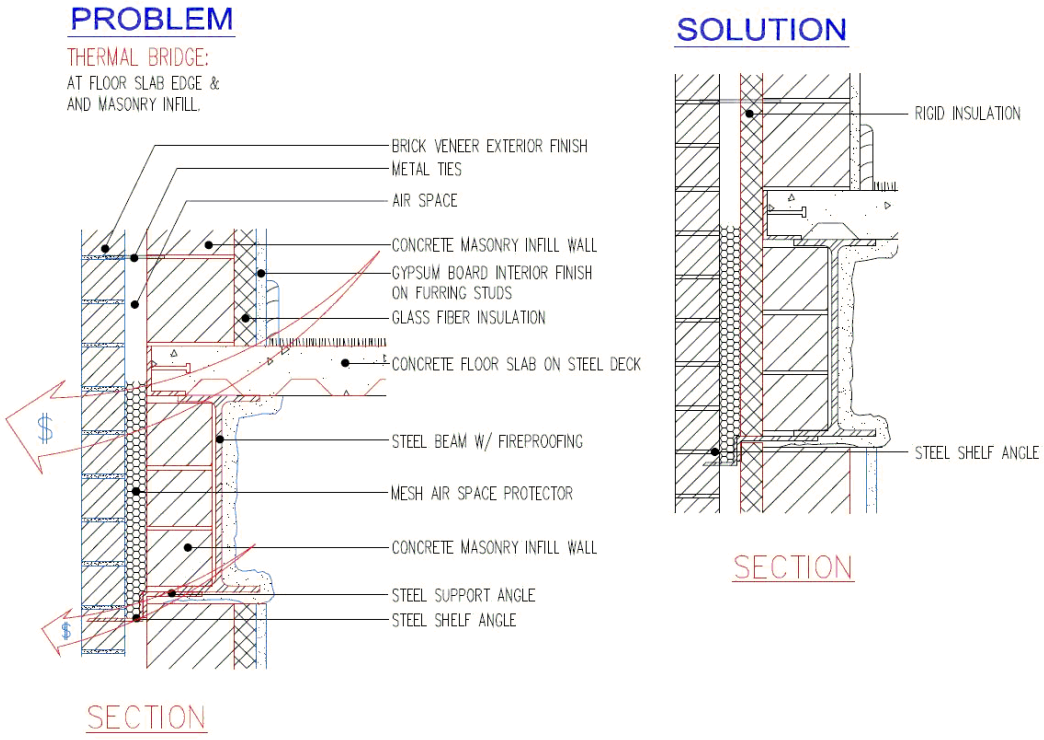

Adapted from (Minnesota DOC 2000).

Figure 19. Slab edge TB with mitigation example. Notice that the mitigation moves the insulation to the exterior, but does not mitigate the shelf angle by setting it off on knife edges and having insulation pass behind it.

If the performance path is chosen, the applicant finds herself simulating a building and comparing this simulation to a simulated "baseline building" designed by the prescriptive bath. Neither simulation has any requirement to accurately account for TBs, except in the limited case described in ASHRAE 189.1 concerning requirements for the building simulation used:

> 1. All uninsulated assemblies (e.g., projecting balconies, perimeter edges of intermediate floor stabs, concrete floor beams over parking garages) shall be separately modeled using either of the following techniques:
>
>   a. Separate model of each of these assemblies within the energy simulation model.
>
>   b. Separate calculation of the U-factor for each of these assemblies. The U-factors of these assemblies are then averaged with larger adjacent surfaces using an area-weighted average method.

As such, slab edges and balconies are only required to be separately simulated if they are "uninsulated." Even thermally broken or insulated balconies and slab edges can represent significant TBs, however, so the applicant is effectively encouraged to overestimate building envelope performance. Even where the detail is simulated, mitigation is not explicitly encouraged, since the "baseline building" would also include the detail.

2.2.2.2 Corners and wall junctions

Corners and wall junctions are both geometrical and material-related TBs. Purely geometrical examples are rare, since these locations generally have structural columns or additional framing. Figure 20 shows a typical corner detail in a light steel-framed wall (Minnesota DOC 2000). The bridge at the corner is caused by the additional framing, and to a lesser extent, by disallowing insulation. Potential solutions are to avoid having all three studs bridge to the outside, or to replace one of the studs with a wallboard nailer strip.

Details 08 and 08a from ASHRAE RP-1365 provides an example of this very wall type, except that it also accounts for the impact of horizontal Z-girts supporting the exterior insulation, and the corner cavity is insulated in both cases. Including corner insulation in such a small cavity should not result in a major difference, as the conductivity is dominated by the high density of steel bridges (Syed and Kosny 2006). With R_{SI}-1.8 m²-K/W (10 sq ft-°F-h /Btu) exterior insulation, the corner with the incorrect framing has a ψ-value of 0.158 W/m-K (0.087 Btu/ft-hr-°F) while the solution shown in the lower right of Figure 20 reduces it to 0.152 W/m-K (0.087 Btu/ft-hr-°F). In

cases such as this, where no large column bridges the exterior insulation (see Figure 14), the user would not expect a major gain from "mitigating" the TB and should consider thicker exterior insulation everywhere.

Wall-wall junctions may also have increased framing and would, similarly, be mitigated with adequate exterior insulation. In some cases, however, a building must be internally insulated and an interior wall would break the continuous insulation envelope. This is often the case for buildings with historically significant facades, such as those at the US Military Academy at West Point, which was recently chosen as a Net Zero Energy pilot program installation (Hemmerlybrown 2011). In such cases, it is important to quantify the impact of the TB and potentially mitigate it by insulating both surfaces of the interior wall some distance from the exterior wall. Unless they represent an "*uninsulated assembly,*" as discussed in Section 2.2.2.1, corner and wall intersection bridges are not treated at all in ASHRAE 90.1 or ASHRAE 189.1.

2.2.2.3 Window and door bridges

Windows and doors are either considered TBs in their entirety or just in their frames and the structural framing associated with their rough opening. An aluminum window frame is a significant TB (discussed and illustrated in detail on p 63); a typical R-value for such a frame is 0.15 m^2-K/W (0.88 h-sq ft-°F/Btu), while argon filled, triple-pane glass with low-e coatings can have R-values as high as 1.2 m^2-K/W (6.7 h-sq ft-°F/Btu) (ASHRAE 2009a). The additional framing could also be significant, as discussed above in Section 2.2.1.1 and shown in Figure 21. As such, this document typically considers fenestration frames and associated structural framing as the TB, while the glazing itself is considered a different type of clear wall.

NFRC Standard 100 is the standard rating system for windows in the United States. It essentially divides simulation of the window into area types such as the frame, a 64 mm (2.5 in.) strip of glass adjacent to the frame called "edge-of-glass" and the remaining glass, called "center-of-glass." An independent agency produces a U-factor by area-weighting simulation results for the area types. In addition to the simulation effort, a separate party physically tests the window according to NFRC Standard 102. If the results are similar enough, the U-factor is published and modifications to the window, such as a different glazing package, can just be simulated for rating purposes (NFRC 2010).

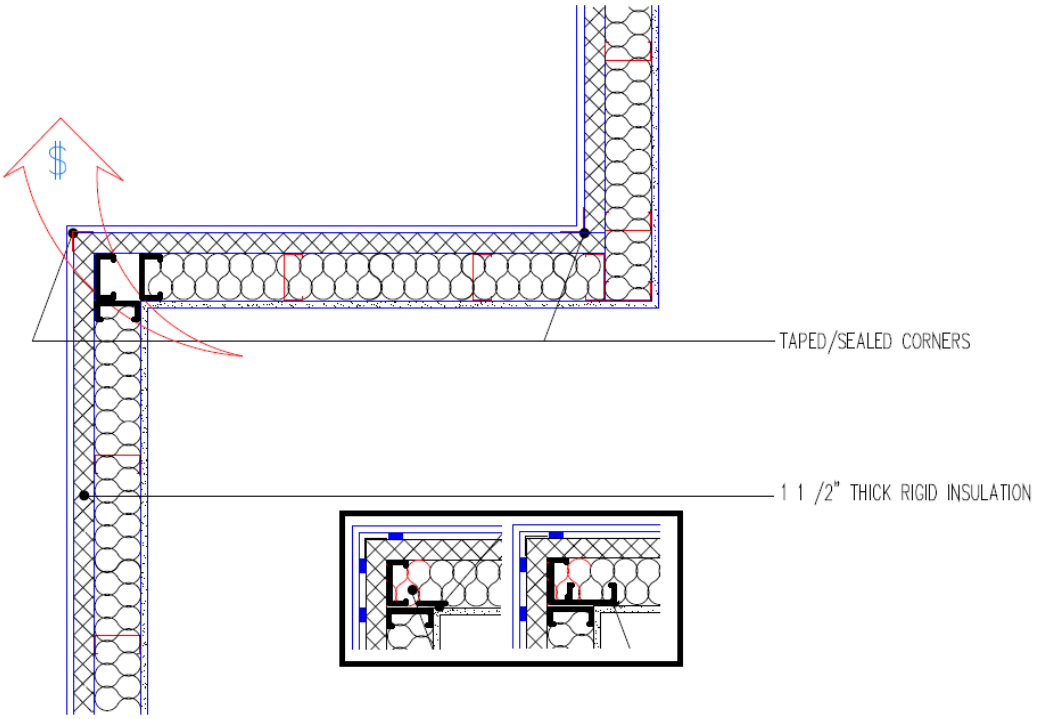

Adapted from Minnesota DOC (2000).

Figure 20. Typical corner in steel-framed building with exterior and cavity insulation.

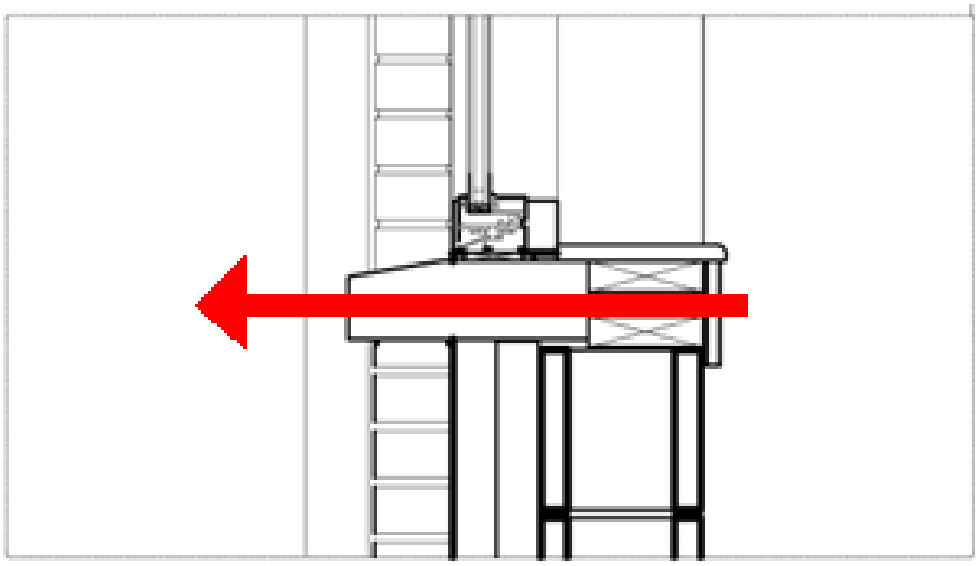

Figure 21. Even if this window were literally adiabatic, the sill framing would represent a significant TB.

Unfortunately, this process is only executed for the NFRC mandated "standard size," but the resulting U-factor is used as the rating for all sizes of the tested window type. As such, the NFRC U-factor is only useful for side-by-side comparison of window types, not actual energy calculations. As Bombino et al. (2010) points out, this "one size fits all" U-factor is the method by which a building designer achieves compliance with ASHRAE 90.1, potentially leading to bad fenestration choices. For instance, if many small windows are used, the highly conductive frame and edge-of-glass regions would dominate, and the performance would be much worse than an equally compliant decision to use one large window (ASHRAE 2007, NFRC 2010). It has been proposed that, since U-factors for the various area types are already calculated during the NFRC process, they should be used to generate published, area-weighted U-factors for windows of all sizes (Bombino and Finch 2010).

Even where accurate window U-factors are used, the "as-installed" TB remains unaccounted for. The implicit assumption for most energy calculations is that the clear-wall U-factor and 1-D conduction assumptions are valid right up to the window area, at which point there is an adiabatic plane and, on the other side of this plane, the window's average U-factor applies over the area of the window (see the right pane of Figure 22). Obviously, the additional sill framing, sealant and flashing details, and 3-D effects between the frame and rough opening can all impact the heat transfer. Simulating or testing both cases and taking the difference can produce an appropriate ψ-value for the "as-installed" TB. Several questions remain, however:

1. Is it important that detailed simulation be done for every window frame, installation method and wall type permutation, or can the window frame be represented by a "black box" of appropriate properties, perhaps determined from existing NFRC frame U-factors?
2. What ψ-value is appropriate for predicting energy use when the drawings leave window installation detail decisions to the construction trades?
3. Is the sill framing part of the clear wall or part of the window TB? In this case, it seems clear that it is part of the TB, as it continues into a sill that penetrates the exterior insulation. Therefore, one needs to avoid including this framing in the framing factor when determining an appropriate clear-wall U-factor, as it is accounted for the window's ψ-value. For other windows, where the additional sill framing does not penetrate the exterior insulation, but only represents an interruption of cavity insulation, this is not always clear.

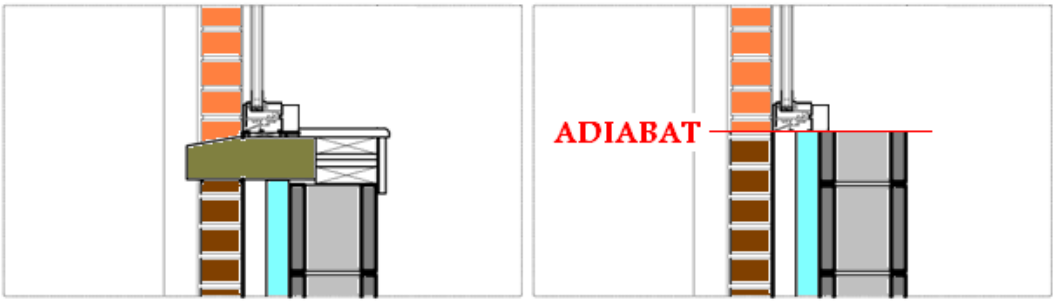

Adapted with different images from report P188 of the ASIEPI (Schild and Blom 2010).

Figure 22. A window as it might be installed (left); how a window is modeled (right).

ASHRAE RP-1365 provides several details that include transitions to windows. The authors chose a representative frame section and glazing unit rather than attempting to generalize results to any choice. In the case of an exterior insulated steel stud wall (Detail 07), the report found ψ-values in the range of 0.077-0.120 W/m-K (0.044-0.069 Btu/ft-°F-h). The impact of choosing different frame sections or glazing units is unclear.

"Details for Passive Houses" also provides ψ-values for windows as installed. Separate catalogue pages are not provided for separate windows, only for separate construction types. Each page indicates that the details are only to be used with windows having a U-factor "significantly lower than 0.8 W/m²-K" (0.14 Btu/sq ft-°F-h).

2.2.2.4 Ground-slab intersections

Ground-slab interactions are considered separately by this report because they behave in fundamentally different ways. First, the time scale is much greater; the ψ-value times the length and temperature difference between indoor and outdoor air may produce the correct heat flux for steady state, but the change in ground temperature can have time scales in the months, so steady state is never achieved in the same way that it is for an exterior wall. Second, the material properties of soil are highly site specific and vary greatly with moisture content. Quantifying the TB must be done with caution.

Because of these difficulties, this type of TB is covered in disproportionate detail by ASHRAE 90.1 and 189.1. Several methods have been proposed to simplify the strongly 3-D and inherently transient nature of ground-coupled heat flux; the one used in 90.1 is based on the work of Wang (1979) and Bligh (1978), which found that heat flux through slab-on-grade floors can be accurately estimated using only the perimeter times an "F-

factor"(Wang 1979; Bligh, Shipp and Meixel 1978; ASHRAE 2007). This is very similar to ψ-values except that the product of the F-factor, building perimeter, and temperature difference estimates the entire ground-coupled heat flux, not just the amount in excess of the clear-wall value. An F-factor requirement is specified for any building built with slab-on-grade floors. The required edge insulation depth can be looked up in a table just like the U-factors discussed in Section 2.2.1.

This approach to compliance risks causing the applicant to choose an inferior, but compliant, detail. For instance, Figure 23 shows a wall with compliant insulation and a footer with insulation reaching the required depth. There is still, however, a clear TB that is nowhere specifically prohibited in ASHRAE 90.1 and 189.1. Though one could argue that it is required to be simulated if the 189.1 performance path is chosen, because it counts as an "uninsulated assembly," this does not actually encourage mitigation of the TB.

ASHRAE RP-1365 does not provide any ground-slab intersection details, likely because it focuses on larger commercial buildings. "Details for Passive Houses" does have several details quantified using a ψ-value rather than an F-factor.

2.2.3 Summary of treatment in ASHRAE standards

ASHRAE 90.1 is the standard commonly used as the foundation for building codes. ASHRAE 189.1 is nearly identical in the structure of its approach to energy compliance, but has more stringent requirements. It also includes issues of material sustainability and indoor air quality. Army policy has recently begun to require meeting or exceeding the energy requirements of ASHRAE 189.1, so it is worthwhile to summarize 90.1 and 189.1's treatments of TBs.

2.2.3.1 Repeating TBs

Repeating TBs are averaged into the U-factors in the tables used for prescriptive compliance. Unfortunately, there is a large risk of underestimating their impact by assuming that these calculated values are always accurate. It is better to think of them as maximum possible performance levels for a given wall type. There is inadequate guidance on when the applicant must use a different method to quantify clear-wall U-factor. Furthermore, fasteners and brick ties are not considered, though they become important at higher building performance levels.

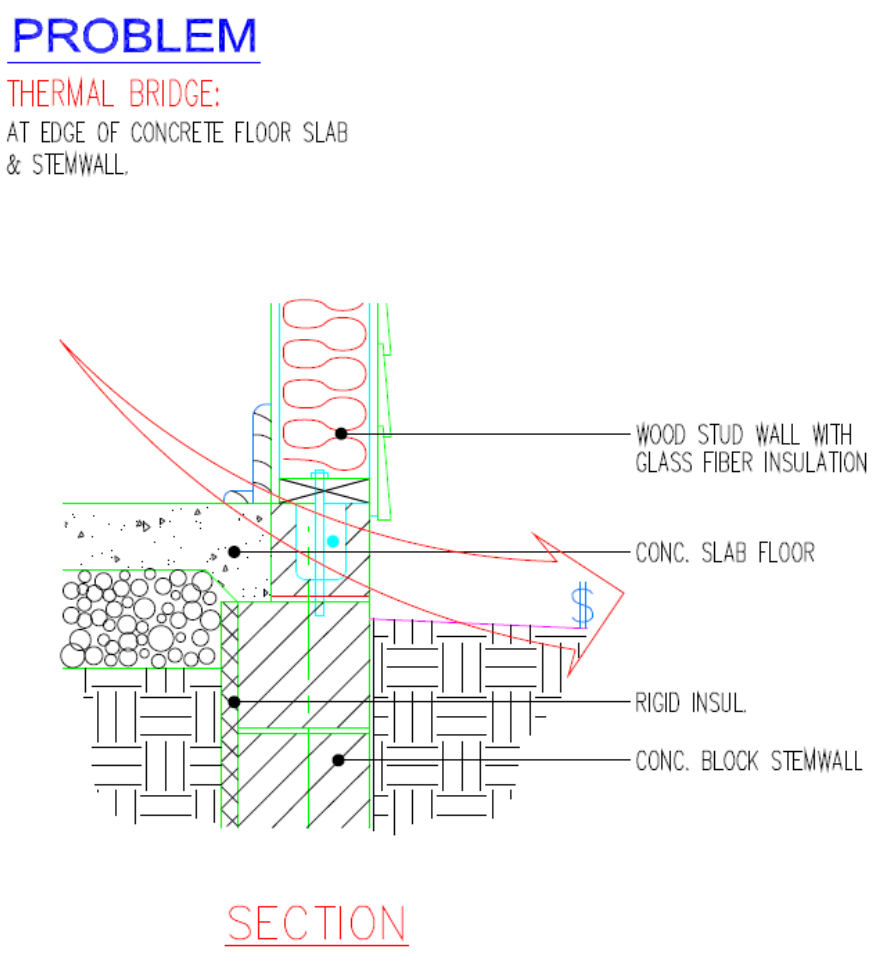

Adapted from Minnesota DOC (2000).

Figure 23. Ground-slab intersection bridge not caused by inadequate insulation depth allowing bridging through the earth, but rather by not continuing the thermal insulation barrier between the footer insulation and clear-wall insulation.

2.2.3.2 Slab edges, balconies, corners and wall intersections

These very important, non-repeating TBs would be ignored by all but the most diligent applicant and building official. There is very limited language in 189.1's performance path specifying that some TBs, if they constitute an "uninsulated assembly," must be simulated. Simulation guarantees that the building with TBs will be simulated in both the baseline form (designed according to the prescriptive approach) and the proposed form. This comparison does not encourage mitigating the bridge, but can potentially cause the applicant to be more aware of a TB.

2.2.3.3 Windows and doors

The standards rely largely on NFRC Standard 100 for ensuring adequate windows and doors are selected. The rated U-factors, however, are often inaccurate because they are applied to windows of all sizes with the same frame cross section and glass package. This fails to encourage good decisions on the part of the applicant. Furthermore, there is no provision for considering the "as-installed" impacts of windows, which can lead to severe TBs even when excellent windows are specified.

2.2.3.4 Ground-slab intersections

The F-factor tables, based on foundation insulation levels, limit or, at least, acknowledge the TB at this location. They attempt to express all heat flux through the slab. For instance, ASHRAE Handbook Fundamentals (ASHRAE 1985) shows four basic slab-on-grade construction examples that address how to prevent the *reverse loss* heat loss (Ch 25, Fig. 7). 1985 Fundamentals suggests the use of perimeter insulation, with the understanding that losses will be reduced even in warmer climates. However, ASHRAE (1985) does not adequately address all of the bridging that is likely to occur at this location, such as a break in insulation continuity at the slab edge above the footer insulation.

2.2.4 Use in whole-building simulations

Throughout this document, "quantifying the impact" of TBs is discussed. That can simply mean the ψ- and χ-values defined in Section 2.1, which are adequate for comparing two detail solutions for the same wall type, but the concern to the designer should actually be the impact on a whole building's annual performance. This typically means that the impact of the TB is incorporated into an annual simulation of a building using 8760 hours of "typical year" weather data (Wilcox and Marion 2008).

Two of the most popular simulation engines, DOE-2 and EnergyPlus, both implicitly encourage the 1-D, parallel paths approximation by defining surfaces as combinations of layers that separate two spaces from each other. The user defines separate surfaces for windows and doors, interior walls, exterior walls, and roofs. To account for the clear-wall bridging accurately, users must somehow average the wall's properties prior to entering them into a simulation program. As discussed in Section 2.2.1, this process is likely done incorrectly as encouraged by the structure of Standard 90.1

and 189.1. Each of these two engines accounts for the transient thermal behavior of the material in the wall as well, keeping track of, for instance, the time lag associated with solar heating of a masonry wall. ψ- and χ-values, however, are inherently steady-state values, and there is no existing interface for integrating them, with the exception of slab-on grade perimeter bridges. These are captured in some cases by F-factors (see Section 2.2.2.4), which are automatically generated from the slab and footer insulation inputs. It is not immediately obvious how to account for the impact of other linear and point bridges, however.

One way is to simply give each side of the building a "dummy surface" in the simulation – something with a U-factor and area to result in the same additional UA as indicated by:

$$UA = \sum_{\substack{All\ Linear \\ Bridges}} \psi_i L_i + \sum_{\substack{All\ Point \\ Bridges}} \chi_i$$

This accounts for all point and linear bridges on a building side. The dummy wall with this UA value would have zero mass and would only represent the additional conduction expected at steady state from inside to outside.

A similar option is to tune the U-factor of one layer of the wall until the overall U-factor is increased by the appropriate amount. This will produce similar results. PHPP, the software package mandated by the Passive House Institute does, in fact, have inputs to accomplish this (Passive House Institute US 2011).

Neither of these options, however, captures the potential impact of TBs on transient conduction. Whether this is significant is unclear, but there has been one major attempt to account for it: ASHRAE RP-1145 "Modeling two- and three-dimensional heat transfer through composite wall and roof assemblies in transient energy simulation programs" (ASHRAE 2001). The output of this method is a wall's transfer function coefficients, used by both EnergyPlus and DOE-2 to capture the transient behavior of walls based on the input of discrete data on outside conditions. (However, because EnergyPlus employs the heat balance method, this transfer function method can be swapped out for another, as in the work of Pedersen [2007].) Essentially, the method produces a simple input for the simula-

tion, representing a wall whose transient behavior is equivalent to what is predicted by a complex, 3-D simulation of a wall.

The authors of this report have never encountered this method used in practical building energy simulations. Generating "equivalent wall" inputs is extremely complex, requiring 3-D-transient simulation or even hot-box testing. An attempt was made in ASHRAE RP-1145 to provide a catalogue of wall types for which this was already done, but the variety of framing factors, window placements, and the occurrence of other TBs, makes use of these walls difficult.

2.3 Army guidance

Many Army goals ultimately refer back to ASHRAE 90.1 or ASHRAE 189.1, but there are many more specific documents that outline criteria or specific solution sets. USACE has combined efforts with the Naval Facilities Engineering Command and the Office of the Air Force Civil Engineer to develop the "Unified Facilities Criteria (UFC)," which makes up the bulk of the Army's building code.

UFC 1-200-01 "General Building Requirements" largely points the reader to other UFC documents or the International Building Code (IBC) (DoD 2010). For exterior walls, the reader is instructed to use Chapter 14 of the IBC, which does not mention TBs (ICC 2009). In place of the IBC's energy efficiency chapter, however, the reader is directed to UFC 3-400-01 "Energy Conservation"; this document also fails to mention TBs (DoD 2002). UFC 4-030-01 "Sustainable Development" does not address TBs, and neither do more material specific UFC documents, such as UFC 3-320-06A "Concrete Floor Slabs on Grade Subjected to Heavy Loads," even though such floors are shown in Section 3.1 to consistently exhibit thermal bridging (DoD 2005, 2007). In fact, the only UFC in which the authors were able to find any mention of TBs was UFC 3-130-07 "Design: Arctic and Sub-Arctic Construction – Buildings," in which the following language appears:

> Concrete has a high thermal conductivity compared with insulative materials, therefore thermal breaks must be provided, and thermal bridges avoided. A concrete slab supporting an exterior masonry wall is one example of a thermal bridge often seen in poorly designed buildings. Even with insulation on the wall's inside surface, heat flows through the slab to the wall, is distributed laterally and dissipated to the outdoors. This process effectively bypasses the insulation. Exterior insulation used with no exposed concrete provides a solution to this problem.

> Other types of thermal breaks are possible, but successful use is difficult. (DoD 2004)

Strangely, language about TBs does appear in "Architectural and Engineering Instructions Design Criteria," the Army document that was superseded by the UFC:

> Opaque wall U-factors must be calculated in accordance with the ASHRAE Handbook of Fundamentals. The calculations must take into account all major thermal bridges and series and parallel heat conductive paths (HQUSACE 1994).

This is certainly more forceful than the guidance in the UFCs, but was still largely unenforced, as is evident from thermography of buildings from this time period.

The USACE document "Energy and Water Conservation Design Requirements for SRM Projects" (Zhivov, Herron, and Liesen 2010a) aims for much higher energy performance than the UFCs. Even the "Building Envelope" design guide document, however, does not fully address TBs, except by specifying exterior insulation in the clear wall in appropriate places (Zhivov et al. 2010a). The "Prescriptive Technology Solution Sets" for specific building types (e.g., Company Operations Facility (COF), TEMF, BdeHQ, Dining facility (DFAC), Unaccompanied Enlisted Personnel Housing (UEPH)) were authored specifically to meet EPAct 2005 high-performance building requirements. EPACT 2005 requires a building to perform 30% better than a similar building built to ASHRAE 90.1, which does not, itself, address TBs adequately. As such, the solution sets do not actually have to address TBs to achieve this goal and, indeed, they do not attempt to provide any specific guidance in avoiding TBs outside of those covered in ASHRAE 90.1 (Zhivov et al. 2010b-h).

2.4 Recommendations of "Good Practice Guidance on Thermal Bridges & Construction Details" (Schild and Blom 2010)

ASIEPI Report P188 (Schild and Blom 2010) compiled the experiences and lessons from the involved European Union (EU) Member States' attempts to provide TB guidance. Its recommendations are summarized as:

1. A maximum or default TB effect should be established. This penalty is applied to the assumed performance buildings for which no TB mitigation has been attempted. This penalty is typically applied on a per-envelope-area basis; i.e., the calculated U-factor used for code compliance must be

increased by some amount (see Section 2.1.1.6 for a discussion of default values). Other options include a per-floor-area approach, or even, as in Denmark, separating the default values into the primary TB types and applying it like ψ- and χ-values. Establishing this value is recommended to facilitate a very simple compliance framework that minimizes the additional work required to account for TBs. For this framework to fit within ASHRAE 90.1, major changes to the standard will be required, as discussed in ASHRAE RP-1365 (ASHRAE 2007, ASHRAE 2011b).

2. Pre-accepted details that mitigate TBs and eliminate condensation risk should be generated. Where appropriate, identify an insulation layer with a minimum acceptable thickness to prevent TB condensation. Again, this recommendation exists so that a designer can put forth minimal additional effort (in this case, selecting pre-approved details) and be rewarded with a smaller performance penalty to use for code compliance.
3. Provided details should be well illustrated and have rich supporting information, including:
   a. climate-dependent changes
   b. construction sequence
   c. Quality Assurance (QA) check-lists to ensure good execution
   d. ψ- and χ-values.
4. Repeating TBs should be incorporated into U-factors, while non-repeating and geometrical TBs should be incorporated under the framework of point and linear thermal transmittances (ψ- and χ-values).
5. General principals of TB avoidance and mitigation should be included with all TB guidance documents, including detail catalogues. The "unbroken" insulation envelope concept should be presented alongside the unbroken air-barrier concept. Moisture issues should also be discussed.
6. Provide calculation methods with examples for TBs not covered by catalogues.

2.5 Conclusions

There is a clear lack of code requirements and Army criteria on the subject of TBs, and, even if this were not the case, there are insufficient tools for a designer to address TBs quickly and accurately. Simplified methods fail to address all the required TB types, especially as performance requirements increase and smaller thermal bridges become important. Numerical methods are too time intensive to treat every TB with a custom model. As such, the authors agree with the recommendations of the ASIEPI Project in sug-

gesting development of a details catalogue designed to provide maximum utility when integrated into UFC and other Army building guidance.

USACE already recognizes the need for detail catalogues. The "CAD Details Library" provides a central location for designers to source details, allowing quick, easy reuse of existing drawings (ERDC 2011). The "2011 – Building Envelope Air and Vapor Barrier Details" provides greater benefit by limiting the details to those that perform to the required level of air tightness, and providing thorough instructions for construction and QA (Carlisle Construction Materials 2011). The catalogue developed as part of this project would aim to replicate this success in the field of mitigating TBs. This catalogue would:

- Provide compliant details, high-performance details and details relevant to renovation
- Provide ψ- and χ-values for performance prediction, with "before" and "after" values to assist in quantifying savings
- Include air-tightness guidance
- Include details that will not lead to condensation or other moisture issues
- Include, where appropriate, simplified correlations or free programs to extend the relevance of the results to all geometry variations
- Instruct the user on order of construction
- Include check-lists for pre- and post-construction inspection.

ASIEPI Report P198 (Tilmans and Orshoven 2010) acknowledges that catalogues can lack generality. As such, many pre-existing catalogues for European construction or commercial construction may not be directly applicable to Army projects. This project will focus on those details of Army buildings not covered by RP-1365 or the catalogues available from Europe.

The early development of the catalogue has already resulted in the cultivation of in-house conduction modeling capabilities in ERDC. USACE districts can request analysis of specific details, and ERDC's rapid turn around capability can both provide them in a timely manner and use the opportunity to generate a new catalogue entry. This plan has led the project team to become familiar with Heat3, an affordable, validated software that facilitates the rapid turn-around time required.

Finally, the success of the USACE Air-Tightness requirements motivates examination of a feasible “post test.” Mandating blower door testing has made the air tightness program a success because the test itself is cheap, reliable and fair to the contractor. No such test currently exists for TB QA. As a step toward developing one, this project will explore quantitative use of surface temperature measurements, using temperature indices on inside and outside surfaces as quick and easy performance metrics. If it is found that the test is reliable and fair to the contractor, it will be included as QA steps in the appropriate catalogue pages.

3 Development of Army Facilities Details List

The first step in producing a catalogue of TBs is to identify the construction details that must be analyzed. The primary method to date has been to use an infrared camera to generate thermal images of a building's exterior, which produces a qualitative understanding of the most important TBs. From here, as-built drawings can be found, or measurements made, to turn the detail into a catalogue page. Section 3.1 describes this activity.

Obviously, this cannot be accomplished for every Army building. Other reports and documents are being reviewed to find the building types that will be or have been constructed in the highest quantity, and the features of these buildings that warrant attention. Section 0 describes this activity.

3.1 Thermography

Thermographic imaging essentially consists of taking photographs in the infrared spectrum. The camera measures and makes an image of long-wave radiation converted to the visible color scale. From these long-wave measurements, a temperature is inferred. This requires assuming an emissivity. Because the camera does not recognize the boundary between, say, bricks and steel door frames, the same user-input emissivity is assumed for all of the field of view. Since this emissivity is an approximation for a single material and is certainly not applicable to all materials, errors are introduced. Also, not all temperature anomalies can be attributed to conduction; some are caused by air leakage. As such, care must be exercised when interpreting TBs from thermographs.

Following ASTM C1060-11a, "Standard practice for thermographic inspection of insulation installations in envelope cavities of frame buildings" (2011), thermographic images were taken at Fort Drum, NY, Fort Bragg, NC, and Fort Carson, CO. These have revealed many TBs, including improperly installed or damaged insulation. Section 3.1.1 describes the buildings inspected and Section 3.1.2 analyzes the thermographs,

3.1.1 Buildings inspected

The building descriptions in this section quote extensively from the Centers of Standardization website's facilities pages. This is also where the standard designs are available (HQUSACE Undated). Relevant detail drawings are including in Appendix B.

Figure 24. DFAC at Fort Carson, CO.

3.1.1.1 Dining facilities

The 500 Person Permanent Party (PP), 800 Person PP, and 1300 Person PP DFAC Army Standards and Standard Design (Ferriter 2012) define functional/operational requirements for PP dining facilities. In general these facilities (e.g., Figure 24) are set up similar to a college cafeteria/food court style serving where larger varieties of food are prepared. Training and Operational Readiness Training Complex Dining Facility (72212) standards are not the same as PP DFACs.

Figure 25. Tactical Equipment Maintenance Facility at Fort Drum, NY.

3.1.1.2 Tactical equipment maintenance facilities

The TEMF Army Standard Design defines an entire complex of facilities for the maintenance, repair, deployment, mission planning/rehearsal, training, and sustainment of equipment assigned to a unit other than aircraft (Figure 25). It defines space and equipment to maintain vehicles and associated equipment for all levels of maintenance below depot level.

3.1.1.3 Company operation facility

The COF Army Standard Design is provided for companies, batteries, and troops as space to perform daily administrative and supply activities (Figure 26). It is also known as a company headquarters building. The COF is comprised of three vertical construction components consisting of an Administrative Module, Readiness Module, and exterior covered hardstand area. In conjunction with this, each site-specific project shall include necessary site amenities, such as vehicle service yards, access drives, and equipment wash stations.

Figure 26. Company Operation Facility, Administration Office Building at Fort Carson, CO.

Figure 27. "Rolling Pin" style Barracks at Fort Carson, CO.

3.1.1.4 UEPH/barracks

UEPH remains the Army's top facility because of the importance Army places on the well being and combat readiness of able-bodied soldiers (Figure 27). UEPH facilities house single soldiers and are intended to be similar both functionally and technically to apartment type housing in the private sector. The soldier's room is similar to an apartment or college dormitory and includes: private sleeping areas, walk-in closets, and a shared bathroom and kitchenette. The varying components for this facility will be: building occupancy requirements, regional soils and climatic conditions, facility structural considerations, heating, ventilating, and air-conditioning (HVAC) systems, and the exterior architectural features. As such, the overall building design and configurations will vary as required to meet project specific requirements. All UEPH facilities are required to meet current DoD Antiterrorism standards. New UEPH facilities are also ex-

pected to meet Leadership in Energy and Environmental Design (LEED) Gold standards.

3.1.1.5 Battalion headquarters

The Brigade and Battalion (BDE & BN) HQ Army Standard Design defines functional/operational requirements for brigade and battalion level headquarters buildings that house the command, personnel, intelligence, operations, supply, communications, and other specialized functions of a regiment/group/brigade and/or a battalion/squadron headquarters, to include all headquarters administrative and command and control operations (Figure 28). Battalion classrooms are included as part of the BN HQ, but shall be accounted for separately under CATCD 17119, Organizational Classrooms. This Standard Design applies to Active, Reserve, and National Guard Component facilities on Army installations, with the exception of facilities intended for Initial Entry Training, Advanced Individual Training, Operational Readiness Training, or Warrior Transition Units, which are addressed by separate standard designs.

Figure 28. Battalion Headquarters at Fort Carson, CO.

Figure 29. Child Development Center Bldg at Fort Drum, NY.

3.1.1.6 Child development center

A Child Development Center (CDC)-Infant and Toddler is used by the Army to support readiness of families by reducing the conflict between military mission workforce requirements and parental responsibilities (Figure 29). CDC facilities covered in this standard were developed to support the

needs of children 6 weeks to 5 years of age. A CDC- School Age (CDCSA) is used by the Army to support readiness of families by reducing the conflict between military mission workforce requirements and parental responsibilities. A CDCSA provides before-school and after-school care during the duty day, summer, school-out days, and holidays. Services are generally provided on a regularly scheduled daily basis for before-school and after-school care, as well as on a full-day basis during the summer, school-out days, and holidays.

3.1.1.7 Army Reserve center

The Army Reserve Center or training center (TC) generally consists of five main functional groups: administrative, assembly/kitchen, weapons, educational, and storage. Supporting these main functional groups are the special training and support areas (Figure 30). Within each group are subordinate functional areas that contribute to the operation of the group. Circulation and structural space are allocated to each project based on the size of the other authorized spaces.

Figure 30. Army Reserve Center Bldg at Fort Carson, CO.

3.1.2 Common TBs in Army facilities

3.1.2.1 Window frame

TBs through window frames are often caused by the typical frame construction material, which is aluminum. Depending on the alloy composition, aluminum's thermal conductivity can be over 200 W/m-K (116 Btu/ft-°F-h), compared concrete's conductivity value, which is approximately 1.4 W/m-K (0.81 Btu/ft-F) (Mills 1999). These TB effects can be reduced if a thermal break is properly installed inside the metallic frame.

Figure 31 shows how window frames at the Army Reserve Center, Fort Carson, CO are easily distinguished by their high temperature profiles (mostly white among the rest of the building walls). This noticeable contrast indicates that the windows' metal frames have poor or nonexistent thermal breaks.)

Figure 31. Window frame joints TB.

3.1.2.2 Door frames

Door frames behave similarly to window frames, as they are also made of highly thermally conductive metallic material. One of the main differences between window and door frames is that the door itself is sometimes more conductive than the insulated glazing unit in a glass frame. This will extend the heat loss problems to a greater area. In the thermograph shown in Figure 32, for example, a door frame at the Army Reserve Center, Fort Carson, CO can be identified by the picture white region (inverted L-shape white section). Like the window frames, door frames should have thermal breaks to avoid this problem. The thermograph also reveals that the door itself might have poor insulation in the upper part. This could also be attributed to air leakage.

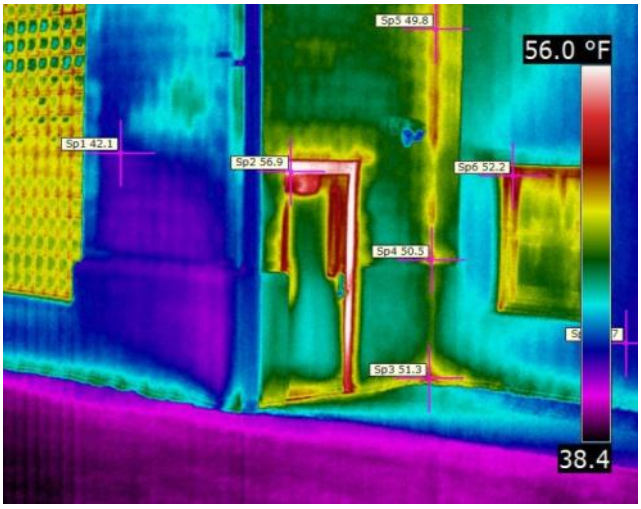

Figure 32. Door frame TB.

3.1.2.3 Overhead door frames

This TB type is mainly found on TEMFs. It is similar to window and door frames, but it comprises greater regions of the whole facility. Air leakage can also be a problem, especially with improperly closed doors. Figure 33 shows a thermograph of an overhead door frame TB at the Tactical Equipment Maintenance Facility, Fort Drum, NY. The thermograph reveals that the door frames used on a large scale (as on an overhead door frame) must be treated with a layer of insulation due to its apparent lack of framing thermal break.

Figure 33. Overhead door frame TB.

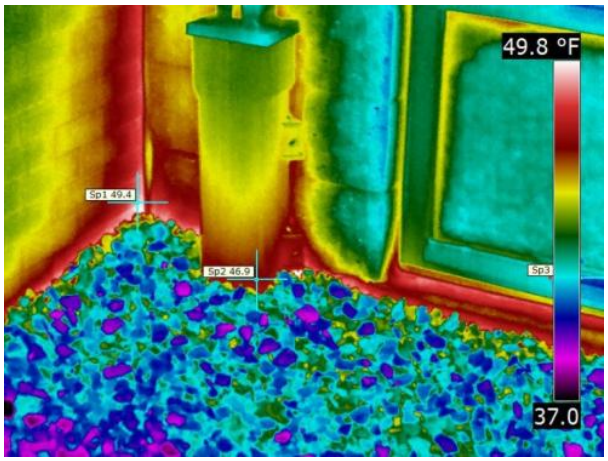

Figure 34. Building Foundation at grade level TB.

3.1.2.4 Building foundation

TBs in building foundations are mainly caused by the lack of insulation around the foundation perimeter and/or the building floor slab. A foundation without the proper insulation will lead to a direct path for heat flow, since the foundation is typically made of a solid-continuous concrete section. Structural and waterproofing requirements result in more constraints on mitigation strategies for this type of bridge than on bridges in other building components. Figure 34 shows a thermograph of a building foundation at grade level TB at a DFAC at Fort Carson, CO. The red region at the grade level indicates that the building internal heating energy is getting lost through the building foundation. The high temperature pattern is also displayed on the vertical wall corner, which also is categorized as a typical TB region in the buildings.

3.1.2.5 Wall/wall intersections

Wall to wall intersections exhibit TB behavior. Depending on whether the designer is considering the inside or outside surface, the ψ-value can be positive or negative if geometry alone causes the bridge. Most corners exhibit TB behavior because of a material change in addition to a geometry change (e.g., a structural column or more structural framing clustered in the corner). TBs caused by geometrical attributes are analogous to stress concentrators in the structural mechanics field.

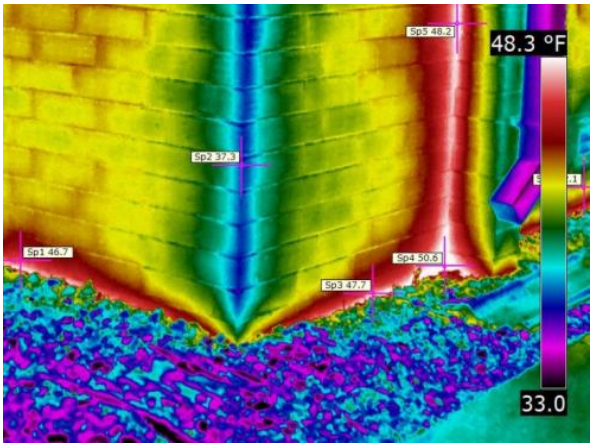

Figure 35. Wall/wall intersection TB.

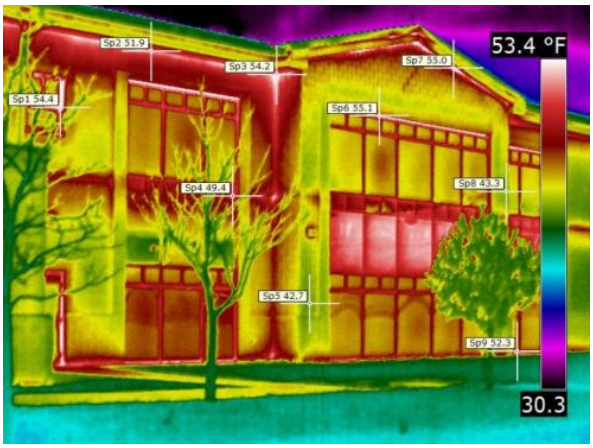

Figure 36. Wall/roof junction TBs. Battalion Head Quarters, Fort Carson, CO.

Figure 35 shows a wall/wall intersection TB at the "yellow brick" Barracks, Fort Carson, CO. The thermograph reveals the two possible scenarios that can be found when two walls intersect each other. The left blue-colored vertical region shows an external wall/wall intersection and the red-colored vertical region shows an external wall/wall intersection. Wall/wall intersections that are concave on their exterior will generally display a temperature increase, while those that are convex on their exterior will display lower temperatures than the rest of the clear field wall.

3.1.2.6 Wall/roof junctions

Wall-roof junctions are similar to wall-wall intersections, except for the structural material involved and the presence of eaves. Figure 36 shows wall/roof junction TBs at the Battalion Headquarters, Fort Carson, CO. The thermograph shows that the highest temperature values are concentrated at the window frames and the roof junction.

3.1.2.7 Mid-floor slab/wall junctions

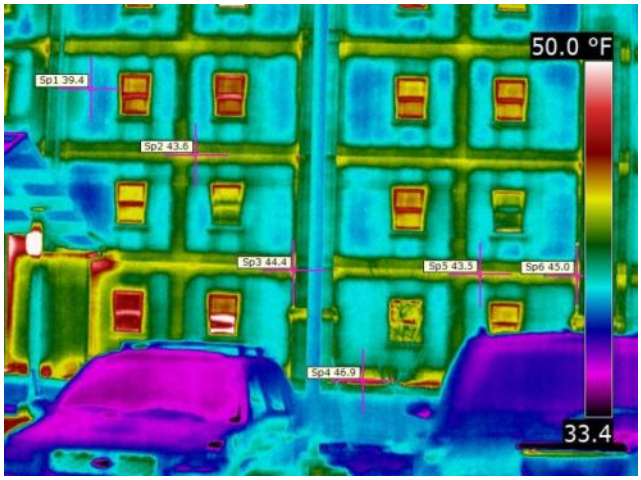

Figure 37. Mid-floor slab/wall junction TB.

These TB types are found in multi-level buildings. Again, the TB is partially developed due to the drastic direction change of the heat flow in the conductive medium. In this case, the intermediate floor causes a fin effect on the inside surface of the building. Additionally, the heavy structure of the floor, often a thermally conductive concrete slab, sometimes penetrates some or all of the way through the envelope's thermal control layer. Figure 37 shows a mid-floor slab/wall junction TB at a "dog bone" barracks at Fort Carson, CO. In this four-story building, the floor slabs and interior wall have been revealed by the thermal bridging effects. These are indicated by the green horizontal and vertical line patterns. The intersections between the green lines turn into a yellowish color, which means that temperatures are even higher, or in other words, there is a local heat transfer increase caused by the super imposed TB types (floor slab, building envelope wall and internal wall).

3.1.2.8 Highly conductive structural/attaching members

Structural members are commonly made of highly thermally conductive materials. They are placed vertically inside the building envelope walls at regular intervals, with additional members to support window and door lintels. Horizontal members can also be found at the floor and ceiling of a wall, and as lintels. The portion of the wall area composed by such members (framing fraction) can exceed 25% in light construction. Figure 38 shows a thermograph of a highly conductive member inside envelope walls at a tactical equipment maintenance facility, Fort Carson, CO. The thermographic image reveals vertical line patterns that are not produced by interior walls, but by a construction component possessing high thermal conductivity in between the walls. This building also exhibits high temperature profiles in the overhead door frames.

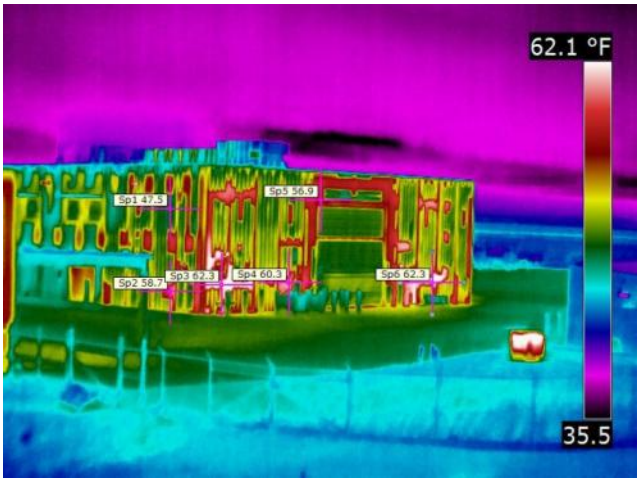

Figure 38. Highly conductive member inside envelope walls.

3.2 Review of Army documents for potential details

Beyond thermographic observation at the installations, this project will examine Army documents to determine the building and construction types that are prevalent enough to warrant detailed study and inclusion in the catalogue. The number and type of existing buildings can be obtained from the Army Real Property Inventory. The commonly used building construction types that are prevalent in the Army inventory should be evaluated against the Rated R-Value of Insulation and Assembly U-Factor, C-Factor, and F-Factor Determinations available and catalogued in Normative Appendix A of ASHRAE 90.1-2010.

3.2.1 Blast windows

Blast resistant windows represent a component not likely handled by DOE and therefore especially deserving of attention. A review of the issue indicates that many manufacturers are planning to release blast resistant, energy efficient windows, presumably NFRC certified. Nevertheless, blast-resistant windows do differ from standard windows; the framing requirements for blast resistant windows is substantially different then for conventional mounting, and the window frames often do not have thermal breaks.

In retrofit applications, blast resistant windows can add significant thermal bridging to existing structures, especially historical structures. Such buildings were often built with insufficient standoff distance from the road and might be subject to extra blast requirements. Some windows, for instance, must have additional reinforcing steel, as shown in Figure 39 (Webster, Reicher,

and Cohen 2006). Unfortunately, such solutions are largely site specific. Thus, it is important to develop a rapid turn-around, in-house capability for specific detail analysis, as discussed in Section 2.5.

Figure 39. Bracing flanks the window and transfers loads to the floor and ceiling. Photo credit: USACE Omaha District Protective Design Center. Used with permission.

3.2.2 Review of historical buildings reports

Reports on stocks of historical buildings over certain periods proved valuable to this work in that they often describe popular construction techniques, or even whole designs, which were repeated throughout the Army. For instance, "Unaccompanied Personnel Housing During the Cold War (1946-1989)" (Kuranda et al. 2003) describes the designs that were used repeatedly across the country during this period, along with features that constitute TBs, such as exposed concrete frames and metal doors and windows. This report has motivated more targeted drawings reviews and will result in useful detail catalogue pages for retrofit efforts.

3.2.3 Conclusions

It is anticipated that the catalogue will grow based on targeted drawing reviews and actual requests for guidance from building designers. The former will be guided by a study of which buildings are most prevalent. Con-

tinued use of thermography at other installations will also suggest details that deserve to be included. All the while, it is important to avoid redundancy, typical Army construction types should be evaluated against the data available in Normative Appendix A of ASHRAE 90.1 (already analyzed by the methods discussed in Sections 2.1.1 and 2.1.2).

4 Computer Models and Results

4.1 Modeling process

As mentioned in previous sections, HEAT2 and HEAT3 were selected as the primary simulation packages for quick analysis of the observed TBs. These model scenarios are selected from Table C1 (in Appendix C, p 126). Table C1 lists scenarios that resulted from several surveys performed at different Army facilities (much of which is described in Chapter 3), which is part of the first step in the modeling procedure adopted in this project. The process shown in Figure 40 gives a simple idea about how the numerical models are elaborated and implemented. Much of the work occurs in the data input acquisition step in an attempt to minimize the uncertainties of construction details, material properties, etc.

4.2 Modeling dimensional assumptions

As much as possible, 2-D simulations are employed over 3-D simulations for their relative simplicity of model construction. When the 2-D modeling is used, it is assumed that the planar heat flow pattern is repeated infinitely along the third axis. It is obvious that this does not happen in the real physical world, but for most cases with sufficiently long TB sections, this assumption generates relatively small discrepancies in the results, compared to the full 3-D scenario (Figure 41).

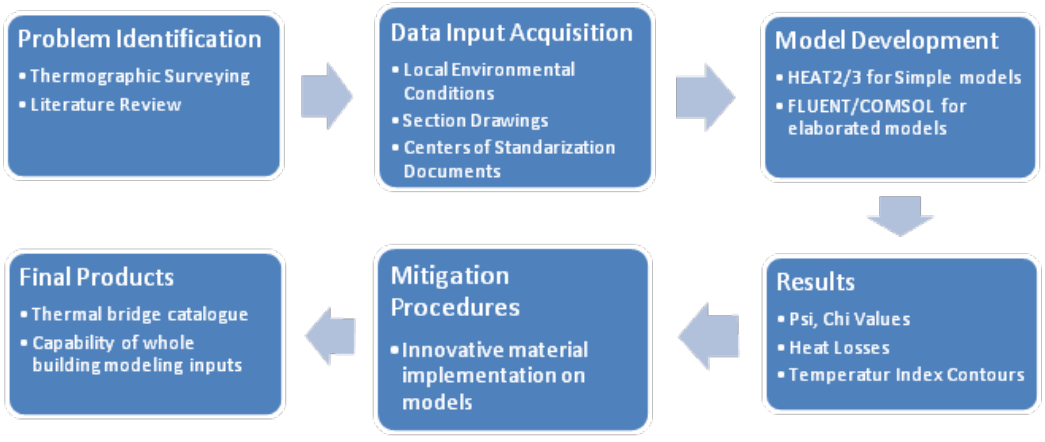

Figure 40. TB treatment process.

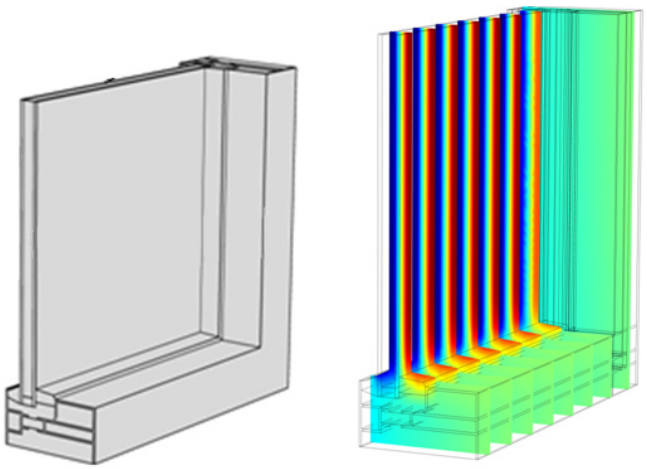

Figure 41. One fourth of a double pane glass window, 3-D geometry.

In Figure 41, the 3-D geometry of a window (left) was created in FLUENT to analyze the conduction heat transfer on a cold day with an exterior temperature of 15 °F outside and a building interior temperature of 72 °F. The window temperature contour profile in the 3-D geometry (right) has been highlighted for different depth sections. The illustration clearly shows that the 2-D temperature profile for each depth section stays relatively constant. Scenarios similar to this one in which a 3-D model will have a close-to-constant behavior in one of the axes will be modeled in 2-D, given that 2-D models are simpler to construct and less computationally expensive.

4.3 Models based on as-built drawings

4.3.1 Window frame/window frame joints

Extensive TBs scenarios were created in most of the facilities at Fort Carson, CO, where as-built drawings were most readily available. A model was developed based on the infrared images taken from Bldg 2132. Figure 42 shows a thermographic image of window frames in Bldg 2132, Fort Carson, CO. The infrared (IR) image color contrast generated by the multiple high temperature profiles indicate that the windows within the white rectangle have frames that show high temperature profiles, which represent high losses, and are therefore good objects for a study.

After identifying the multiple TBs scenarios in this building, the next step is to acquire the building's as-built drawings, specifically architectural detail drawings showing window frame junction with the wall.

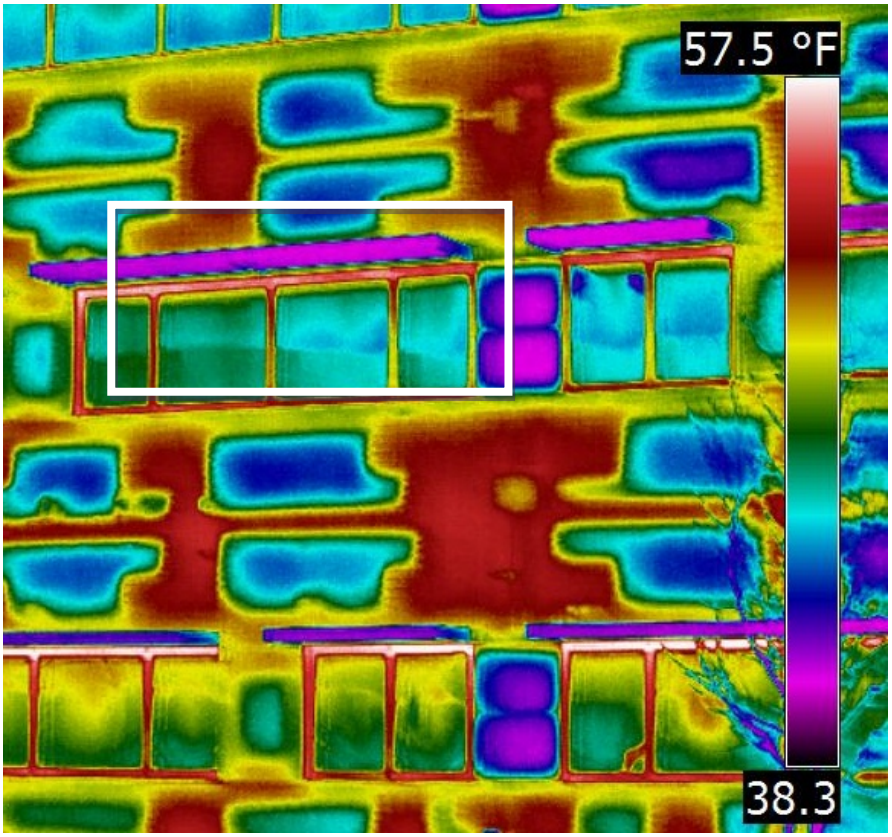

Figure 42. Thermographic image of window frames in Bldg 2132, Fort Carson, CO.

Figure 43 shows several geometrical complexities in the window frame section. It can be seen that the actual window frame joint shown in Figure 43 has a relatively complex geometrical configuration. For modeling purposes, this geometry is simplified as far as it does not affect the heat propagation from the interior side of the building to the exterior side. For the 2-D model, some of them will be omitted, while for the 3-D model some of them will be included. The 2-D model, for instance, will not include the impact of the bolt shown here.

The model shown in Figure 44 is intended to be used to study the temperature profile and heat flux effects through the window frame, along with the frame/wall joint TB effects. (Note that the model shown in Figure 44 includes several geometrical simplifications, such as removing the window frame connecting bolt, etc.) The manufacturer does not consider these joint effects by in the window U-factor calculation. Some computational details such as the frame cavities' heat convection are modeled by the software based on the ISO Standard 10077-2 algorithm.

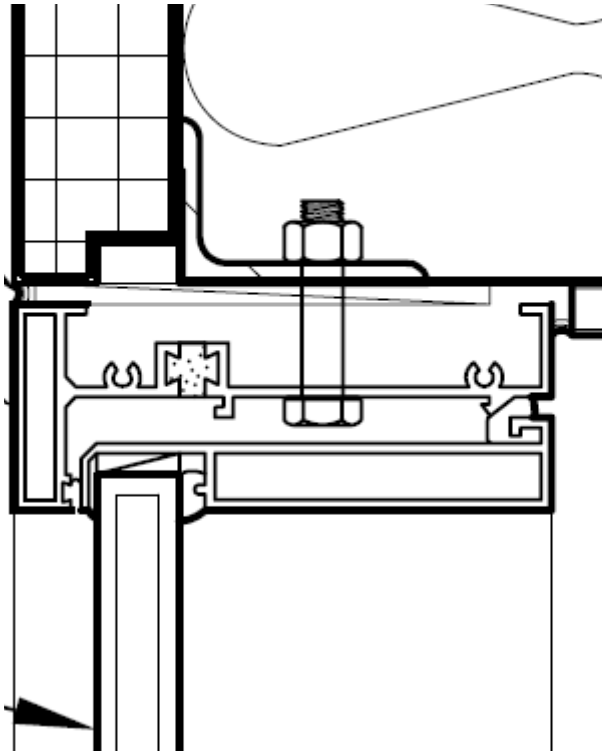

Figure 43. Window frame joint section detail drawing.

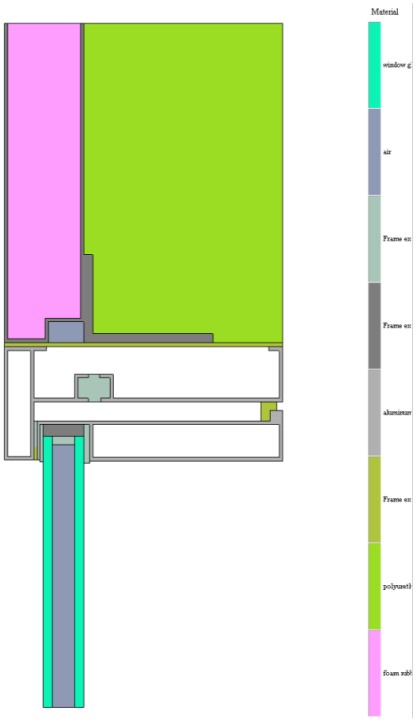

Figure 44. HEAT2 model of a window frame and joint in Bldg 2132, Fort Carson, CO.

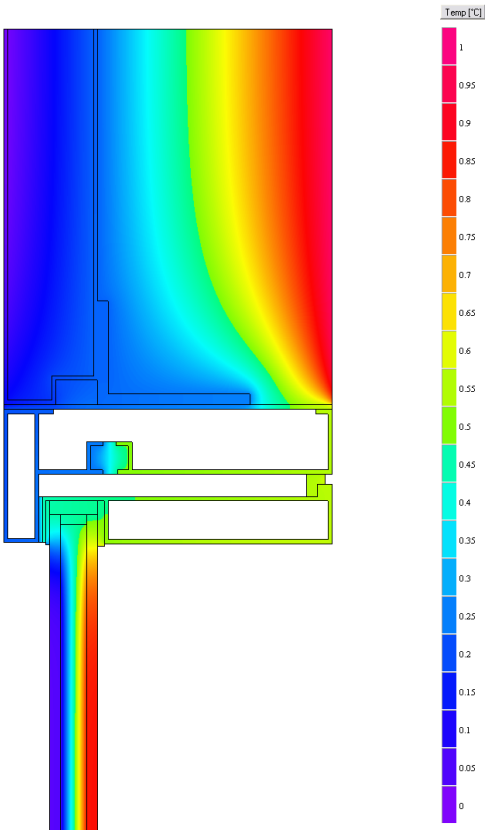

Figure 45. Window frame joint temperature profile.

Figure 45 shows model simulation temperature results, in which the building envelope wall and the window glazing stay at building interior temperatures while the window frame demonstrates its high thermal conductivity by having the lower temperatures in the interior section. This plot contains temperature index values, not the actual interior/exterior temperature values. According to the window temperature profile results, most of the building interior stays warm while the exterior stays cold (blue on the left side and red on the right side). This is expected. One exception is that the window frame has much lower temperatures than other interior surfaces. Due to the high thermal conductivity of the metal frame, the heat is conducted to the outside of the building envelope wall even though this frame has a thermal break. Also, the wall joint plays an important role in the transferred thermal energy to the outside, as described in Figure 22 (p 48).

4.3.2 Building foundation/ground heat transfer

Similar to the window frame/ window frame joint scenario, most of the inspected Army facilities in Fort Carson, CO experienced thermal losses through their foundations, as evidenced by the IR images.

Figure 46 shows a close up IR picture of one of the Dining Facilities that reveals the heat losses through the ground. Yellow regions indicate that the bricks posses uniform temperature with the exception of the "at grade" regions. The mixture of blue, purple and green regions indicate the low temperatures found in the soil surrounding the building envelope. The image reveals where the losses are at the grade level but it does not reveal the ones that are below the grade level, which, in the model discussed below, are shown to be higher. In other words, this profile reveals the absence of an effective thermal break component between the wall and the floor slab or, similarly, the improper installation of foundation edge insulation.

An evaluation of the foundation detail drawings (Figure 47), intuitively confirms what the IR image shows; there is a direct heat path between the inside and outside regions of the building through the cast concrete medium. As mentioned in Chapter 2 (Figure 23, p 50), an inadequately insulated foundation is expected to have these heat losses.

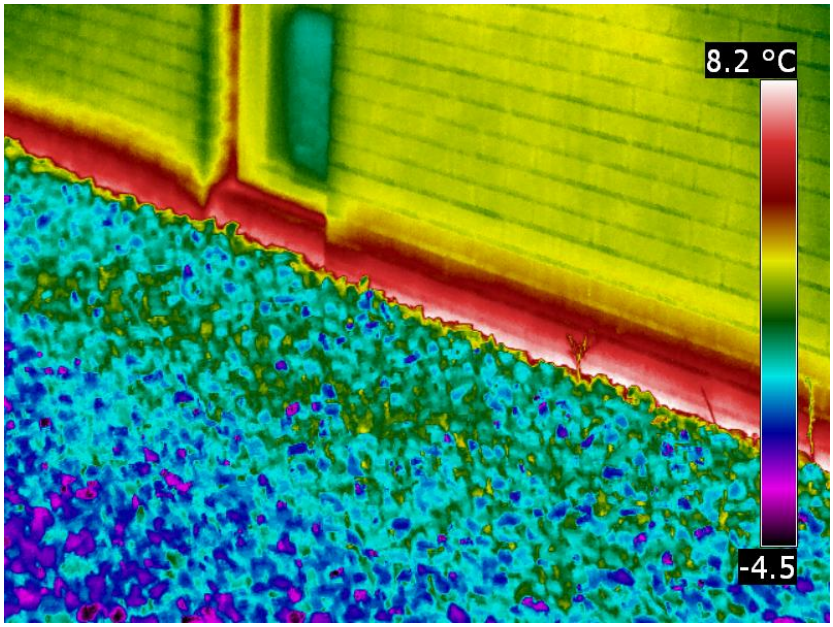

Figure 46. Thermographic image of slab-ground and slab-wall interaction in Bldg 1444, Fort Carson, CO.

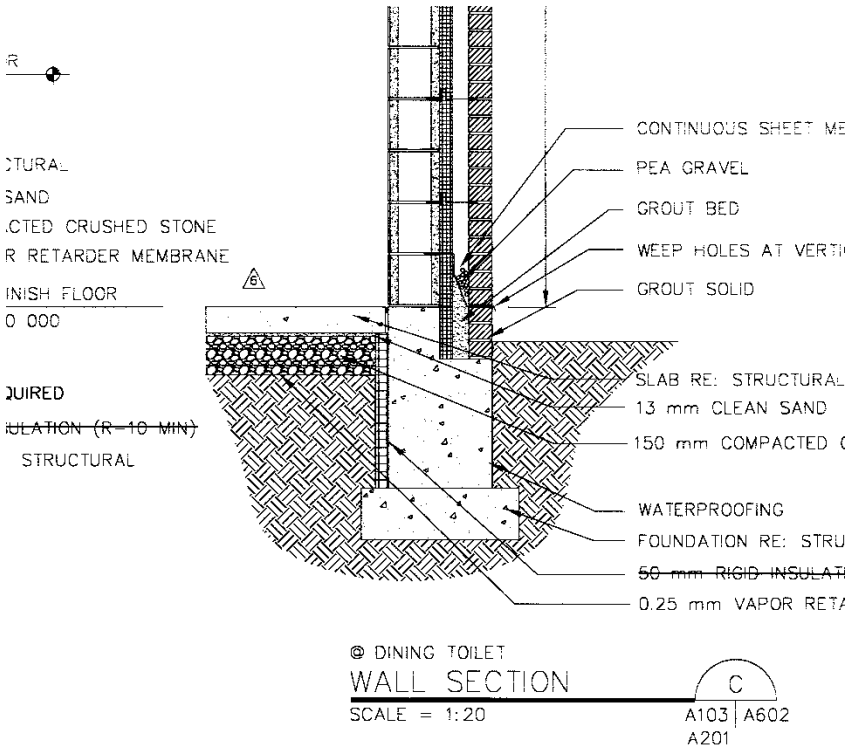

Figure 47. Bldg 1444 foundation as-built detail drawing. Air, brick mortar and cast concrete are some of the materials contained in the building envelope wall.

The building foundation is one of the most challenging TB scenarios to model, due to all the uncertainties associated with the soil properties and equivalent thermal transmittances (Figure 48). ISO 10211 provides a guideline to select the appropriate boundary conditions for this scenario based on several building geometrical parameters. This model has been made with the inclusion of the edge insulation (as shown in Figure 47). Components such as flashing and steel studs also have been included in this 3-D model.

The building foundation thermal simulation results show the relative increase in temperature at the grade level (Figure 49). Temperature index has been used instead of actual temperature values, and the temperature scale has been adjusted to highlight the high temperature profiles outside the building envelope. The soil was assumed to be uniform, having a flat geometry with a constant thermal conductivity. This might be the main reason why the highest exterior temperatures profiles are found in the soil grade/wall interface and not in the wall itself, as would be inferred from Figure 46. Note that the temperature scale in this image has been biased to create more contrast in the region of interest, thus the homogenous pink area in the rest of the figure.

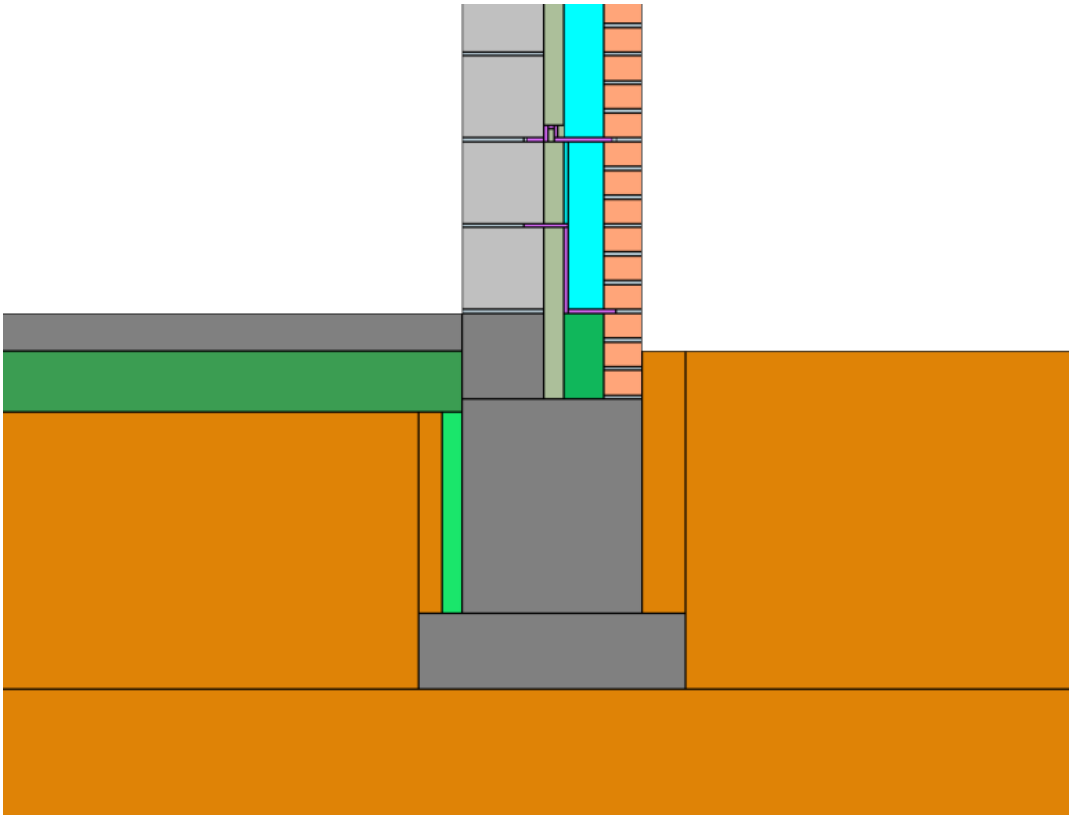

Figure 48. HEAT3 Bldg 1444 foundation model. Bricks, CMUs, cast concrete and a rigid insulation have been implemented in the wall section, as indicated in the as-built detail drawing.

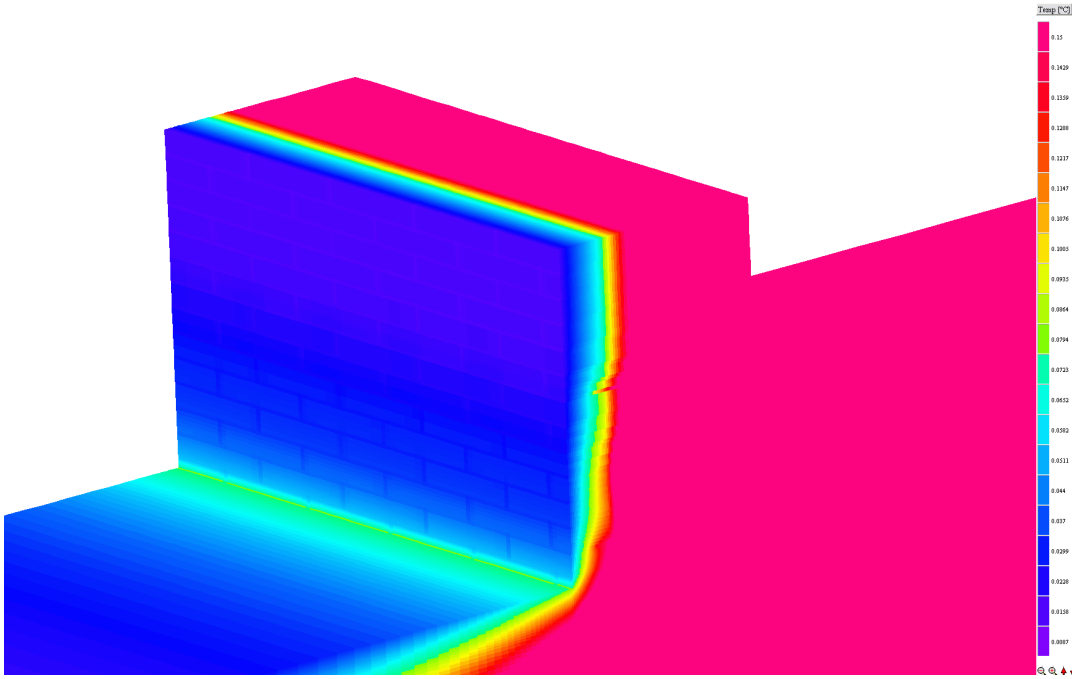

Figure 49. Bldg 1444 foundation temperature profile.

4.3.3 Wall/wall intersections

Given the exterior concave wall/wall intersection in Bldg 1552 at Fort Carson, CO, a positive external ψ-value would be expected, i.e., external ψ-values are computed in comparison with a UA computation using the external area of the building (see Section 2.2.2.1). Indeed, the geometric anomaly is evident in the thermographic image shown in Figure 50; the intersection has the highest temperature profiles. Two-dimensional heat transfer can be assumed in a top plane view cross section given that this geometry has only minor variations along the wall height.

The top view wall/wall intersection detail drawing (Figures 51 and 52) show a uniform construction layering despite the corner (CMU-Insulation-Air-CMU). The wall shown in Figure 51 consists of simple geometry and components. CMU's of 200 and 100 mm (8 in. and 4 in.) compose the interior and the exterior sides of the wall respectively, enclosing an air cavity and a rigid insulation. As such, this geometrical TB is not caused by the choice of materials used in the wall. Note that the drawing also shows the junction of a window frame jamb, which is not included in the model.

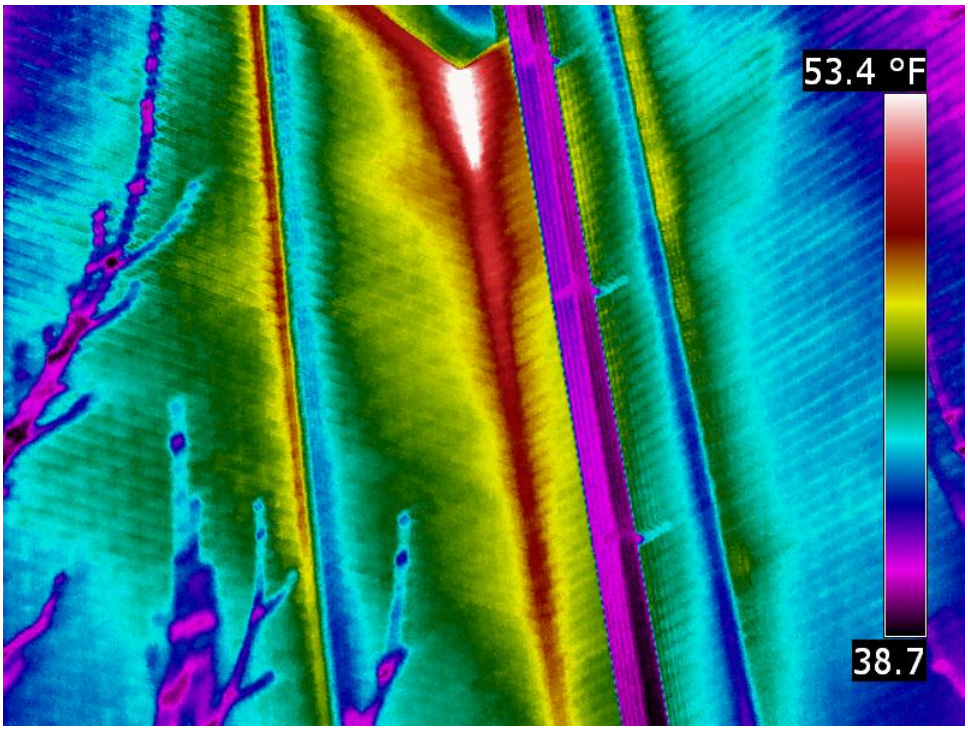

Figure 50. Thermographic image of wall/wall intersection at Bldg 1552, Fort Carson, CO.

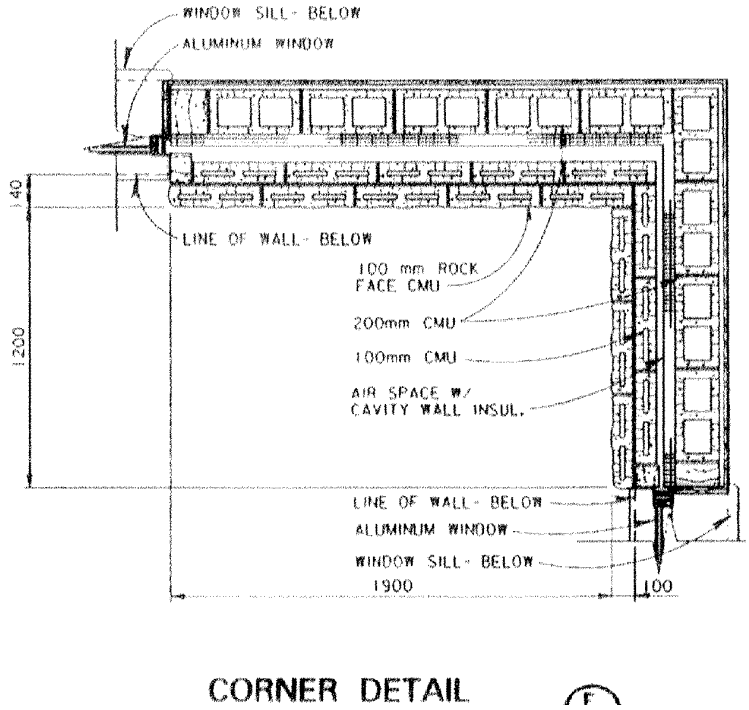

Figure 51. Bldg 1552 wall/wall intersection as-built detail drawing.

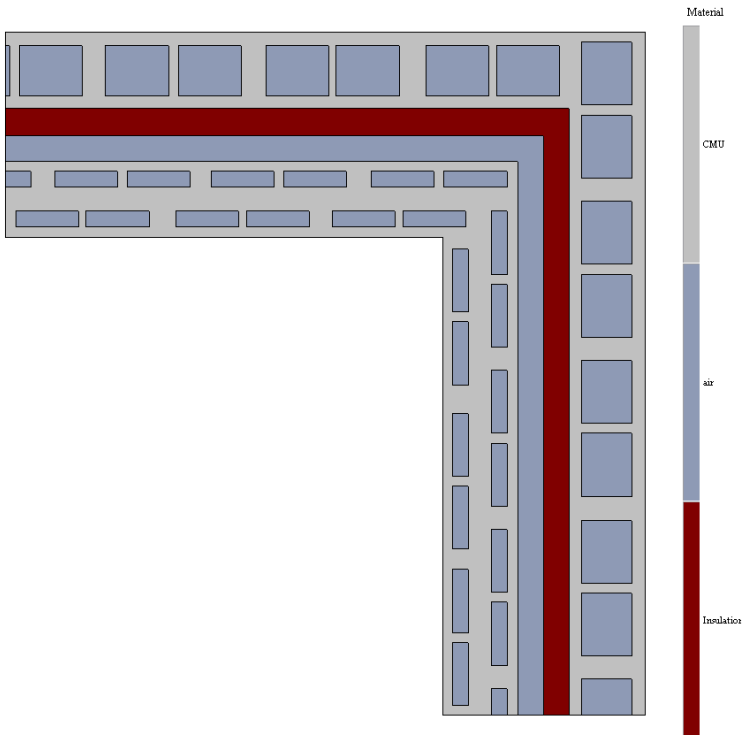

Figure 52. Wall/wall intersection model of Bldg 1552, Fort Carson, CO. Grey indicates the CMU concrete, red indicates the insulation and light purple indicates the air spaces.

The 2-D model of the wall intersection incorporates 1 meter measured from the interior surface intersection point. Because this model simulates heat transfer only in two directions, an implicit assumption is that any displayed result will be the same along the wall height.

Figure 53 shows the temperature contour plot of this model. The wall insulation and air gap cause the majority of the temperature change gradient in the all, similar to the thermal break inside the metal window framing (Figure 45). Unlike Figure 49, the temperature profile is scaled to the actual indoor and outdoor temperature, so this effect is visible. Zooming in on the corner and adjusting the temperature scale allows one to observe some of the warm corner effect seen in Figure 54; it also fails to fully explain the temperature anomaly, and causes one to question whether some of the apparent problem results from poor execution at this detail. Note that a magnification and a temperature scale adjustment were made in Figure 54 to identify this apparent thermal "discontinuity" generated by the geometrical anomaly. This "warm corner" explains some of what is seen in the thermograph in Figure 50.

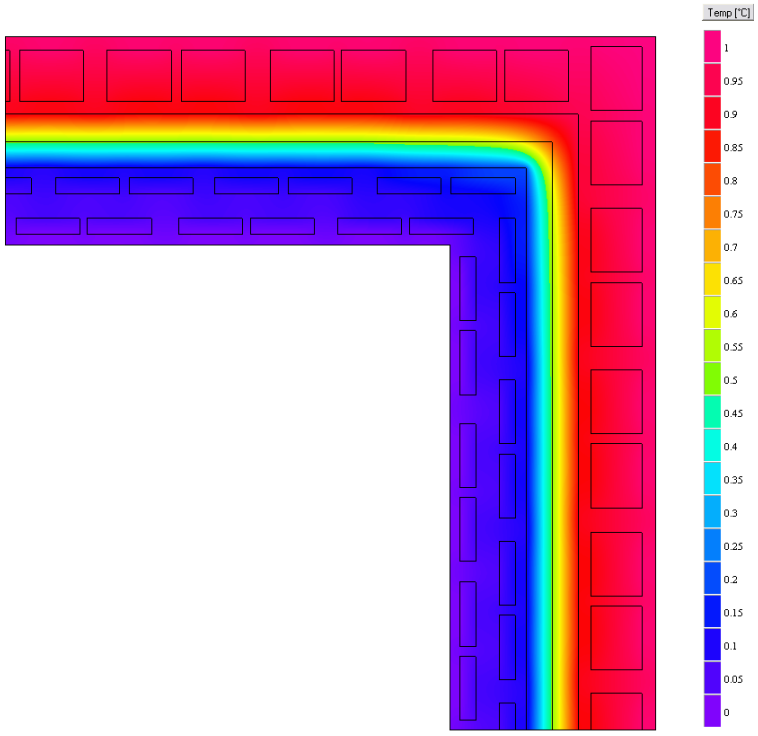

Figure 53. Bldg 1552 wall/wall intersection thermal simulation temperature index contour plot. Red indicates the highest temperatures and blue indicates the lowest temperatures, corresponding to the exterior environment temperature.

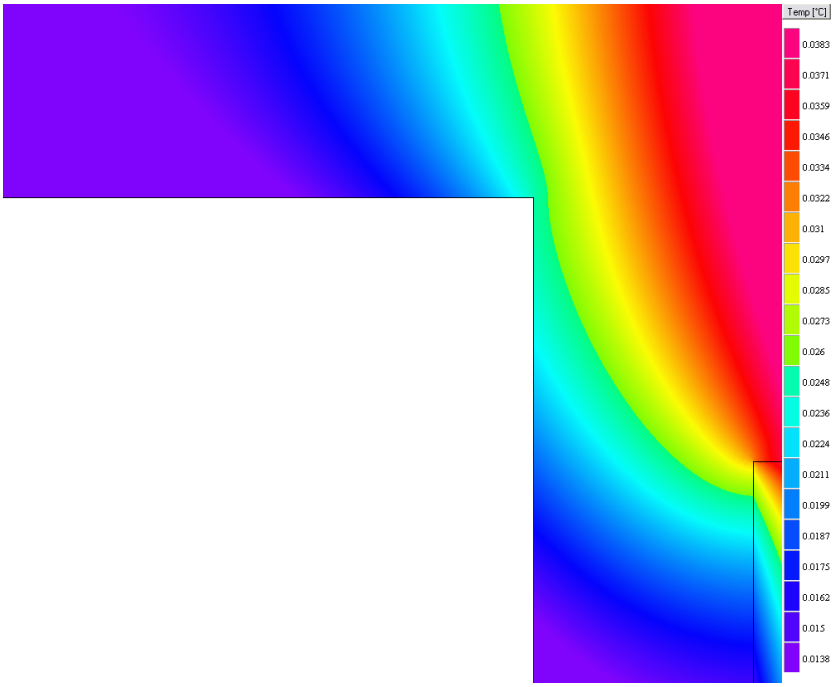

Figure 54. Temperature index profile in the same wall/wall intersection shown in Fig. 53.

4.4 Parametric simulation approach

Parametric simulation results can be used to define optimum design regions, combining variables such as long-term durability, cost, insulation thickness, length, and thermal conductivity, among others. It is also possible to do return on investment (ROI) analyses according to the selected material and the proportions used. An example of this can be how cost effectively we can implement the use of aerogel on specific sites compared to conventional polyurethane foam insulation.

Figures 55 and 56 show two examples of preliminary parametric studies done on this project. Such analyses will be used to settle on optimum mitigation strategies where there are competing ideas. The parametric simulations shown in Figure 55 consisted in running simulations using different insulation materials and changing the insulation material thickness for each of the used materials and study what are their effects on the overall heat transfer coefficient of the window (U-factor). The costs are proportional to the material type and also proportional to the material volume. This graph in Figure 56 is a 3-D representation of the plot in Figure 55, which makes it easier to distinguish the “knee” region of the surface and to focus on that region in the material type-dimension selection.

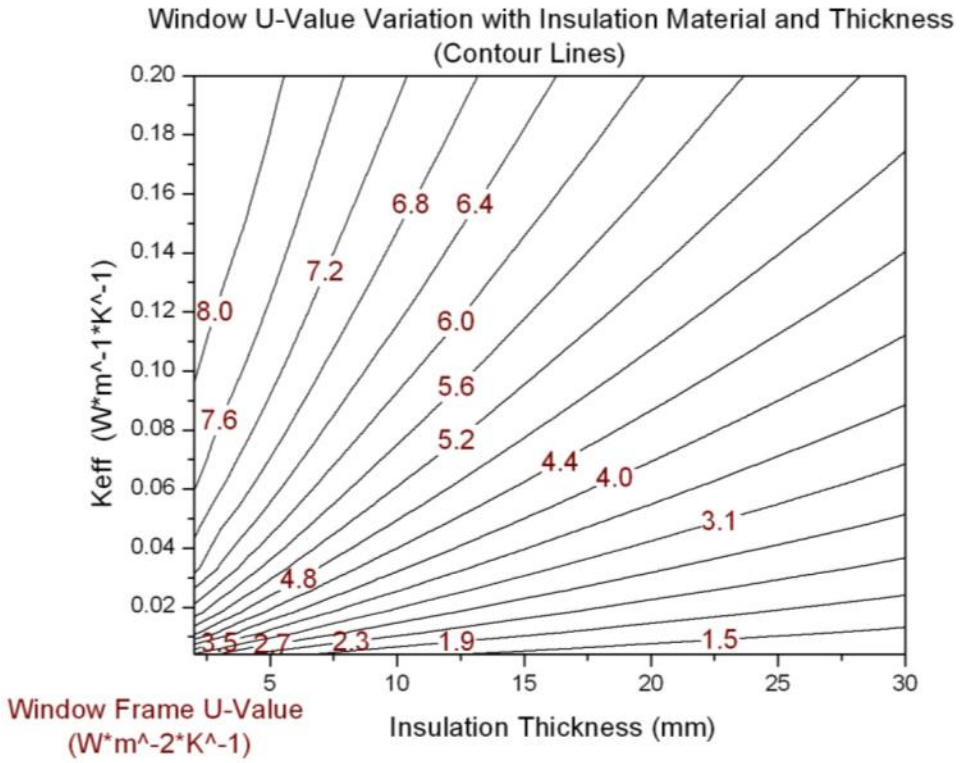

Figure 55. Parametric simulation results plot of heat transfer in window frame.

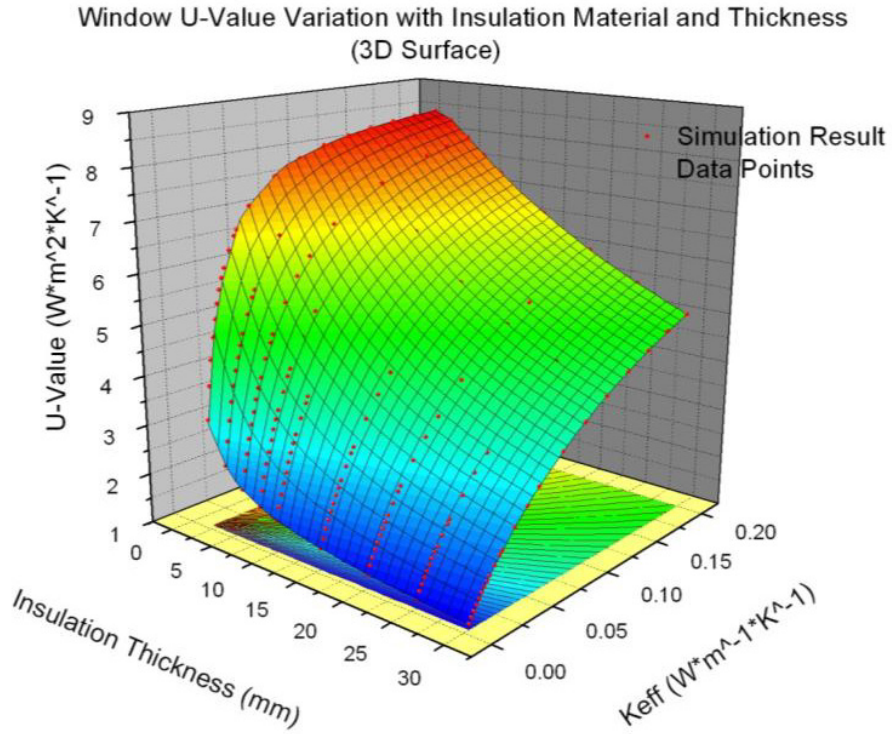

Figure 56. Parametric simulation results plot of heat transfer in window frame, 3-D plot.

5 Energy Efficient Insulation

5.1 Introduction

The energy efficiency of the building enclosure is based on the material properties in the building envelope. When properly installed, building insulation has been determined to save energy by reducing the heating and cooling cost of maintaining the comfort levels. ERDC-CERL recently performed infrared photography of buildings at Fort Bragg and Fort Carson to determine where the heat losses were located. The results pointed to many retrofit possibilities, of which the most important would be to install an insulating layer over the TBs. Retrofit applications, especially, place unusual demands on building materials. This chapter describes efforts in testing the properties of several cutting edge building materials that have, to date, not been tested sufficiently to specify their use in building envelopes.

The energy efficiency of a building can be further improved by using materials known as phase-change material (PCM). Insulation materials that contain PCMs attempt to dampen the extreme temperatures a building will experience through one daily cycle and keep the building at a more steady-state. By dampening the extreme temperatures through one daily cycle, the demands on the environmental control systems are reduced as are the overall energy demands of the building. The use of PCMs also shifts the time when the energy is needed, thus reducing energy costs (when energy demand is lower).

5.2 Conventional insulation

Conventional insulation materials reduce heat flow by using materials that have a low effective thermal conductivity. This is often achieved by trapping air or an inert gas in small pockets in the material. Although inert gasses are less conductive than air, they can leak out of the insulation over time.

The efficiency of the insulation is measured by the insulation R-value, or thermal resistance. The R-value is the ratio of the temperature difference across the insulation to the heat flux, which is given by:

$$R = \frac{\Delta T}{\dot{Q}_A}$$

where:

ΔT = the change of temperature
$\dot{Q}_A$ = the heat transfer per unit area and R is the R-value.

5.2.1 Insulation materials

This study tested four commercially available, standard insulation types: (1) Dow polystyrene, (2) standard fiberglass, (3) Aspen Aerogel, and (4) Honeywell's polyurethane. Table 14 lists the four tested insulation materials, their experimental thermal properties (derived through testing), and the cost per square foot. The sample size needed to test in the LaserComp Fox801 (Heat Flux Analyzer) was 30 x 30 in. Thus, each material sampled was cut or formed to this size.

Table 14. Experimental thermal properties of the insulation materials and the standard deviations of the values.

Sample	Conductivity (W/mK)	Heat Flux (W/m²K)	Thickness (mm)	R /in. (sq ft°Fh/BTU)/in	Cost (per sq ft)
Dow Polystyrene	0.02807	13.7915	51.1015	5.1169	$1.28
	σ = 0.00063	σ = 0.08	σ = 0.0636	σ = 0.0318	
Standard Fiberglass	0.05680	11.8337	88.9000	3.4324	$0.31
	σ = 0.07706	σ = 0.43956	σ = 0.00000	σ = 0.12956	
Aspen Aerogel	0.01569	39.5919	9.9265	9.1932	$4.00
	σ = 0.00038	σ = 1.80142	σ = 0.36341	σ = 0.22168	
Honeywell Polyurethane	0.02516	12.1600	51.7563	5.7569	$2.00
	σ = 0.00048	σ = 0.22925	σ = 0.39726	σ = 0.08363	

5.2.1.1 Closed-cell spray polyurethane foam (CCSPF)

CCSPF is a two component mixture that is sprayed into structural cavities and is then allowed to expand to fill a cavity to provide insulation. CCSPF insulation materials work by trapping a gaseous blowing agent inside the structure of the foam. Sprayed applied polyurethane foam reduces air infiltration and reduces energy consumption. The CCSPF insulation that was used in this study is manufactured by Honeywell and was precut into 30 x 30-in. size samples. Figure 57 shows the CCSPF sample used for testing.

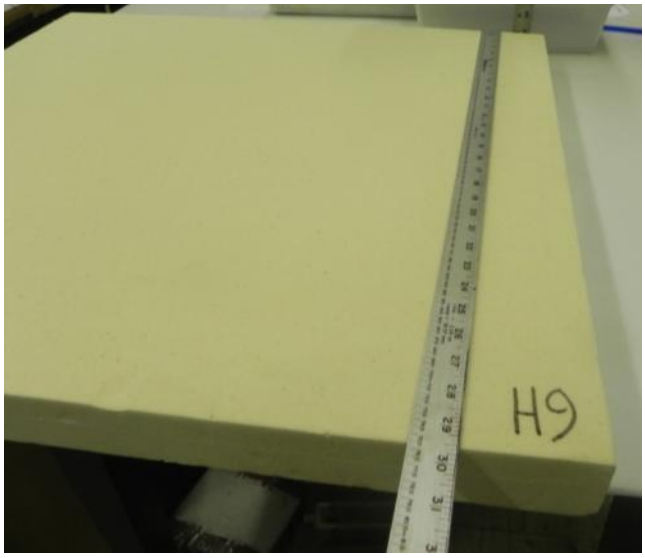

Figure 57. CCSPF sample.

5.2.1.2 Aerogel insulation

Aerogels are extremely low-density solids with a very low thermal conductivity. The porous silica traps gas inside the structure of the aerogel, with 99.9% volume being gas; the high gas content allows for the aerogel's density and thermal conductivity to be very low. The average density of an aerogel is about 1.9 mg/cm^3 (6.86·10^{-5} lb/in^3). The structure of aerogel prevents the gas, which typically has a very low thermal conductivity, from circulating. The composition and structure of aerogels greatly restricts the three methods of heat transfer (convection, conduction, and radiation). Silica aerogels conductivities range from 0.03 W/m·K (0.05 Btu/[hr·ft·°F]) down to 0.004 W/m·K (0.007 Btu/[hr·ft·°F]), corresponding to R-values of 14 (RSI-value of 2.47) to 105 (RSI-value of 18.49). Aerogel's melting point is 1200 °C (2192 °F).

This work studied and tested the aerogel insulation Spaceloft®, made by Aspen Aerogels® (Figure 58). Spaceloft® is a flexible, nanoporous aerogel blanket insulation. The insulation is composed of silica aerogel and is reinforced by polyester fibers, which allows the insulation to have low thermal conductivity, and gives it flexibility and resistance to compression.

Figure 58. Aspen Aerogel's Spaceloft® insulation.

5.2.1.3 Fiberglass insulation with backing

The fiberglass insulation used in the study is the traditional insulation installed in buildings, manufactured by Johns Manville (Figure 59). Fiberglass insulation consists of intertwined, flexible glass fibers that trap air. The trapped air, which has low thermal conductivity, is prevented from circulating, which reduces heat transfer through convection and conduction. The fiberglass tested has a paper coated backing material to prevent moisture from entering the product.

Figure 59. Fiberglass insulation.

5.2.1.4 Extruded polystyrene

Extruded Polystyrene insulation is closed-cell foam that is composed of rigid, cell structures that trap a gas. Like the other insulation materials being studied, the gas trapped in the polystyrene structure reduces the thermal conductivity below what would be achieved with air. The polystyrene being used in this study is produced by Dow Chemical Company. In applications, this polystyrene is part of an insulation system called Exterior Insulation and Finish System (EIFS). Figure 60 shows one of the polystyrene samples used in our study. Since this insulation system comes in 24-in. widths; an extra 6 in. was required for a complete 30 in. sample.

5.2.2 Thermal properties test methods

The thermal properties of the insulation materials (thermal conductivity, heat transfer, etc.) were determined by using a LaserComp Fox 801 Heat Flux Analyzer (H/F Analyzer, see Figure 61). A total of 9 samples of each of the four products were used to determine and verify the thermal properties of the insulation materials. The testing of the samples followed ASTM Standards C518 and C1058. The heat-flux analyzer determines the thermal properties of samples by creating a temperature gradient between a hot and cold plate. By using ASTM Standard C1058, the upper and lower temperatures were set to 18 °C (64.4 °F) and 43 °C (109.4 °F).

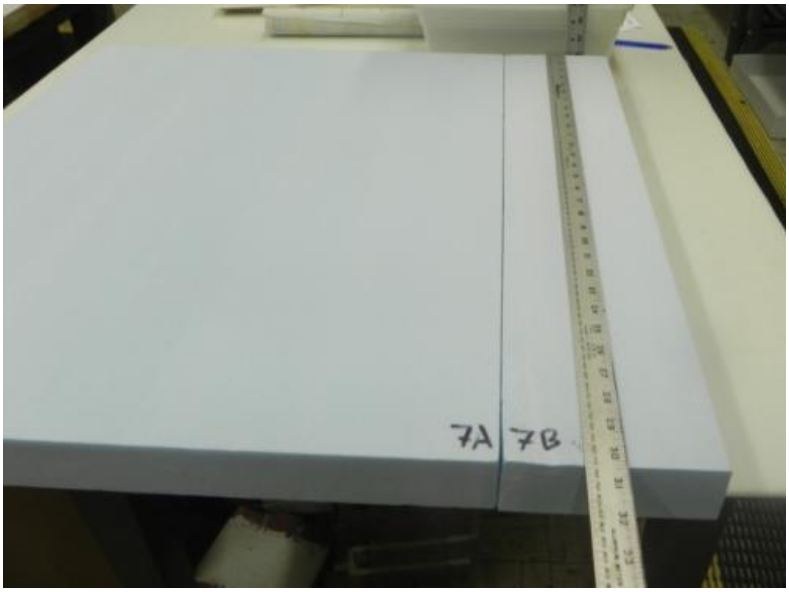

Figure 60. Polystyrene insulation.

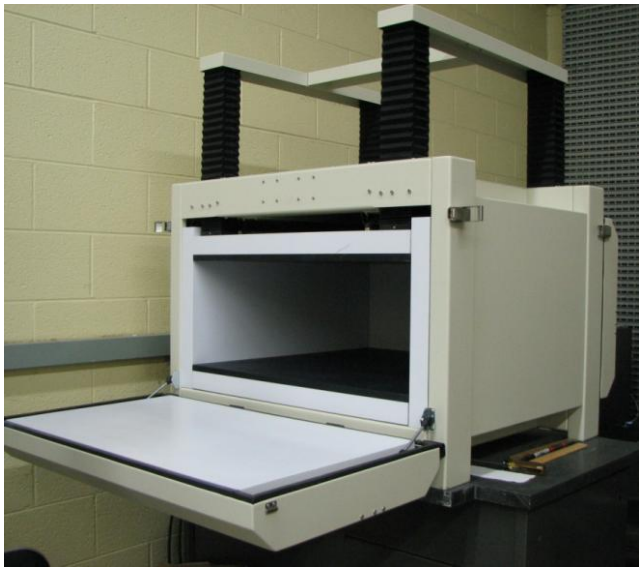

Figure 61. LaserComp Fox801 Heat Flux Analyzer.

After analyzing the sample, the heat-flux analyzer outputs the average temperature, conductivity, and heat flux. All of the samples were cut to the dimensions of 30 x 30 in, and the thickness of the samples was determined by the heat-flux analyzer. For non-rigid insulation materials, such as the fiberglass insulation, the thickness was set to 3.5 in. Table 14 lists the experimental thermal properties of the tested insulation.

To determine the aging effects of the insulation materials, all of the samples were placed in a temperature and humidity chamber (T/H Chamber) for different increments of time. The samples were left in the temperature and humidity chamber for 1 week and 1 month under steady-state conditions, and were thereafter put under cyclic conditions for 3 months. The samples were conditioned in the T/H chamber under steady-state conditions followed ASTM Standard C870. In future testing, the samples will be under cyclic conditions following ASTM Standard C1512. After conditioning in the temperature and humidity chamber, the samples were immediately tested in the heat-flux analyzer following the test methods described above. For each time increment (1 week, 4 weeks), three samples were tested. For the steady-state tests, the temperature and humidity was set to 65.56 °C (150 °F) and 90%, respectively. For the cyclic testing, the temperature and humidity will be varied between 4.44 °C (40 °F) and 10% to 65.56 °C (150 °F) and 90% in a 24-hr time period, respectively. Figures 62 and 63 show the experimentally derived aging effects of the thermal properties of the tested insulation.

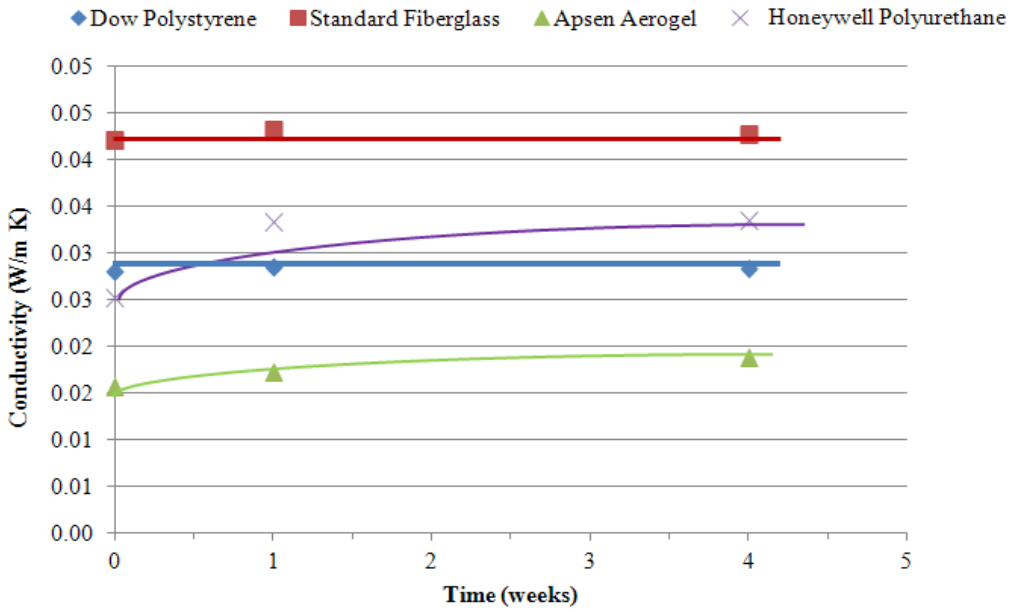

Figure 62. Degradation effects of the thermal conductivity for given increment of time.

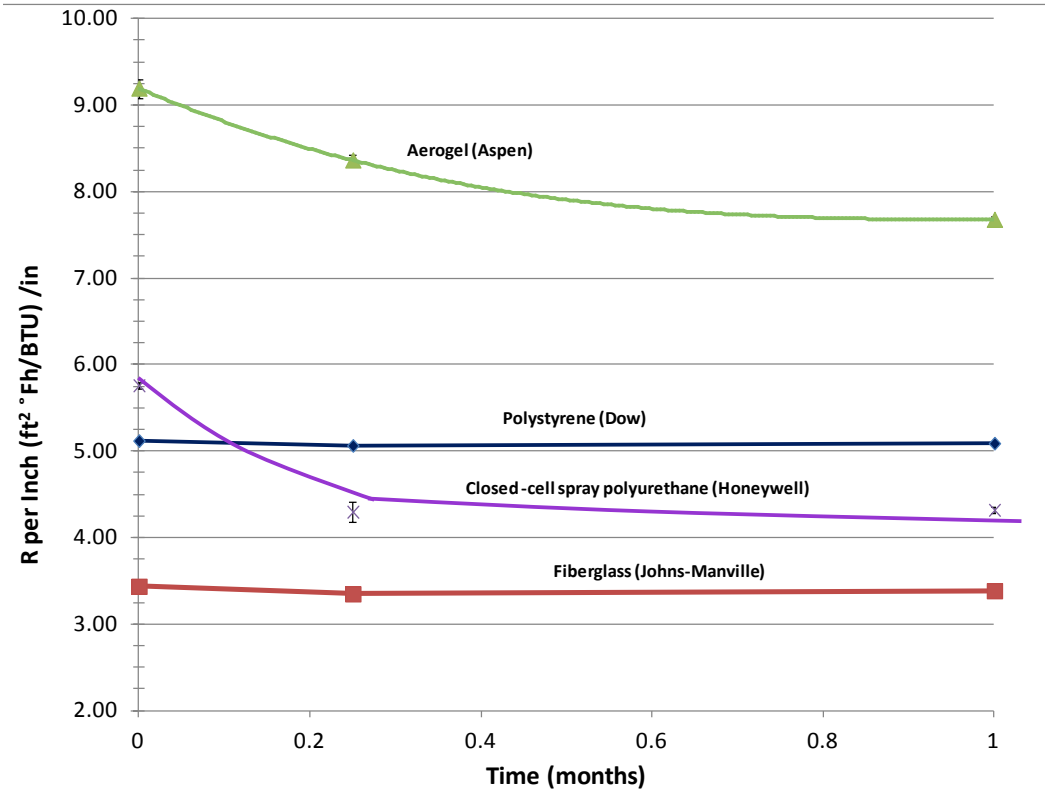

Figure 63. Degradation effects of the R-value for given increment of time.

5.2.3 Insulation aging

The four different insulation materials were tested under controlled conditions to observe the effects that prolong exposure to high temperature and humidity had on the insulation materials. As stated in Section 5.2.2, the samples were left in the temperature and humidity chamber for 1 week and 1 month under steady-state conditions, and were then left in the chamber for 3 months under cyclic conditions. For the steady-state tests, the temperature and humidity were set to 65.56 °C (150 °F) and 90%, respectively. For the cyclic testing, the temperature and humidity will be varied between 4.4 °C (40 °F) and 10% to 65.56 °C (150 °F)and 90% in a 24-hour time period, respectively.

For the steady-state testing, all four insulation materials experienced some degradation for the R-value and thermal conductivity from the original samples. The thermal conductivity of the Dow Polystyrene and the standard fiberglass insulation materials degraded less than 2.5%, and the R-value remained fairly constant between the 1-week and 1-month samples. The thermal conductivity of the Aspen Aerogel and the Honeywell polyurethane insulation materials degraded by roughly 10% and 33% in the 1-week samples, respectively. The Aspen Aerogel insulation degraded a further 10% between the 1-week and 1-month samples, while the Honeywell polyurethane insulation R-value remained relatively constant between the 1-week and the 1-month samples.

Since the R-value is the inverse of the thermal conductivity of the sample, the same degradation trends that are seen in the thermal conductivity of the samples are also seen in the degradation of the R-value of the samples. The R-value of the Dow Polystyrene and the standard fiberglass insulation materials degraded by less than 3%, and there was not much change between the 1-week and the 1-month samples. The R-value of the Aspen Aerogel and the Honeywell polyurethane insulation materials degraded by roughly 10% and 25%, respectively. The Aspen Aerogel insulation degraded a further 3% between the 1-week and 1-month samples, while the Honeywell polyurethane insulation degradation remained relatively constant between the 1-week and the 1-month samples.

Beyond the degradation of the thermal properties of the samples, there were minor physical changes to the specimens. After conditioning, the Aspen Aerogel sample A1, started to develop crystals on the surface (Figure 64).

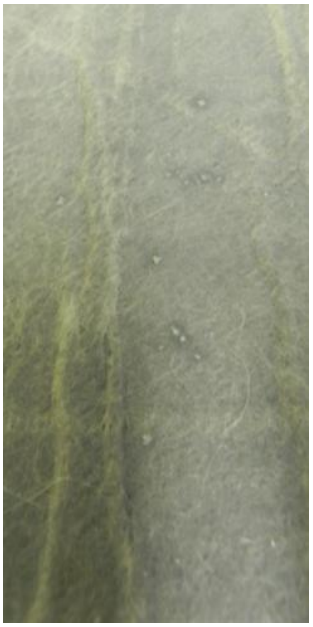

Figure 64. Crystals on a post-conditioned Aspen Aerogel sample.

Figure 65. Post-conditioned polyurethane samples in the temperature and humidity chamber. Note: the middle samples are the post-conditioned samples.

Only one of the aerogel samples showed signs of crystal growth, but it is difficult to determine if the crystals were from an external source, or if they grew naturally from materials within or on the sample. The Aspen Aerogel appears to be hydrophobic (rejecting moisture), as evidenced by the fact that water droplets pool on the surface of the sample.

A few of the polyurethane samples started to bow and deform as a result of exposure to 65.56 °C (150 °F) and 90% relative humidity. This was likely due to the samples being recently manufactured by the producer and not given enough time to cure properly, or the "skin" being removed to have a correctly sized sample. In general construction applications, the sprayed -on polyurethane will not be cut. Figure 65 shows three polyurethane samples being placed in the temperature and humidity chamber with varying degrees of deformation. The other two insulation materials showed little or no physical changes when conditioned in the temperature and humidity chamber. A new sample preparation strategy for closed-cell polyurethane foam samples will be employed in the next round of thermal cycling/LaserComp

tests, which is expected to circumvent these deformation problems. Also, in future conditioning and R-value testing, moisture accumulation will be ascertained for each sample by using differential mass analysis.

5.2.4 Future testing and service life prediction

These initial testing results indicate that two of the insulation materials (viz., aerogels and polyurethanes) decrease in R-value over time as they are exposed to elevated temperatures and moisture. It is not clear from these early experiments which parameter is more important; in fact, plans for future experiments have been developed to evaluate the R-values as a function of time at several temperatures and relative humidity exposure in accordance with the test matrix shown in Figure 66.

It is believed that the mechanism of degradation may be due to diffusion of moisture into the materials. Generally the degradation of properties of materials under these conditions may be expressed in accordance with the following equations (McManus et al. 2009):

$$\frac{\partial c}{\partial t} = k_c M_c (1-c)^n exp\left(\frac{-E_c}{N_A K T}\right)$$

$$c = \frac{(R_{t0} - R_t)}{(R_{t0} - R_f)}$$

where:

C = the dimensionless parameter of hydrothermal degradation; c=0 is new material, c=1 is fully degraded material.
M_c = moisture content, and is dimensionless so that M_c=0 when the material is dry and M_c = 1 when the material is fully saturated
E_c = activation energy (from empirical data fit).
T = temperature
N_A = Avogadro's number
K = Boltzman's constant
k_c = rate parameter (to be fitted from test data)
n = exponent from empirical data fit
R_{t0} = R-value at time, t_0
R_t = R-value at time, t
R_f = fully degraded R-value.

Thus the rate of R-value degradation is predicted by $\frac{\partial c}{\partial t}$.

Test Matrix for Insulation Steady State																	
		Round 1		Round 2		Round 3		Round 4		Round 5		Round 6					
Sample Type	Thickness	Temperature (deg F)	Humidity	Temperature (deg F)	Humidity	Temperature (deg F)	Humidity	Temperature (deg F)	Humidity	Temperature (deg F)	Humidity	Temperature (deg F)	Humidity	Exposure Time (Month)	Exposure Time (Week)	Laser Comp 801 Conductivity Testing
Honeywell Polyurethane (PU) Foam	2 inch	180	90%	150	90%	120	90%	90	90%	180	30%	90	30%	1	1	Before/After Exposure
Aspen Aerogel	0.4 in	180	90%	150	90%	120	90%	90	90%	180	30%	90	30%	1	1	Before/After Exposure
Dow Polystyrene-Xnergy	2 inch	180	90%	150	90%	120	90%	90	90%	180	30%	90	30%	1	1	Before/After Exposure
Standard: Fiberglass	3.5 inch	180	90%	150	90%	120	90%	90	90%	180	30%	90	30%	1	1	Before/After Exposure

Figure 66. Test Matrix for future experiments to determine R-values as a function of temperature, moisture and time.

This model assumes an Arrenhius-type term for hygrothermal degradation, dependant on activation energy (E_c), temperature (T), and moisture concentration (M_c), and variance with time (t). This sort of model was employed by McManus, who incorporated a moisture concentration term in his modification of existing Time-Temperature-Superposition (TTS) equations for predicting the long-term behavior of composite materials based on short-term testing. In future experiments, the weight gain due to increased moisture content as a result of exposure will be measured, and the data will be used in the analysis described above.

It is anticipated that the results of such experiments will enable the use of the TTS, as is used in service life prediction of composites. It is expected that TTS results will show that short exposure degradation of R-values at an elevated temperature is equivalent to that of long-term degradation at lower temperatures, and that R-value degradation increases faster at higher moisture concentrations, as shown by the conceptual plot in Figure 67. In the plot at the left (Figure 67a), for moisture concentration M1, equivalent R-values at high temperatures occur at earlier times than R-values at lower temperatures. In the right plot (Figure 67b), for moisture concentration M2 (where M2>M1), equivalent R-values occur at earlier times for a given temperature than in the plot on the Fort. If this analysis is successful, it is expected to result in a methodology for prediction of long-term insulation parameters based on short-term testing.

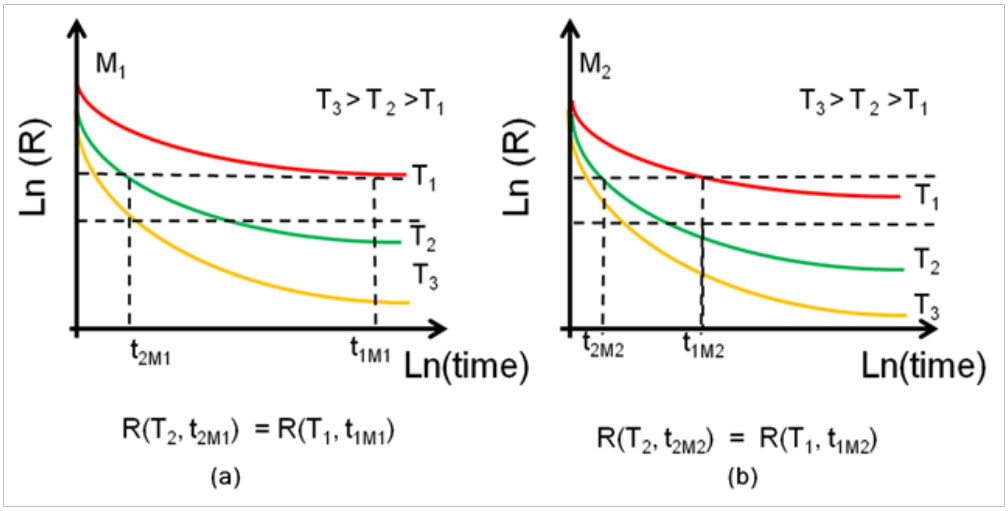

Figure 67. Conceptual TTS plots.

5.3 Phase-change material (PCM)

PCMs are materials that have a high thermal storage density for a small temperature range. The high thermal storage density is created by the material changing phases between a solid to a liquid state, or a liquid to a solid state, when the temperature of the material is shifted across its melting point. Currently, there many different PCMs on the market with a wide range of melting points that allow for phase-change material to be used in any temperature region.

In one application, PCMs are embedded in conventional insulation or blown-in cellulose insulation. When the insulation is introduced to a temperature difference that runs across the PCMs melting point, the phase-change materials either absorbs or expels heat depending on the direction in which the temperature is been driven. This process dampens the changing temperature and allows for an insulated room to remain at more stable temperature, which reduces energy demands on the rooms environmental control systems.

5.3.1 PCM theory

PCMs are materials that store large amounts of latent heat at their liquid-solid phase-change temperature. An ideal material without phase-change, also known as sensible heat storage material, has a change of temperature that is linearly related to the heat that is absorbed or released. Similarly, a PCM follows the same linear relationship above and below its phase-

change temperature, but at its phase-change temperature, the temperature remains fairly constant while a large amount of heat is either absorbed or dissipated. The heat that is absorbed or released by the PCM can be described by the enthalpy function of the material. Enthalpy of a material, h, depends on the integrated function of the specific heat, c_p, which is given by:

$$h(T) = h_{ref} + \int_{T_o}^{T} c_p(T)dT$$

where:

h_{ref} = the reference, or initial, enthalpy
$c_p(T)$ = specific heat function integrated from the initial temperature T_o to some variable temperature T.

Figure 68 details the enthalpy function of a material across a typical phase-change. An ideal PCM can be modeled by using the specific heats, c_p, at the liquid and solid states, and a change of enthalpy, Δh, at the T_m, the ideal phase-change temperature. However, real PCMs have a broad melting range and the change in enthalpy occurs over a range of temperatures, which is correctly modeled by the enthalpy function h(T).

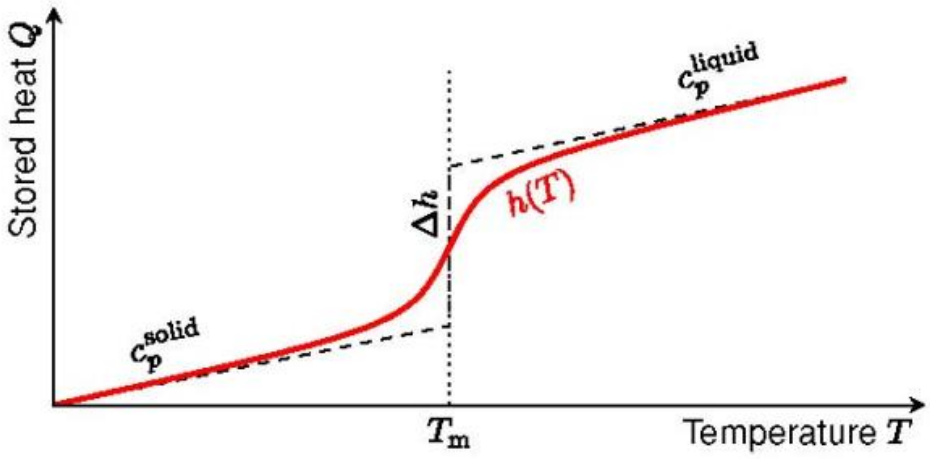

Figure 68. Thermal storage capacity Q(T) of an ideal PCM (dashed) and a real PCM (solid) (Gunther et al. 2009).

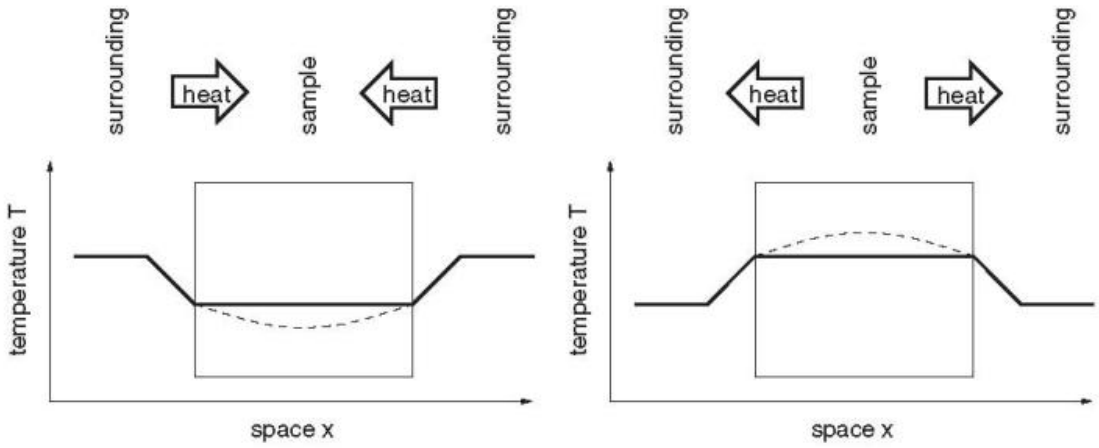

Figure 69. Sketch of the temperature gradient inside the sample during heating (left) and cooling (right) (Castellon et al. 2008).

One of the major difficulties in conducting experimental analysis on PCMs is the presence of a temperature gradient in the material. In an ideal experiment, the temperature is assumed to be constant throughout the material, but in reality, the temperature is not constant due to heat transfer limitations, causing a temperature gradient to form in the sample. This problem causes the measured temperature at the surface to be higher than the average temperature of the sample during heating and lower than average temperature of the sample during cooling. When conducting both heating and cooling tests, the real temperature effects on the thermal properties of the sample can be assumed to be between values obtain during the heating and cooling tests. Furthermore, the uncertainty in the experimental data can be indicated by the distance between the values obtained from the heating and cooling tests. Figure 69 shows the temperature gradient problem present inside PCMs.

In the experimental analysis of PCMs, several different methods are used to calculate the enthalpy and specific heat functions of a material while overcoming the problem of a temperature gradient being present. For microscopic, homogenous samples of PCMs, three different methods are used to measure the thermal properties: dynamic, step, and T-history method. Both the dynamic and step methods can be implemented by a differential scanning calorimeter (DSC). The T-history method typically uses a custom made apparatus not available for this research, and will not be further discussed. The dynamic and step methods can also be used to measure insulation materials that incorporate PCMs. While conducting a

test on a DSC with either the dynamic or step methods, the DSC outputs voltage signal that is proportional to the thermal response of the sample.

The dynamic method is the most widely used testing method that uses a constant heating or cooling ramp with a constant rate. Typical heating and cooling rates for measurements range from 2 K/min to 10 K/min. As the heating and cooling rate increases, the enthalpy determination becomes more accurate, but the uncertainty of the temperature increases greatly. The increased uncertainty of the temperature is caused by the internal temperature gradient of the sample increasing in magnitude. The dynamic method uses three different measurements with the crucible empty, filled with a standard material, and filled with a sample material, all using the same constant heat or cooling rate to find the specific heat function. The specific heat function of the sample material is given by:

$$c_{p,sample}(T) = c_{p,standard}(T) \cdot \left[\frac{U_{sample} - U_{empty}}{U_{standard} - U_{empty}}\right](T) \cdot \frac{m_{sample}}{m_{standard}}$$

where:

m = the mass of the sample and standard material
U = the voltage signals of the empty, standard, and sample runs.

This method relies on the known thermal properties of a standard material. The enthalpy function can be determined by integrating the specific heat function over a given temperature range. Figure 70 shows a typical temperature profile and heat flow signal. The peaks in the heat flow signal indicate a change of the heat flux into the sample and bound the region that phase-change is occurring in the sample.

The step method is another commonly used measurement method for PCMs. Unlike the dynamic method, the heat or cooling rate is not constant and continuous, but instead increases or decreases in increments. During each temperature increment, the temperature is kept constant and the sample is allowed to reach thermal equilibrium. The step method produces a temperature profile that has small steps, and a signal that has a sequence of varying peaks. The size of the temperature step needs to be long enough for the sample to reach thermal equilibrium, which is when the signal goes back to the baseline.

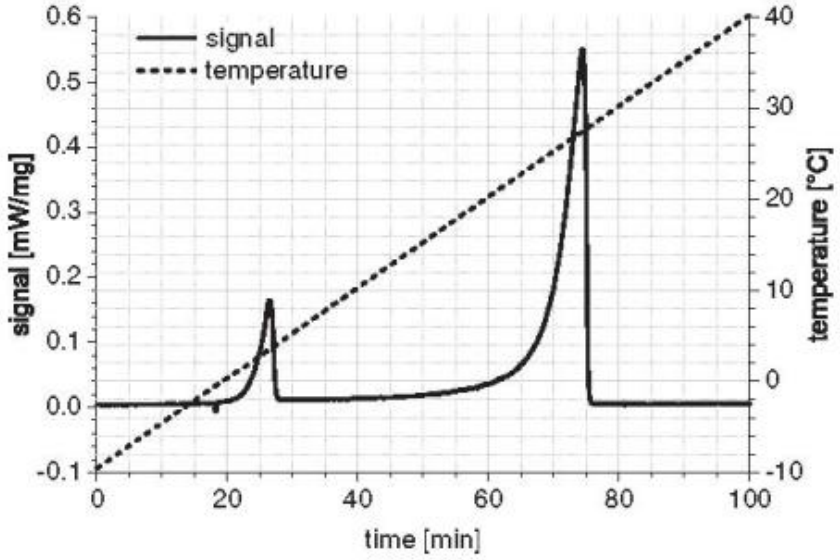

Figure 70. Typical heat flow and temperature profile for a dynamic test (Gunther et al. 2009).

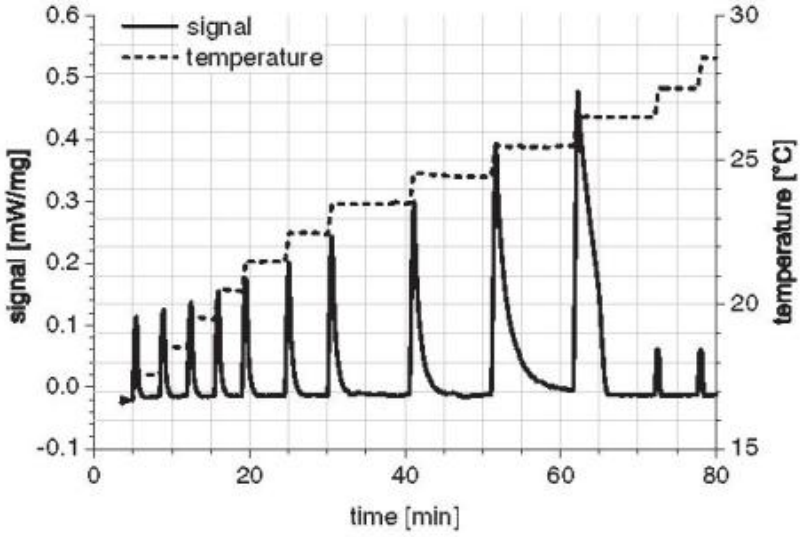

Figure 71. Typical heat flow and temperature profile for step test (Gunther et al. 2009).

The temperature resolution of the obtained data is equal to the step size. The resolution of the temperature can be increased by reducing the step size, but as the step size becomes very small, the signal will vanish and the precision in the measurement disappears. The enthalpy function is determined by integrating all of signal peaks. Figure 71 shows a typical temperature profile and heat flow signal.

5.3.2 PCM test methods

The testing of PCMs will be accomplished by two different approaches. The first approach will try to determine the thermal properties of the PCM that is imbedded in traditional insulation. The second approach will look at the thermal properties of the PCMs in a pure state. Both approaches will use the same two testing methods, but with different measuring equipment to obtain experimental results. The PCM embedded in traditional insulation will be tested by the LaserComp Fox801 (Heat Flux Analyzer) in conjunction with special dynamic testing software. The PCM that is in a pure state will use a DSC.

The PCMs/insulation materials will be analyzed by using a dynamic and a step mode, both described above. The dynamic mode uses a ramp function to raise or lower the temperature at a constant rate from the upper to lower bound temperatures. The step mode raises or lowers the temperature at increments while waiting for the sample to reach thermal equilibrium at each increment. Both processes have distinct advantages and disadvantages. The dynamic mode is simple and provides continuous data on the thermal properties. Since the dynamic mode heats or cools the sample at a constant rate, the sample is never in thermal equilibrium, producing a temperature gradient to form inside the sample. This results in deviations in data between the different heating rates and samples sizes. The step mode provides high resolution data that is equal to the temperature step size. The advantage that the step mode has over the dynamic mode is that the uncertainty in the temperature is precisely known, as it is restricted to the step size. Temperature resolution and accuracy of the data improves as the step size decreases. As the step size decreases in size, the observable change in data vanishes and the precision in the measurement is lost.

Cyclic testing will be conducted on PCM samples that have been conditioned in the temperature/humidity chamber over a range of temperatures and humidity's for multiple cycles, simulating 20 to 30 years of normal usage. Testing of the PCM imbedded in traditional insulation will closely follow a draft of ASTM Standard that is currently in the process of being reviewed for final publication (Stovall 2011) and that is closely related to ASTM Standard C518 (ASTM 2012a). For PCMs that are mixed in with loose-fill insulation, ASTM Standard C687 (ASTM 2012b) will be followed. From ASTM Standard C687, a test frame made of material that has low

thermal conductivity while be used to contain loose-fill insulation for testing. For both the loose-fill and rigid insulation materials, the samples will be pre-conditioned before testing to ensure that the moisture content inside the samples is negligible. The samples will tested using both the dynamic and step modes that are described above, with the tests being repeated three times to gather accurate data. Both of the tests will be tested in the temperature range of 3·dT below and above the minimum and maximum temperature at which the phase-change behavior is observed, respectively. The temperature increment dT is the change of temperature that the PCM is observed to undergo phase change.

The testing of the pure PCM will be conducted by a TA Instruments DSC (Figure 72). A total of three samples of each material will be tested in the DSC by using both the step and dynamic modes. The sample sizes will be 10 mg, but to ensure that the influence of the sample size is negligible, additional tests will be carried out at 5 mg and 15 mg.

Figure 72. TA Instruments DSC for testing PCMs.

All PCM samples will be exposed to multiple temperature/humidity cycles in the environment chamber to simulate long-term usage. The samples will be tested in the DSC before and after exposure in the environmental chamber to determine any degradation of their thermal properties. The results of these tests of candidate PCM materials will be used to determine their relative abilities to store energy under simulated conditions, and more importantly, their estimated service life, as predicted by the number of cycles for which their performance remains unchanged. The number of cycles will be set to simulate at least 20 years.

5.3.3 PCMs to be tested

Typical emerging PCMs to be evaluated in this research are: (1) BioPCM™, (2) Microtek microencapsulated PCM, (3) DuPont™ Energain (Figure 73). The BioPCM bubblepacks (Figure 73 top row) can be unrolled and readily installed on top of insulation. Microtek PCM (Figure 73 middle row) is encapsulated, and is often mixed with cellulose insulation. Energain (Figure 73 bottom row) has PCM incorporated into a ready-to-use panel. (PCM is sandwiched between two sheets of aluminum.) Each is discussed separately below.

5.3.3.1 BioPCMTM

BioPCM™ is a mat composed of packets of PCM made from soy oils and palm oils. BioPCM™ mat can be integrated into fiberglass rolls or bat insulation in place of the craft layer. The BioPCM™ mat integrated with an insulation roll can be installed in the same manner as traditional insulation. The company claims that BioPCM™ mat has demonstrated an energy savings of up to 30% and has life span of at least 13,000 phase-change cycles, which is equivalent to 48 years. The packets of BioPCM™ contain between 5 ml and 10 ml, so that if a packet is punctured, the PCM that leaks out is can be absorbed by the surrounding insulation.

5.3.3.2 Microtek's microencapsulated PCM (MicroPCMTM)

Microtek's MicroPCMs are very small bi-component particles consisting of a core material of PCM and a acrylic microcapsule shell. The PCM core material typically used is either hexadecane or octodecane. For installation, the MicroPCM™ is mixed with a loose-fill insulation, such as cellulose insulation.

5.3.3.3 DuPont™ Energain

DuPont™ Energain insulation is aluminum-laminated panels that contain copolymer and paraffin wax. The paraffin wax used in DuPont™ Energain insulation melts and solidifies from 22 to 18 °C (72 to 64 °F). The company claims that their tests on DuPont™ Energain insulation have shown energy savings of up to 35%.

BioPCM blanket installed over insulation.

"Bubble Pack BioPCM product for placement in wall cavities.

Sample of "Microtek PCM."

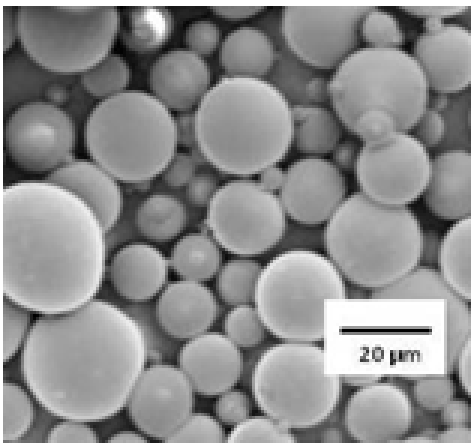

Magnified image of encapsulated Microtek PCM.

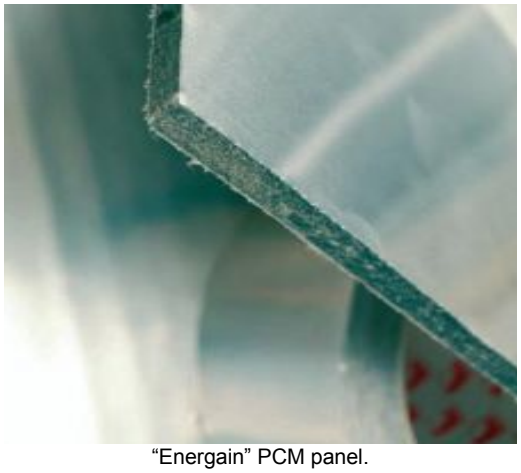
"Energain" PCM panel.

Figure 73. Samples of PCM materials to be tested.

6 Conclusions and Recommendations

The building envelope represents an area of much needed improvement in Army facilities. Although guidance has already been published to encourage much more efficient building envelopes, that guidance does not address thermal bridging despite the fact that failure to mitigate it has been shown to represent relatively high losses in otherwise high performing buildings. Existing mitigation strategies fail to exploit the potential for novel materials to contribute to more efficient building envelopes, in part because the properties are not yet well understood. The absolute impact of TBs has often been thought of as small relative to an envelope's overall losses; however, as buildings become more energy efficient, this relative contribution has increased. As additional insulation improvements in the "clear wall" show diminishing returns, mitigating TBs becomes the wiser investment.

TBs can also decrease the interior surface temperature during the heating season, allowing the potential for condensation on interior surfaces leading to material degradation, soiling, and mold growth. As standards for building envelope performance become more stringent, the complex, three-dimensional impact of TBs can become unpredictable and even lead to condensation after a retrofit where there was none prior to a retrofit.

This work developed capabilities to characterize energy losses through building envelopes and devise potential mitigation strategies using advance materials to meet mandated energy reduction goals. After identifying the areas of high energy losses in standard Army buildings at two military bases using infrared technology, several 3-D models were used to characterize energy losses and develop dynamic models.

This work recommends that additional Army guidance be enacted to require adequate mitigation of TBs in new construction and in retrofits. To assist the building designer in complying with this guidance, a catalogue of building details will be composed, which will include:

1. A detailed drawing with rich construction notes (for new construction details) or diagnosis tips (for identifying existing versions of the detail for ret-

rofit). QA and verification tips should be included for new construction details.
2. Detail thermal performance with climate-dependent changes. This will allow comparison between the standard or existing detail and the improved or retrofitted detail which will, in turn, allow the improvement to be economically justified.
3. An indication of whether the detail meets certain guidance, which will provide for quick decision making where quantifying the detail's impact is not desired.

Performance estimation can be performed with 2- and 3-D heat transfer simulations. Mitigation can include advanced materials, especially where retrofits make conventional materials inadequate.

Deciding which details are to be included in the catalogue is an ongoing effort. Many have been selected based on drawing review and, more importantly, on actual observations of existing buildings using infrared imaging.

References

American Society of Heating, Refrigerating and Air-Conditioning Engineers (ASHRAE). 2001. *Modeling Two- and Three-Dimensional Heat Transfer through Composite Wall and Roof Assemblies in Transient Energy Simulation Programs*. Atlanta, GA: ASHRAE.

———. 2007. *Energy Standard for Buildings Except Low-Rise Residential Buildings*. Atlanta, GA: ASHRAE.

———. 2009. *Fundamentals*. Atlanta, GA: ASHRAE.

———. 2009a. *Standard for the Design of High-Performance, Green Buildings Except Low-Rise Residential Buildings*. Atlanta, GA: ASHRAE.

———. 2011. *HVAC Applications*. Atlanta, GA: ASHRAE.

———. 20011a. *Thermal Performance of Building Envelope Details for Mid- and High-Rise Buildings*. Atlanta, GA: ASHRAE.

———. 1985. *ASHRAE Handbook 1985 Fundamentals: Inch-Pound Edition*. Atlanta, GA: ASHRAE.

American Society for Testing and Materials (ASTM). 2012. ASTM Standard C518-10. *Standard Test Method for Steady-State Thermal Transmission Properties by Means of the Heat Flow Meter Apparatus*. West Conshohocken, PA: ASTM.

ASTM. 2012. ASTM C687 – 07. *Standard Practice for Determination of Thermal Resistance of Loose-Fill Building Insulation*. West Conshohocken, PA: ASTM.

ANSYS, Inc. 2012. ANSYS FLUENT. Product overview. Web page, http://www.ansys.com/Products/Simulation+Technology/Fluid+Dynamics/ANSYS+Fluent

Bligh, T. P., P. Shipp, and G. Meixel. 1978. Energy comparisons and where to insulate earth sheltered buildings and basements. *Earth Covered Settlements*. Fort Worth, TX: US DOE Conference.

BLOCON. 2005. *Heat3 Manual*. Reading, MA: BLOCON USA. Accessed 4 November 2011, http://www.buildingphysics.com/manuals/HEAT3%205%20update%20manual.pdf

Bombino, Robert, and Graham Finch. *Reconsidering the Approach towards Determining Overall Building Enclosure Thermal Performance for Code Compliance*. ASHRAE Buildings XI, 2010.

California Energy Commission. 2001. *Public Interest Energy Research Program. Characterization of Framing Factors for Low-Rise Residential Building Envelopes in California*. Sacramento, CA: California Energy Commission.

Carlisle Construction Materials. 2011. *2011 - Building Envelope Air and Vapor Barrier Details*. Carlisle, PA: Carlisle Construction Materials.

Castellon, C., E. Gunther, H. Mehling, S. Hiebler, and L. F. Cabeza. 2008. *Determination of the Enthalpy of PCM as a Function of Temperature Using a Heat-Flux DSC—a Study of Different Measurement Procedures and Their Accuracy*. International Journal of Energy Research. 32(13):1258-1265. DOI: 10.1002/er.1443.

Choudhary, M. K., C. Kasprzak, R. H. Larson, and R. Venuturumilli. 2010a. ASHRAE Standard 90.1 Metal building U-factors—Part 1: Mathematical modeling and validation by calibrated hot box measurements. *ASHRAE Transactions*. 116.

———. 2010b. ASHRAE Standard 90.1 Metal building U-factors—Part 2: A systems based approach for predicting the thermal performance of single layer fiberglass batt insulation assemblies. *ASHRAE Transactions*. 116.

Christensen, Dane. 2010. Thermal impact of fasteners in high-performance wood-framed walls. *ASHRAE Buildings XI*.

Christian, J. E., and J. Kosny. 1995. Toward a national opaque wall rating label. *Thermal Performance of the Exterior Envelopes of Buildings VI*, December 4-8, 1995, Sheraton Sand Key Hotel, Clearwater Beach, Florida. Conference Proceedings. Atlanta, GA: ASHRAE.

Christianson, Les. 2010. ASHRAE Standard 90.1 Metal building U-factors—Part 4: Development of U-factors for walls and roofs based on experimental measurements. *ASHRAE Transactions*. 116.

Citterio, Marco, Manuela Cocco, and Heike Erhorn-Kluttig. 2008. *Thermal Bridges in the EPBD Context: Overview on MS Approaches in Regulations*. Information paper P64. European Building Platform Directive (EBPD), http://www.buildup.eu/system/files/P064_EN_ASIEPI_WP4_IP1_p3073.pdf

Centre Scientifique et Technique de la Construction (CSTC). *Logiciel KOBRA*. Bruissels, Belgium: CSTC. Accessed 4 November 2011, http://www.cstc.be/homepage/index.cfm?cat=bbri&sub=rd&pag=projects&art=kobra_software

Department of the Army (DA), The Army Senior Energy Council and the Office of the Deputy Assistant Secretary of the Army for Energy and Partnerships. 2009. *Army Energy Security Implementation Strategy*. Washington, DC:, http://www.asaie.army.mil/Public/Partnerships/doc/AESIS_13JAN09_Approved%204-03-09.pdf

Department of Defense (DoD). 2002. *Energy Conservation*. UFC 3-400-01 http://www.wbdg.org/ccb/DOD/UFC/ufc_3_400_01.pdf

———. 2004. *Design: Arctic and Subarctic Construction - Buildings*. UFC 3-130-07, http://www.wbdg.org/ccb/DOD/UFC/ufc_3_130_07.pdf

———. 2005. *Concrete Floor Slabs on Grade Subjected to Heavy Loads*. Unified Facilities Criteria (UFC) 3-320-06A, http://www.wbdg.org/ccb/DOD/UFC/ufc_3_320_06a.pdf

———. 2007. *Sustainable Development*. UFC 4-030-01, http://www.wbdg.org/ccb/DOD/UFC/ufc_4_030_01.pdf

———. 2010. *General Building Requirements*. UFC 1-200-01, http://www.wbdg.org/ccb/DOD/UFC/ufc_1_200_01.pdf

———. 2011. UFC 1-200-01, *General Building Requirements*. Washington, DC: DoD, http://www.wbdg.org/ccb/DOD/UFC/ARCHIVES/ufc_1_200_01_2010.pdf

The Energy Independence and Security Act of 2007 (EISA). 2007. PL 110-140. 110th Congress.

Energy Policy Act of 2005 (EPAct 2005). 2005. Public Law 109-58. 109th Congress. http://www.fedcenter.gov/_kd/Items/actions.cfm?action=Show&item_id=2969&destination

Engineer Research and Development Center (ERDC). 2011. CAD/BIM Technology Center for Facilities, Infrastructure, and Environment. CAD Details Library, http://www.erdc.usace.army.mil/pls/erdcpub/!www_fact_sheet.capability_page?ps_capability_numb=4980989&tmp_Main_Topic=&page=SUCCESS&page=TEAM#TECHNOLOGY

Erhorn, Hans, and Heike Erhorn-Kluttig. 2010. *Advanced Thermal Bridge Driven Technical Developments*. EPBD, http://www.buildup.eu/system/files/content/P190_Advanced_thermal_bridge_driven_technical_developments_ASIEPI_WP4.pdf

Erhorn, H., M. Gierga, and H. Erhorn-Kluttig. 2002. *Demonstrationsvorhaben 3-Liter-Häuser in Celle*. Lindau, Germany: Fraunhofer-Institut für Bauphysik.

Erhorn-Kluttig, Heike. 2010.Assessment and improvement of the EPBD Impact. *An Effective Handling of Thermal Bridges in the EPBD Context*. PowerPoint Presentation. Valley, Germany: Fraunhofer Institute for Building Physics, http://www.asiepi.eu/fileadmin/files/WebEvents/WebEvent_4.1/ASIEPI_WP4_WebEvent1_04_Impact.pdf

Erhorn-Kluttig, Heike, and Hans Erhorn. 2009. *Impact of Thermal Bridges on the Energy Performance of Buildings*. EPBD, http://www.buildup.eu/system/files/content/P_148_EN_ASIEPI_WP4_IP2.pdf

Ferriter, Michael, LTG. 15 February 2012. Memorandum for Commander, US Army Corps of Engineers and Commander, Installation Management Command. Subject: Revised Army standard for permanent party enlisted personnel dining facilities (EPDF). Washington, DC: Assistant Chief of Staff for Installation Management (ACSIM).

Gorgolewski, Mark. 2007. Developing a simplified method of calculating U-factors in light steel framing. *Building and Environment* 42(1):230-236, http://www.sciencedirect.com/science/article/pii/S0360132306001776

Gunther, Eva, Stefan Hiebler, Harald Mehling, and Robert Redlich. 2009. Enthalpy of phase change materials as a function of temperature: Required accuracy and suitable measurement methods. *International Journal of Thermophysics*. 30(4):1257-1269.

Hemmerlybrown, Alexandra. 2011. Army launches 'Net Zero' pilot program. *WWW.ARMY.MIL, The Official Homepage of the United States Army*. Accessed 9 November 2011, http://www.army.mil/article/55280/

Headquarters, US Army Corps of Engineers (HQUSACE). 1994. *Architectural and Engineering Instructions Design Criteria*. Washington, DC: HQUSACE http://www.wbdg.org/ccb/ARMYCOE/AEICOE/ARCHIVES/aei.pdf

HQUSACE. Undated. *Centers of Standardization: Facility Type Links*. Web page. Accessed 7 November 2011, http://mrsi.usace.army.mil/cos/Lists/Links/AllItems.aspx

International Code Council (ICC). 2009. *International Building Code (IBC)*. Washington DC: ICC.

International Organization for Standardization (ISO). 2007a. *Thermal Bridges in Building Construction - Heat Flows and Surface Temperatures - Detailed Calculations*. Geneva, Switzerland: ISO.

ISO. 2007b. *Thermal Bridges in Building Construction - Linear Thermal Transmittance - Simplified Methods and Default Values*. Geneva, Switzerland: ISO.

ISO. 2007c. *Thermal Performance of Buildings - Transmission and Ventilation Heat Transfer Coefficients - Calculation Method*. Geneva, Switzerland: ISO.

Kosney, Jan, J. E. Christian, Edward Barbour, and John Goodrow. 1994. *Thermal Performance of Steel Framed Walls*. Oak Ridge, TN: Oak Ridge National Laboratory.

Kosny, Jan, David Yarbrough, Phillip Childs, and Syed Azam Mohiuddin. 2007. *How the Same Wall Can Have Several Different R-Values: Relations between Amount of Framing and Overall Thermal Performance in Wood and Steel-Framed Walls*. Buildings X. Atlanta, GA: ASHRAE.

Kosny, Jan, and Jeffrey E. Christian. 2001. *Whole Wall Thermal Performance*. Oak Ridge, TN: ORNL.

Kuranda, Kathryn M., Brian Cleven, Nathaniel Patch, Katherine Grandine, and Christine Heidenrich. 2003. *Unaccompanied Personnel Housing during the Cold War (1946-1989)*. Washington, DC: Department of the Army (DA).

Lahmidi, H., and F. Leguillon. Undated. *Study for the ASIEPI Project: Thermal Bridges Influence on the Primary Energy Consumption*. Summary report of ASIEPI WP4.

Larbi, Ben A. 2005. Statistical modeling of heat transfer for thermal bridges of buildings. *Energy and Buildings* 37(9):945:951. DOI: 10.1016/j.enbuild.2004.12.013.

Lstiburek, Joseph W. October 2007. A bridge too far. *ASHRAE Journal*, http://www.google.com/url?sa=t&rct=j&q=Lstiburek%2C+Joseph+W.+2007.+A+bridge+too+far.+ASHRAE+Journal.+&source=web&cd=1&ved=0CCEQFjAA&url=http%3A%2F%2Fwww.ashrae.org%2FFile%2520Library%2FdocLib%2FJournal%2520Documents%2FOctober%25202007'%2F20070926_buildingsciences.pdf&ei=hLYxT-_MBsaKgwex7L2gBQ&usg=AFQjCNF1peiRY7I4-XW7IRhOlig1DCBRHA

McBride, Merle F., and Patrick M. Gavin. 2010. ASHRAE Standard 90.1 Metal building U-factors–Part 3: Equations for double layers of fiberglass batt insulation in roof and wall assemblies. *ASHRAE Transactions*. 116.

McManus, H. L., S. Kessler, A. Raghavan, M. Hyer, S. Case, and J. Cain. 2009. Service life assessment methodology for composites. San Francisco, CA: *International Conference on Fiber Reinforced Polymer (FRP) Composites for Infrastructure Applications - Focusing on Innovation, Technology Implementation, and Sustainability*.

Mills, A. F. 1999. *Heat Transfer*. Saddle River, NJ: Prentice-Hall Inc.

Minnesota Department of Commerce (DOC), Energy Division. 2000. *Catalog of Thermal Bridges in Commercial and Multi-Family Construction*, http://www.google.com/url?sa=t&rct=j&q=Catalog+of+Thermal+Bridges+in+Commercial+and+Multi-Family+ConstructionASHRAE+Transactions+116&source=web&cd=2&ved=0CCsQFjAB&url=http%3A%2F%2Fwww.state.mn.us%2Fmn%2FexternalDocs%2FCommerce%2FThermal_Bridges%2C_pdf_file_111302111336_ThermalBridgesCat.pdf&ei=NLgxT6mdIMGqgwfItqCeBQ&usg=AFQjCNERPJyAyEhqR4Xe6DF4wbjitng6Og

National Fenestration Rating Council (NFRC). 2010. *NFRC 100: Procedure for Determining Fenestration Product U-Factors*. Silver Spring, MD: NFRC.

O'Brien, Sean M. 2006. *Thermal Bridging in the Building Envelope. The Construction Specifier*.

Office of the Assistant Secretary of the Army for Installations, Energy and the Environment (ASAIEE). 2012. *Army Vision for Net Zero*, http://army-energy.hqda.pentagon.mil/netzero /

Passive House Institute US. 2011 accessed 8 November 2011, http://www.passivehouse.us/passiveHouse/PHIUSHome.html

Pedersen, C. O. 2007. *Advanced Zone Simulation in Energyplus: Incorporation of Variable Properties and Phase Change Material (PCM) Capability*. Beijing, China: 10th International Building Performance Simulation Association (IBPSA) Conference.

Pokorny, Walter, Thomas Zelger, Karl Torghele, Hildegund Motzl, and Barbara Bauer. 2009. *Passivhaus-Bauteilkatalog, Okologisch Bewertete Konstruktionen (Details for Passive Houses, a Catalogue of Ecologically Rated Constructions*). Heidelberg, Germany: Springer Verlag GmbH.

Schild, Peter G. 2010. *Good Practice Guidance on Thermal Bridges & Construction Details, Part II: Good Examples*. EPBD, http://www.buildup.eu/system/files/content/P189_Thermal_bridge_guidance_examples_ASIEPI-WP4_0.pdf

Schild, Peter G., and Peter Blom. 2010. *Good Practice Guidance on Thermal Bridges & Construction Details, Part I: Principles*. EPBD, http://buildup.eu/system/files/content/P188_Thermal_bridge_guidance_principles_ASIEPI-WP4.pdf

Spiekman, M. 2009. *Summary of a Dutch Study on the Quantification of Thermal Bridge Effects on the Energy Performance*. Summary report of ASIEPI WP4.

Stovall, Therese. 31 March 2011. Personal communication between Therese Stovall, Oak Ridge National Laboratory (ORNL) and Jonathon Trovillion, Engineer Research and Development Center, Construction Engineering Research Laboratory (ERDC-CERL).

Syed, Azam Mohiuddin, and Jan Kosny. 2006. Effect of framing factor on clear-wall r-value of wood and steel framed walls. *Journal of Building Physics* 30(2):163-180.

Theodosiou, T.G., and A.M. Papadopoulous. 2008. The impact of thermal bridges on the energy demand of buildings with double brick wall constructions. *Energy and Buildings* 40(11):2083-2089, http://dx.doi.org/10.1016/j.enbuild.2008.06.006

Thomsen, Kristen Engelund, and Jorgen Rose. 2009. *Analysis of Execution Quality Related to Thermal Bridges*. EPBD, http://www.buildup.eu/system/files/content/P%20159%20ASIEPI_Execution%20Quality_%28WEB%29.pdf

Tilmans, Antoine, and Dirk Van Orshoven. 2010. *Software and Atlases for Evaluating Thermal Bridges*. EPBD, http://www.buildup.eu/system/files/content/P198_Software_and_atlases_for_evaluating_thermal_bridges_0.pdf

UK Department for Communities and Local Government. Undated. *Accredited Construction Details for Part L. Regulations Planning Portal*. Web page. Accessed 4 November 2011 http://www.planningportal.gov.uk/buildingregulations/approveddocuments/partl/bcassociateddocuments9/acd

Wang, F. S. 1979. Mathematical modeling and computer simulation of insulation systems in below grade applications. Kissimmee, FL: *Proceedings of the ASHRAE/DOE-ORNL Conference, Thermal Performance of the Exterior Envelopes of Buildings*. Atlanta, GA: ASHRAE. pp 456-470.

Webster, Julie L., Patrick E. Reicher, and Gordon L. Cohen. 2006. *Antiterrorism Measures for Historic Properties*. ERDC/CERL TR-06-23. Champaign, IL: ERDC-CERL, http://www.cecer.army.mil/techreports/erdc-cerl_tr-06-23/erdc-cerl_tr-06-23.pdf

Wilcox, S., and W. Marion. 2008. *Users Manual for TMY3 Data Sets*. Technical Report NREL/TP-581-43156. Golden, CO: National Renewable Energy Lab, http://www.nrel.gov/docs/fy08osti/43156.pdf

Wojnar, S., S. Firlag, and A. Panek. 2009. *Quantitative Study of Thermal Bridges in Residential Buildings*. Summary report of ASIEPI WP4.

Zhivov, Alexander, Dale Herron, and Richard Liesen. 2010a. *Energy and Water Conservation Design Guide (for Sustainment, Restoration and Modernization [SRM] Projects and Military Construction [MILCON])*, Accessed 4 November 2011, http://wbdg.org/pdfs/usace_ewcdr_execsummary.pdf

———. 2010b. Building Envelope. *Energy and Water Conservation Design Requirements for SRM Projects*, http://www.wbdg.org/pdfs/usace_ewcdr_execsummary.pdf

———. 2010c. ARC prescriptive technology solution sets. *Energy and Water Conservation Design Requirements for SRM Projects* http://www.wbdg.org/pdfs/usace_ewcdr_execsummary.pdf

———. 2010d. CDC Prescriptive Technology Solution Sets. *Energy and Water Conservation Design Requirements for SRM Projects* http://www.wbdg.org/pdfs/usace_ewcdr_execsummary.pdf

———. 2010e. COF Prescriptive Technology Solution Sets. *Energy and Water Conservation Design Requirements for SRM Projects* http://www.wbdg.org/pdfs/usace_ewcdr_execsummary.pdf

———. 2010f. DFAC Prescriptive Technology Solution Sets. *Energy and Water Conservation Design Requirements for SRM Projects* http://www.wbdg.org/pdfs/usace_ewcdr_execsummary.pdf

———. 2010g. Prescriptive technology solution sets. *Energy and Water Conservation Design Requirements for SRM Projects* http://www.wbdg.org/pdfs/usace_ewcdr_execsummary.pdf

———. 2010h. TEMF prescriptive technology solution sets. *Energy and Water Conservation Design Requirements for SRM Projects* http://www.wbdg.org/pdfs/usace_ewcdr_execsummary.pdf

Acronyms and Abbreviations

Term	Definition
AC	Alternating current
ACDs	Accredited Construction Details
ANSI	American National Standard Institute
ASHRAE	American Society of Heating, Refrigerating, and Air-Conditioning Engineers
ASIEPI	ASessment and Improvement of the EPBD Impact
ASTM	American Society for Testing and Materials
CCSPF	Closed-Cell Spray Polyurethane Foam
CDC	Child Development Center
CDCSA	CDC- School Age
CEERD	US Army Corps of Engineers, Engineer Research and Development Center
CERL	Construction Engineering Research Laboratory
CMU	Concrete Masonry Unit
COS	Centers of Standardization
DC	Direct Current
DoD	US Department of Defense
DPW	Directorate of Public Works
DSC	Differential Scanning Calorimetry
ECDs	Enhanced Construction Details
EIFS	Exterior Insulation Finishing System
EISA	US Energy Independence and Security Act of 2007
EPACT	Energy Policy Act
EPBD	Energy Performance of Buildings Directive
ERDC	Engineer Research and Development Center
EU	European Union
HVAC	Heating, Ventilating, and Air-Conditioning
IBPSA	International Building Performance Simulation Association
IEE	Institution of Electrical Engineers
IES	Illuminating Engineering Society
IESNA	Illuminating Engineering Society of North America
IR	Infrared
ISO	International Standards Organization
MS	Member State
NFRC	National Fenestration Rating Council
PCM	Phase-Change Material
SF	Standard Form
TB	Thermal Bridge
TR	Technical Report
TTS	Time-Temperature Superposition
UPH	Unaccompanied Personnel Housing
USACE	US Army Corps of Engineers
USGBC	US Green Building Council

Appendix A: Summary of ISO 10211:2007 and 13770:2007

Pre-processing procedures: Specifications for numerical model construction -ISO 10211

ISO 10211 provides the following information regarding the model construction:

- Boundary Conditions: Where is acceptable to assign temperature or no transverse heat transfer condition?
- Geometry Simplifications: What can be assumed linear or uniform rather than a complex shapes?
- Material Omissions: What material can be excluded without affecting the quality of the results?
- Cutoff plane locations: At what distance an adiabatic plane should be placed without drastically modifying the actual heat transfer physics of the modeled scenario?

Thermal transmittance calculations

Psi and chi values are computed using the model simulation results, along with semi-empirical equations that are provided in ISO standards. These equations are found in the ISO Standard accordingly the scenario to be modeled. Several simulation packages provide a direct psi and/or chi value calculation, in which care must be taken due to the uncertainty of the used methodology to compute them.

Linear and Point Thermal Transmittances- ISO 10211

- Linear Thermal Transmittance

$$\psi_{TB} = L_{2d} - \sum_{i=1}^{n} U_i \, l_i$$

- Foundation TB, internal surface assumption

$$\psi_{TBg} = L_{2d} - h_w U_w - 0.5 B' U_g$$

- Foundation TB, external surface assumption

$$\psi_{TBg} = L_{2D} - (h_w + h_f)U_w + 0.5(B' + w)U_g$$

- Point Thermal Transmittance

$$\chi_{TB} = L_{3d} - \sum_{i=1}^{n} U_i\, l_i - \sum_{i=1}^{n} \psi_{TB\,i}\, l_i$$

Ground heat transfer equations-ISO 13370

- Basement
  - Well-insulated basement floors

$$For\ (d_t + 0.5z) \geq B'$$

$$U_{bf} = \frac{\lambda}{0.547B' + d_t + 0.5z}$$

  - Uninsulated floors

$$For\ (d_t + 0.5z) < B'$$

$$U_{bf} = \frac{2\lambda}{\pi B' + d_t + 0.5z} \ln\left(\frac{\pi B'}{d_t + 0.5z} + 1\right)$$

  - Basement walls

$$U_{bw} = \frac{2\lambda}{\pi z}\left(1 + \frac{0.5d_t}{d_t + z}\right) \ln\left(\frac{z}{d_w} + 1\right)$$

where:

$$d_t = w + \lambda(R_{si} + R_f + R_{se})$$

$$d_w = \lambda(R_{si} + R_w + R_{se})$$

$If\ d_w < d_t, then\ d_t\ should\ be\ replaced\ by\ d_w\ in\ the\ U_{bw}\ formula$

- Simple floor, slab on ground
  - Insulated floor

$$For\ d_t \geq B'$$

$$U\_g = [(R\_f + R\_si + R\_se + w/\lambda) + (0.457B\text{^}')/\lambda]\text{^}(-1)$$

- Uninsulated floor

$For\ d_t < B'$

$$U_g = \frac{2\lambda}{\pi B' + d_t} \ln\left(\frac{\pi B'}{d_t} + 1\right)$$

- Building with edge insulation

$$R' = R_n - \frac{d_n}{\lambda}$$

- Vertical edge insulation

$$\psi_{g,e} = -\frac{\lambda}{\pi}\left[\ln\left(\frac{2D}{d_t} + 1\right) - \ln\left(\frac{2D}{d_t + d'} + 1\right)\right]$$

- Horizontal edge insulation

$$\psi_{g,e} = -\frac{\lambda}{\pi}\left[\ln\left(\frac{D}{d_t} + 1\right) - \ln\left(\frac{D}{d_t + d'} + 1\right)\right]$$

where (for ISO equations above):

$A = Floor\ Area\ enclosed\ by\ room\ walls\ P = Exposed\ perimeter\ floor$
$w = thickness\ of\ external\ walls$
$\lambda = Unfrozen\ thermal\ conductivity\ of\ the\ ground$
$D = Depth\ of\ vertical\ edge\ insulation$
$R_f = Thermal\ resistance\ of\ floor\ construction$
$R_{si} = Internal\ surface\ resistance\ R_{se} = External\ surface\ resistance$
$d_t = total\ equivalent\ thickness\ for\ slab - on - ground\ floor\ R_n =$
$thermal\ resistance\ of\ vertical\ edge\ insulation$
$d_n = vertical\ edge\ insulation\ thickness$
$B' = Characteristic\ floor\ dimmension$
$U_g = Ground\ thermal\ transmittance\ U_w = wall\ thermal\ transmittance$
$\psi_{g,e} = Edge\ insulation\ linear\ thermal\ transmittance, negative\ value.$
$h_w =$
$wall\ height\ from\ the\ ground\ to\ the\ addiabatic\ cut\ plane\ (at\ least\ 1\ meter)$
$h_f = overall\ floor\ thickness$
$L_{2D} = thermal\ coupling\ coefficient\ on\ 2D\ calculations$
$(calculated\ in\ the\ simulation)$
$R' = addional\ thermal\ resistance\ due\ to\ edge\ insulation\ Q'_{int} =$
$Total\ heat\ flux\ crossing\ the\ selected\ internal\ boundary$

Appendix B: Army Facilities Detail Drawings Examples

Dining Facilities

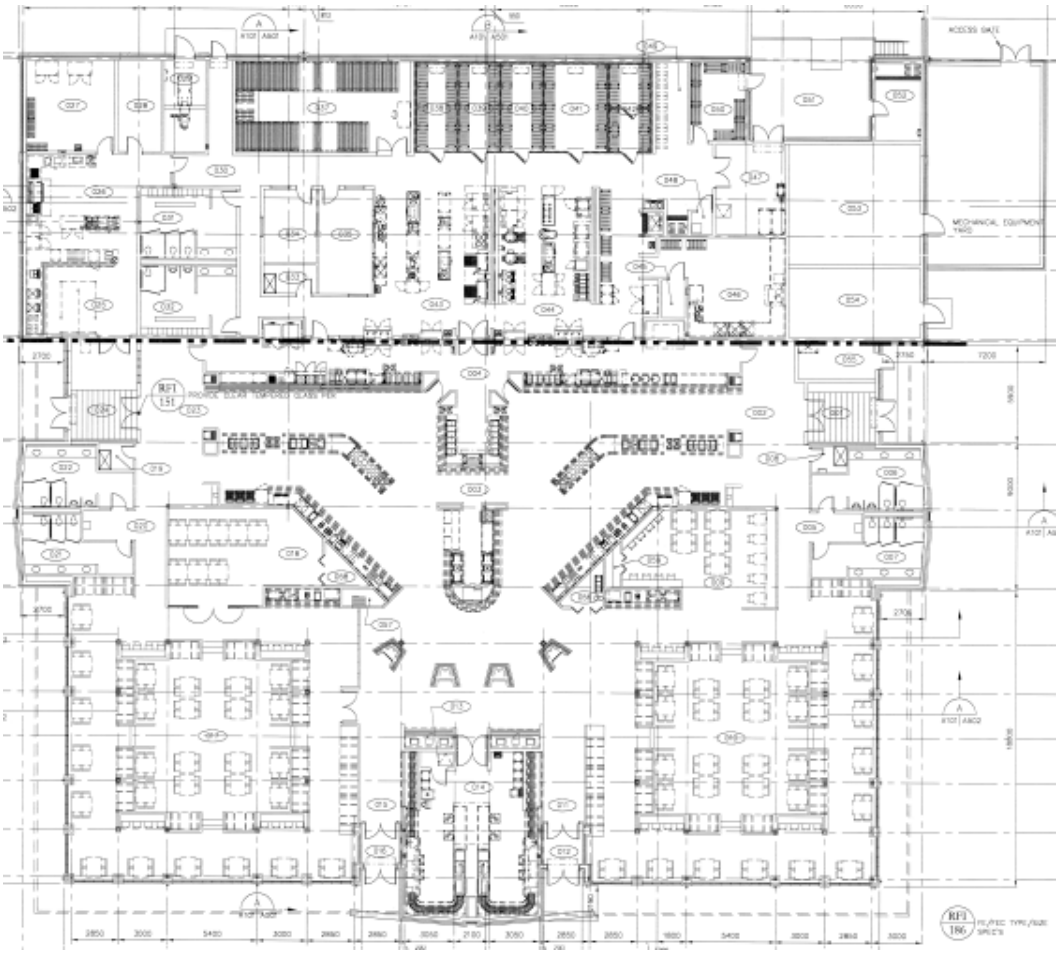

Figure B1. DFAC floor plan. Bldg 1444, Fort Carson, CO.

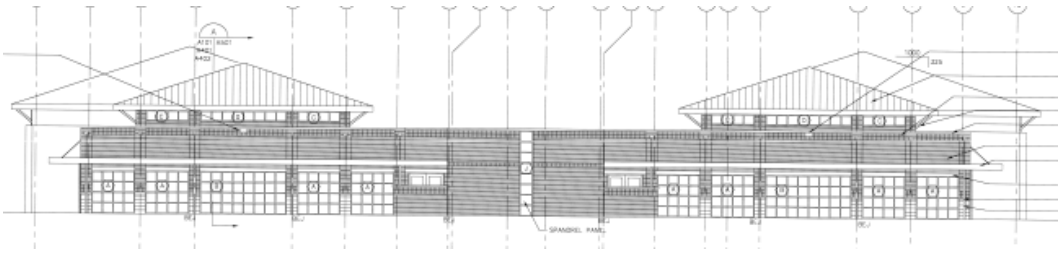

Figure B2. DFAC elevations. Bldg 1444, Fort Carson, CO.

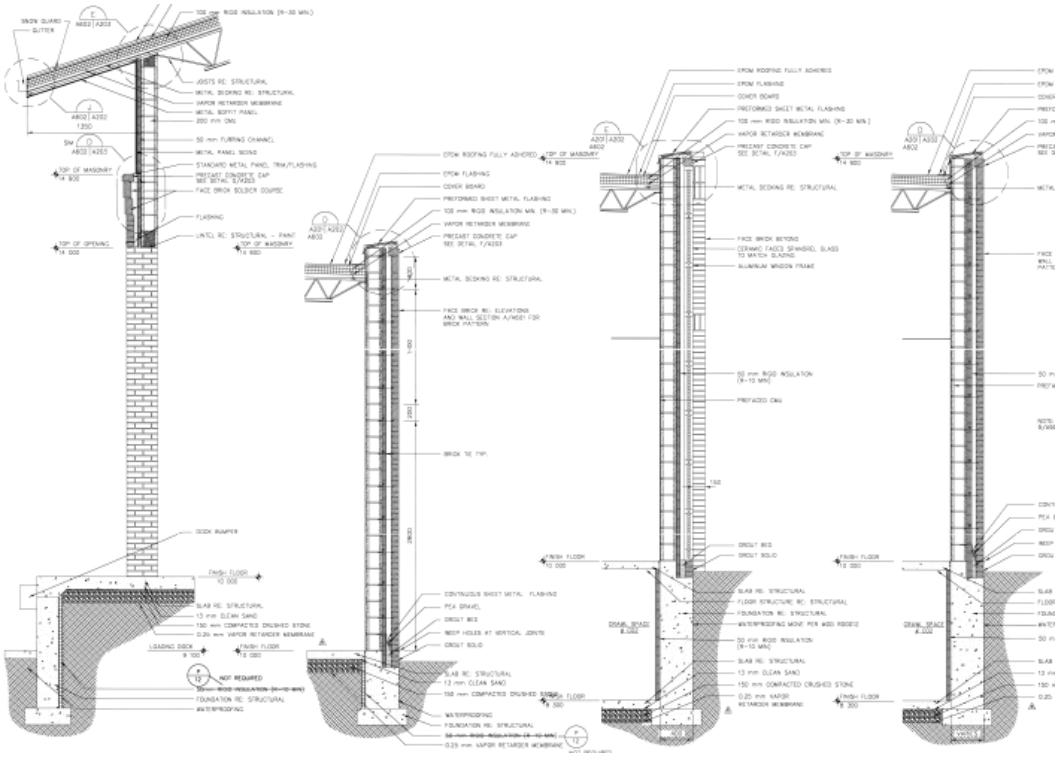

Figure B3. DFAC wall sections. Bldg 1444, Fort Carson, CO.

Tactical Equipment Maintenance Facility

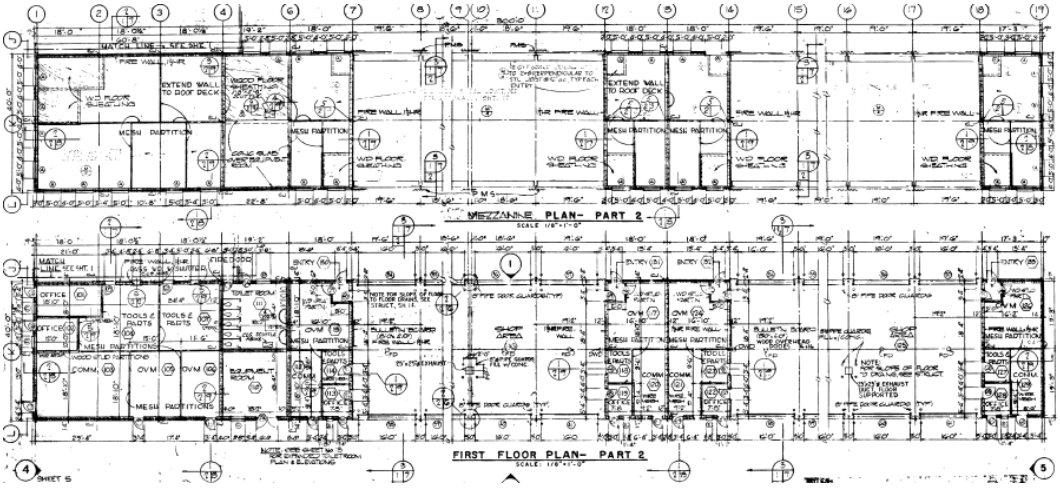

Figure B4. Tactical Equipment Maintenance Facility floor plan. Bldg 3492, Fort Carson, CO.

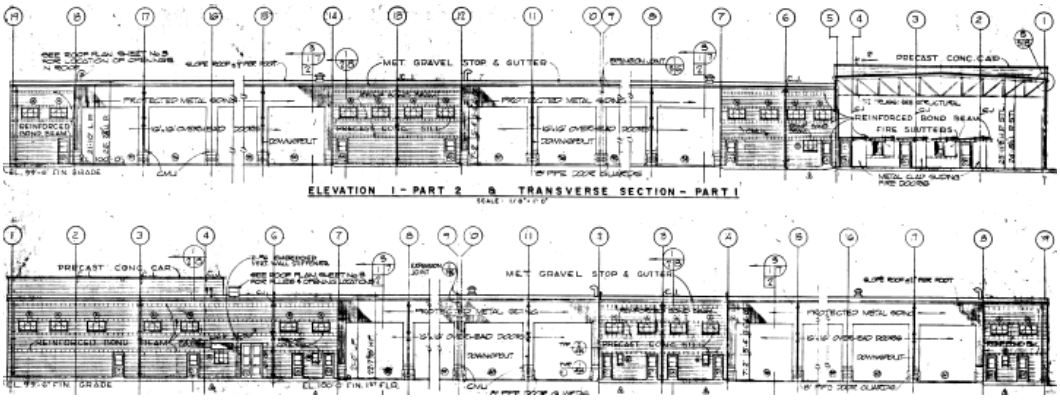

Figure B5. Tactical Equipment Maintenance Facility elevations, Bldg 3492, Fort Carson, CO.

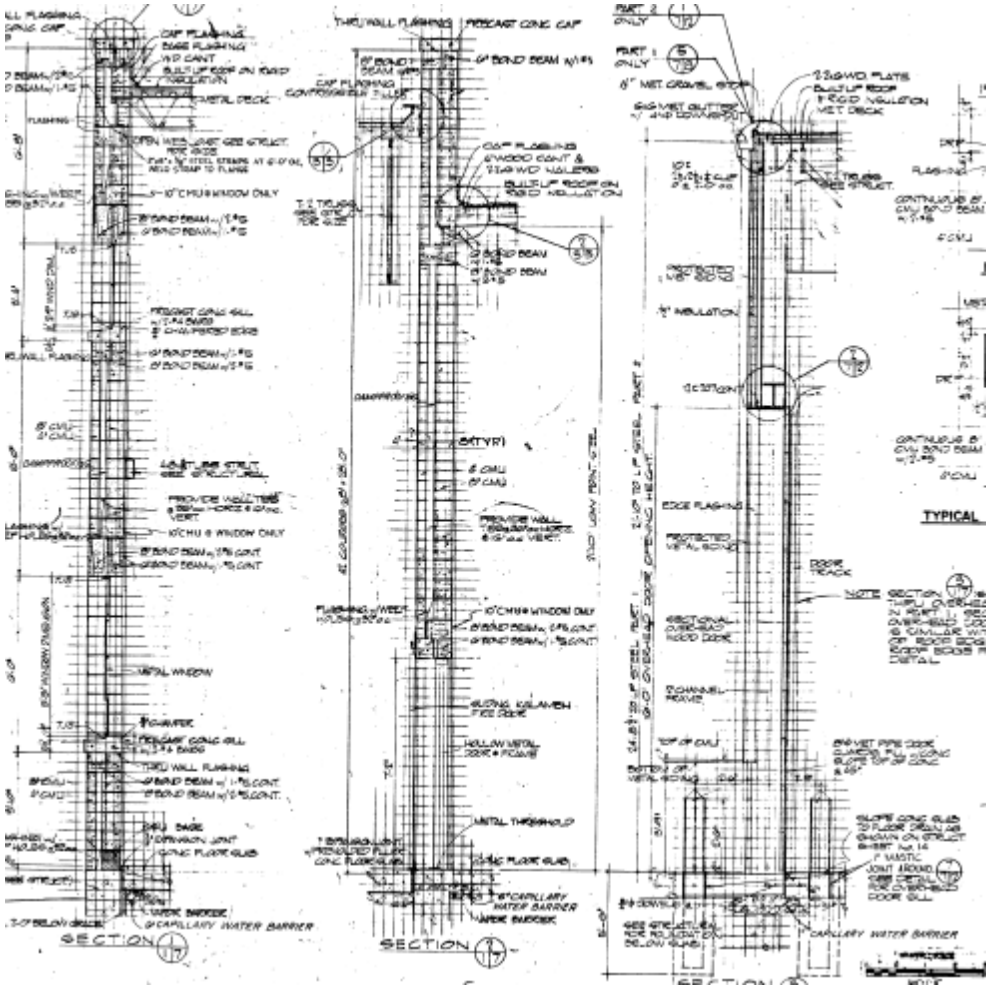

Figure B6. Tactical Equipment Maintenance Facility wall sections, Bldg 3492, Fort Carson, CO.

Company Operation Facility

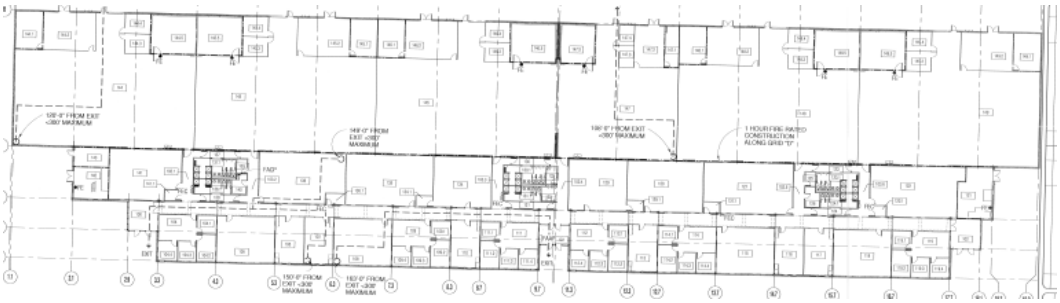

Figure B7. Company Operation Facility, administration offices floor plan, Bldg 2620, Fort Carson, CO.

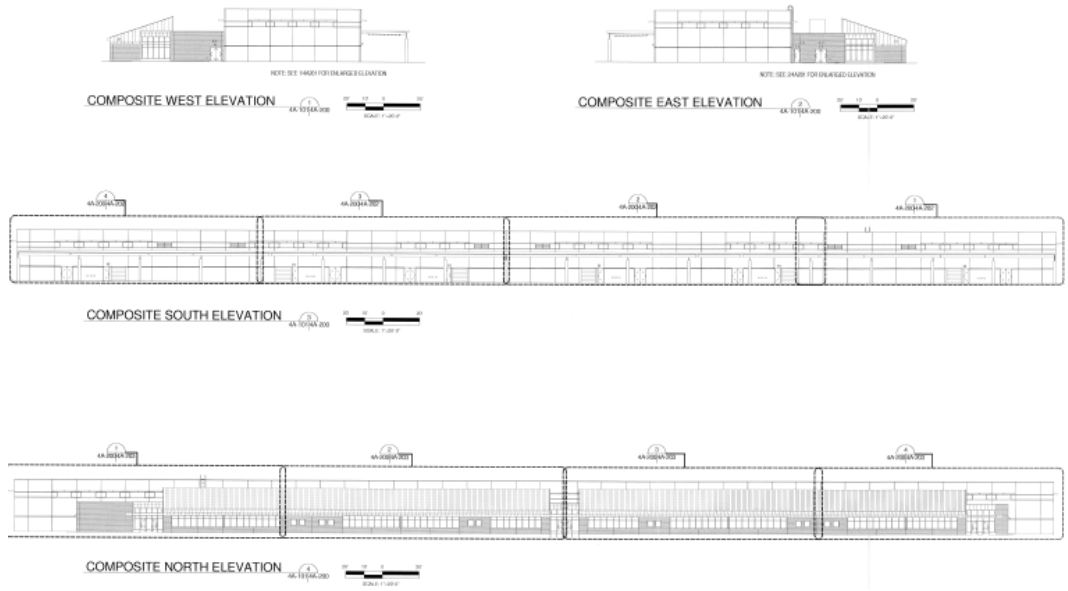

Figure B8. Company Operation Facility, administration offices elevations, Bldg 2620, Fort Carson, CO.

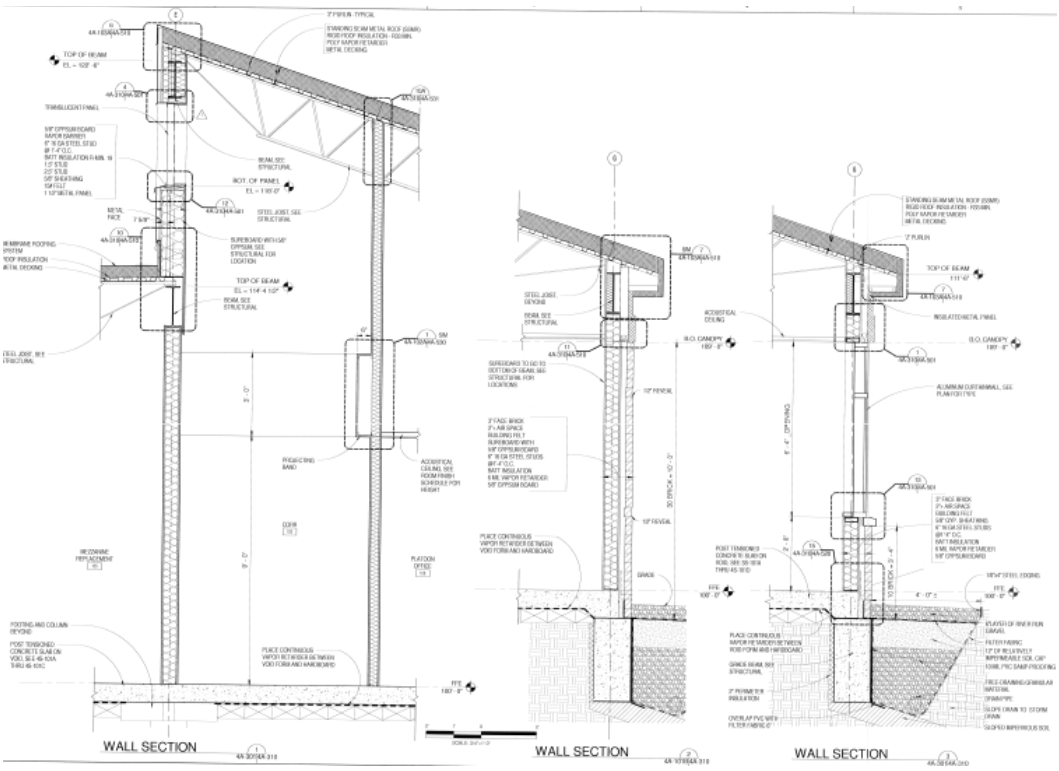

Figure B9. Company Operation Facility, administration offices wall sections, Bldg 2620, Fort Carson, CO.

UEPH/Barracks

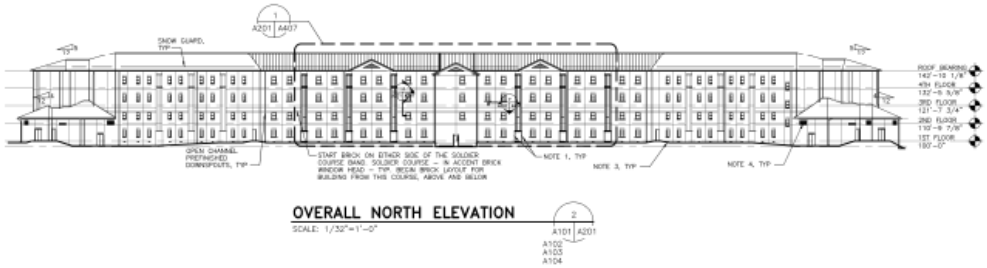

Figure B10. "Dogbone" Barracks elevations, Bldg 2144, Fort Carson, CO.

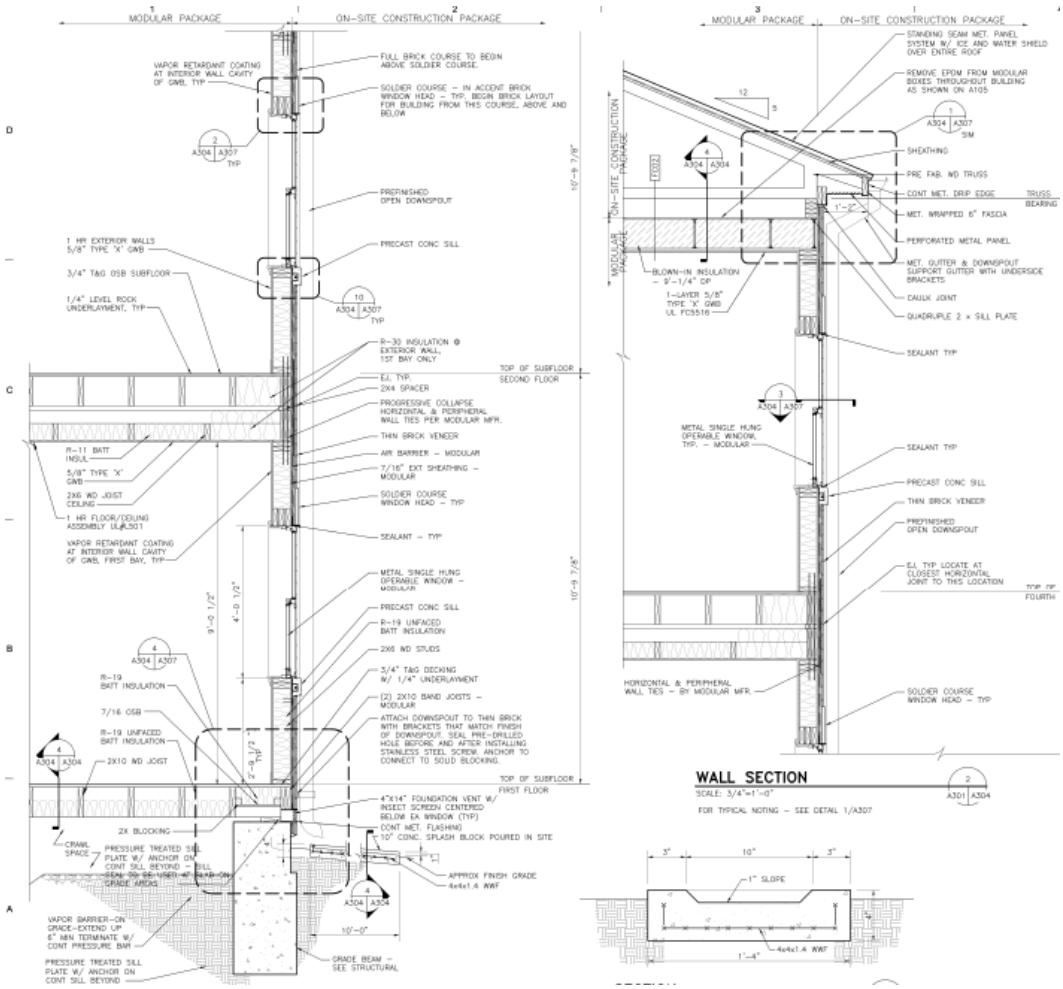

Figure B11. "Dogbone" Barracks wall sections, Bldg 2144, Fort Carson, CO.

Battalion Head Quarters

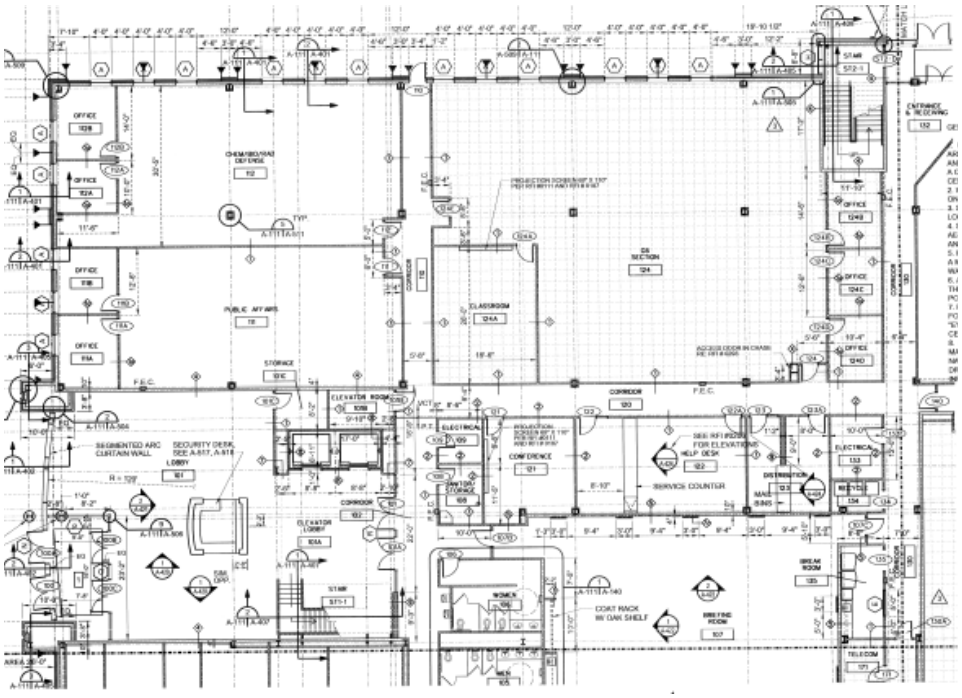

Figure B12. Battalion Head Quarters floor plan, Bldg 1435, Fort Carson, CO.

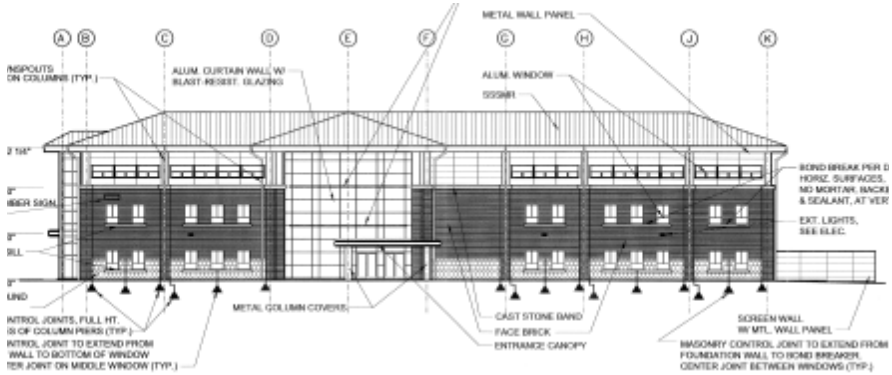

Figure B13. Battalion Head Quarters elevations, Bldg 1435, Fort Carson, CO.

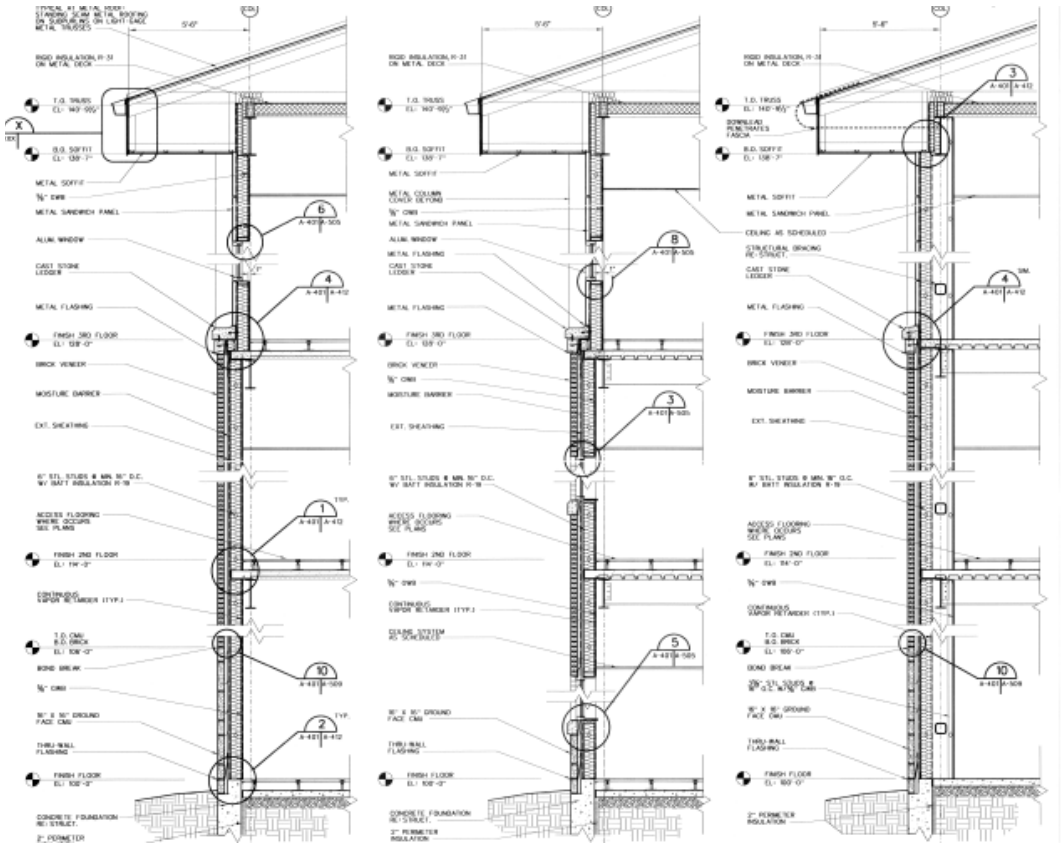

Figure B14. Battalion Head Quarters wall section, Bldg 1435, Fort Carson, CO.

Army Reserve Facilities

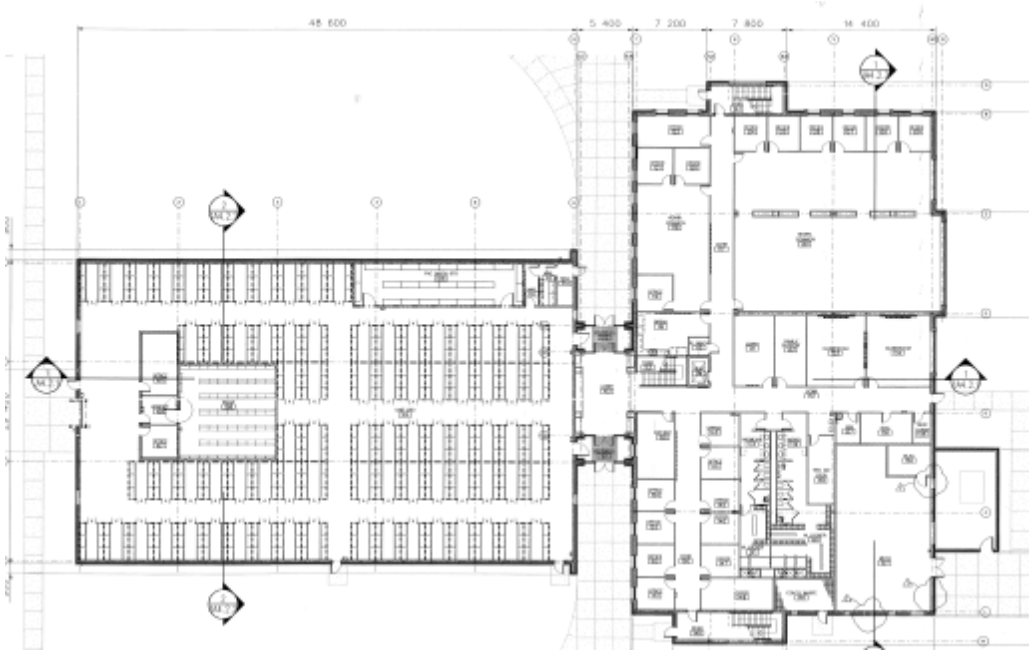

Figure B15. Army Reserve Center floor plan, Bldg 3450, Fort Carson, CO.

Figure B16. Army Reserve Center elevations, Bldg 3450, Fort Carson, CO.

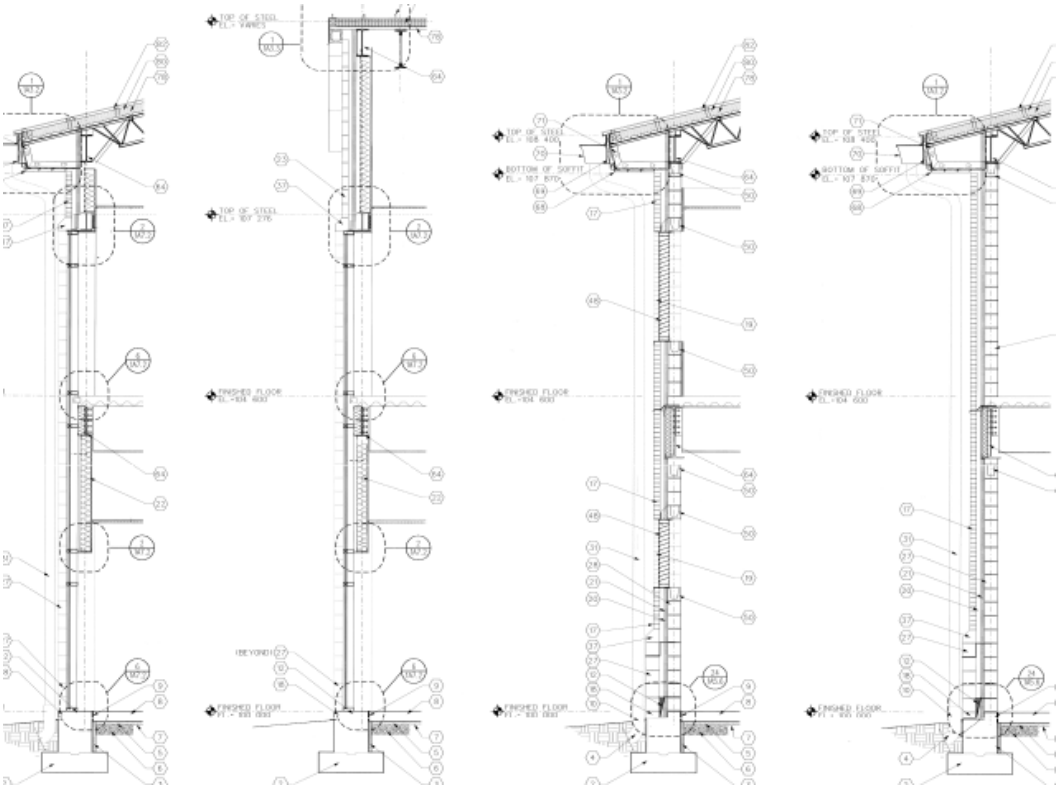

Figure B17. Army Reserve Center wall sections, Bldg 3450, Fort Carson, CO.

Appendix C: Army Facilities Thermal Bridge Index

Table C1. Summary data on several of the TB scenarios identified with the thermographic camera, which provides a guideline and facilitates the modeling start up process, which begins with the selection of appropriate drawings based on the different construction configurations (building types) that can be found among the Army facilities

				Thermal Bridge Type								
List Picture #	Installation	Building #	Building Category	Window Frames	Door Frames	Overhead Door Frames	Building Foundation	Wall/Wall Intersection	Three way Corners	Wall-Roof Junction	Mid Floor Slab/Wall	Internal Wall Framing
1	Carson	1444	DFAC		x		x		x			
2	Carson	1444	DFAC		x		x		x			
3	Carson	1444	DFAC				x	x	x			
4	Carson	8930	TEMF			x	x					x
5	Carson	8930	TEMF		x	x	x					
6	Carson	2630	ADMIN	x			x					
7	Carson	2630	ADMIN	x	x			x	x			
8	Carson	2630	ADMIN	x	x							
9	Carson	2630	ADMIN	x								
10	Carson	3074	Barracks	x			x	x	x			
11	Carson	2144	Barracks				x				x	
12	Carson	1552	Barracks	x			x	x	x			
13	Carson	2132	Battalion HQ	x	x		x	x			x	
14	Carson	1435	Battalion HQ				x					
15	Carson	1435	Battalion HQ	x								
16	Carson	1435	Battalion HQ	x			x					
17	Carson	3450	ARC	x						x	x	
18	Carson	3450	ARC	x	x					x		
19	Carson	3450	ARC		x				x			
20	Carson	3450	ARC	x	x			x	x	x		
21	Drum	D#1	DFAC	x	x							
22	Drum	D#2	DFAC	x								x
23	Drum	D#3	DFAC									x
24	Drum	D#4	DFAC							x		
25	Drum	D#5	TEMF	x		x				x		
26	Drum	D#6	Barracks	x						x		
27	Drum	D#7	Barracks				x					
28	Drum	D#8	Barracks				x	x			x	
29	Drum	D#9	Battalion HQ	x	x							
30	Drum	D#10	Battalion HQ	x								
31	Drum	D#11	Battalion HQ	x								
32	Drum	D#12	CDC							x		
33	Bragg	B#1	Battalion HQ	x						x		
34	Bragg	B#2	Battalion HQ									x
35	Bragg	B#3	Battalion HQ	x	x					x		

REPORT DOCUMENTATION PAGE

Form Approved
OMB No. 0704-0188

1. REPORT DATE (DD-MM-YYYY)	2. REPORT TYPE	3. DATES COVERED (From - To)
06-08-2013	Final	

4. TITLE AND SUBTITLE
Analysis Techniques, Materials, and Methods for Treatment of Thermal Bridges in Building Envelopes

5a. CONTRACT NUMBER

5b. GRANT NUMBER

5c. PROGRAM ELEMENT

6. AUTHOR(S)
Benjamin P. Barnes , Axy Pagán-Vázquez , Andrew P. Heffron , Brenda B. Mehnert , Michael P. Case , Ashok Kumar , Jeffrey L. Lattimore , Richard J. Liesen , Larry D. Stephenson , and Jonathan C. Trovillion

5d. PROJECT NUMBER
622784AT45

5e. TASK NUMBER

5f. WORK UNIT NUMBER

7. PERFORMING ORGANIZATION NAME(S) AND ADDRESS(ES)
US Army Engineer Research and Development Center (ERDC)
Construction Engineering Research Laboratory (CERL)
PO Box 9005,
Champaign, IL 61826-9005

8. PERFORMING ORGANIZATION REPORT NUMBER
ERDC TR-13-7

9. SPONSORING / MONITORING AGENCY NAME(S) AND ADDRESS(ES)
Headquarters, US Army Corps of Engineers (HQUSACE)
400 G St., NW
Washington, DC 20314-1000

10. SPONSOR/MONITOR'S ACRONYM(S)
CEMP-CI-I

11. SPONSOR/MONITOR'S REPORT NUMBER(S)

12. DISTRIBUTION / AVAILABILITY STATEMENT
Approved for public release; distribution is unlimited.

13. SUPPLEMENTARY NOTES

14. ABSTRACT

To meet mandated energy reduction goals, this work developed capabilities to characterize energy losses through building envelopes (especially thermal bridge losses), and to devise potential mitigation strategies using advanced techniques and materials. This report reviews existing thermal bridge quantification and mitigation strategies, as well as Army and building code requirements. It is proposed that, first, additional guidance must be authored to encourage treatment of thermal bridges and, second, that an easy to use thermal bridge catalogue must be composed. To this end, important thermal bridges in Army buildings are identified by infrared imaging and drawings review. Next, several 3-D heat transfer simulations are performed on these details as the first step to predicting their performance for inclusion in a details catalogue. Finally, advanced materials are characterized to better serve as mitigation options for thermal bridge retrofits.

15. SUBJECT TERMS
building envelope, energy conservation, thermal bridge

16. SECURITY CLASSIFICATION OF:			17. LIMITATION OF ABSTRACT	18. NUMBER OF PAGES	19a. NAME OF RESPONSIBLE PERSON
a. REPORT	b. ABSTRACT	c. THIS PAGE			19b. TELEPHONE NUMBER (include area code)
Unclassified	Unclassified	Unclassified	SAR	142	